Republic of Iraq

Ministry of higher education

and Scientific Research

University of Al-Mustansiriyah

College of Pharmacy

LOADING OF CLARITHROMYCIN AND PACLITAXEL ON PREPARED CdS/NiO NANOPARTICLES AS PROMISING NANOCARRIERS

Submitted to the Department of Pharmaceutics and the Committee of Graduate Studies of the College of Pharmacy/University of Al-Mustansiriyah in Partial Fulfillment of the Requirements for the Degree of Master of Science in Pharmacy "Pharmaceutics"

By

Mustafa Raad Abdulbaqi

BSc Pharmacy 2009

Supervisors

Assist.Prof. Dr.
Nidhal K. Maraie

Prof. Dr.
Ashour H. Dawood

2016 AD ***1437 AH***

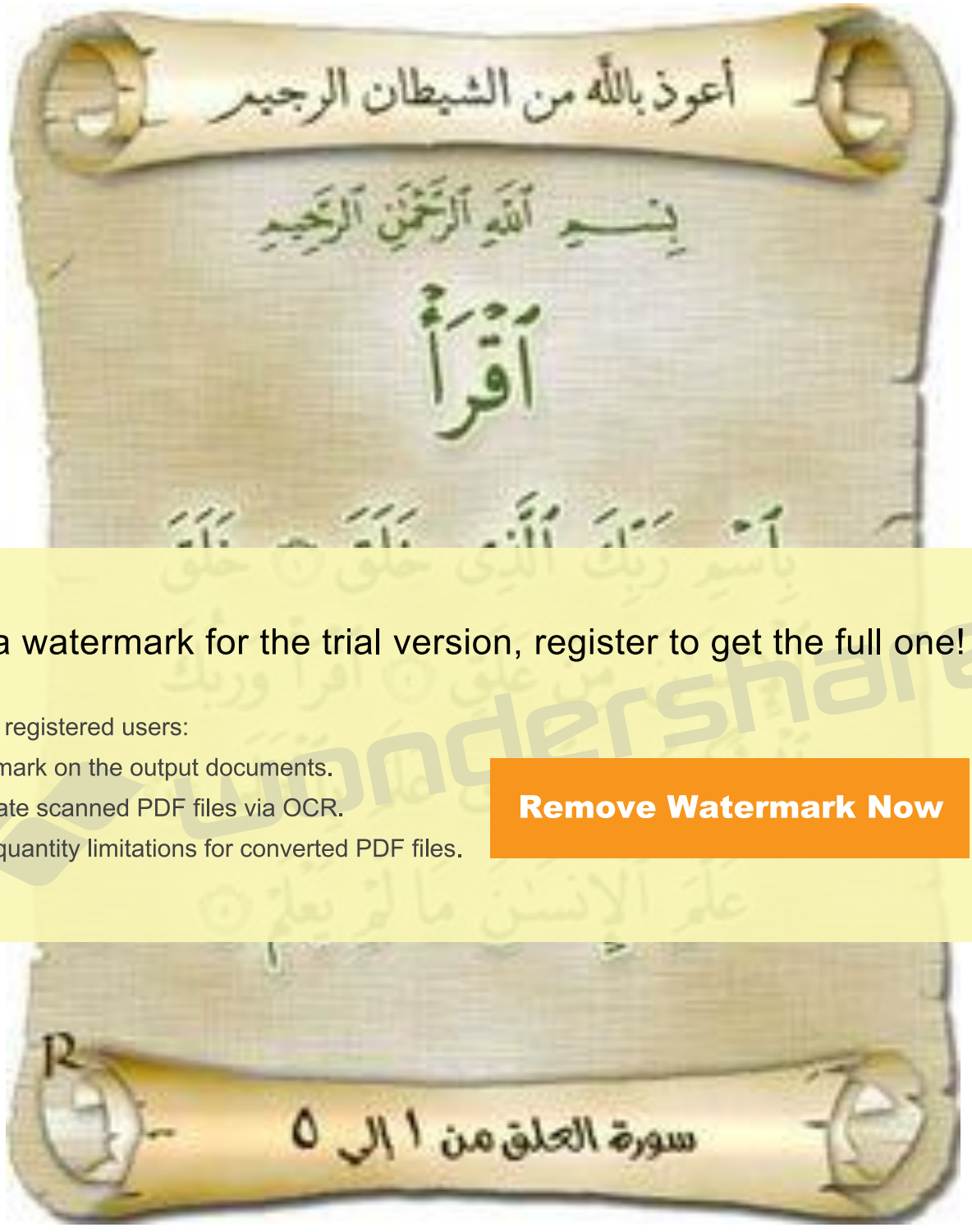

صدق الله العظيم

Supervisor certificate

We certify that this thesis, titled **(Loading of Clarithromycin and Paclitaxel on Prepared CdS/NiO Nanoparticles as Promising Nanocarriers)**, was prepared under our Supervision at College of Pharmacy/Al - Mustansiriyah University, as a partial fulfilment of the requirements for the degree of Master of Science in Pharmacy (Pharmaceutics).

Signature:

Name: **Assistant Prof. Dr. Nidhal K. Maraie**

Department: Department of Pharmaceutics/College of Pharmacy/Al - Mustansiriyah University

Date: / / 2016

Signature:

Name: Prof. Dr. Ashour H. Dawood

Department: Department of Pharmaceutical Chemistry/College of Pharmacy/Al - Mustansiriyah University

Date: / / 2016

In view of the available recommendations, I forward this thesis for debate by the examining committee.

Signature:

Name: Dr. Inam S. Arif

Chairman of the Committee of Graduate

Date: / / 2016

Committee Certificate

We, the examining committee, after reading this thesis, titled

(Loading of Clarithromycin and Paclitaxel on Prepared CdS/NiO Nanoparticles as Promising Nanocarriers),

And examining the student (Mustafa Raad Abdulbaqi) in its content, find it is adequate as a thesis for the degree of Master of Science in Pharmacy (Pharmaceutics).

Signature:

Name: Assist. Prof. Dr. Monther F. Mahdi

Address: College of Pharmacy/ Uni. Of Al-Mustansiriyah

(Chairman)

Date: / / 2016

Signature: Signature:

Name: Asst. Prof. Dr. Name: Asst. Prof. Dr.

Address: College of Pharmacy/ Uni. Of Baghdad Address: Uni. Collage of Humanities

(Member) (Member)

Date: / / 2016 Date: / / 2016

Approved by; The University Committee of Graduate Studies.

Signature:

Name: Assistant prof. Dr. Monther F. Mahdi

Dean of College of Pharmacy

University of Al - Mustansiriyah

Date: / / 2016

Dedication

To My Dear Parents …
I am grateful for your endless

support, assistance and patience.

…

Mustafa

Acknowledgments

Thanks and praise be to **God Allah Almighty**, the lord of whole creation who made all this work possible.

I would like to express my sincere gratitude to my supervisor **Assist. Prof. Dr. Nidhal K. Maraie** for her continuous support, patience, motivation, and immense knowledge. Her guidance helped me in all the time of research and writing of this thesis.

I would like to express my heartfelt gratitude and appreciation to my co-supervisor **Prof. Dr. Ashour H. Dawood** for his guidance, valuable advice and constant help through the whole work.

My deep thanks with respect to **Assist. Prof. Dr. Monther F. Mahdi**, Dean of Collage of Pharmacy/University of Al-Mustansiriya for his valuable generosity and support.

I would like to deep thanks **Dr. Inam S. Arif**, Dean assistant for scientific affairs for her generosity and support.

Deepest appreciations are to **Dr. W[illegible] K. Ali** for her help and support.

[illegible] **Dr. [illegible]umah M[illegible]** [illegible]sity.

Deepest appreciations are to **Dr. Sabah J. Salih** and **Pharmacist Zina S. Dhiab** for their help and support.

Deep thanks to **Lecturer Dr. Mohammed M. Mohammed** and **Dr. Ishraq Al-Dahhan** for their help and generosity.

Deep thanks to **Assist Prof. Dr. Hazim I. Abdulbari** for his help.

My heartfelt gratitude to **Pharmacist Zainab H. Mahdi**, for her continuous help and support.

Finally my deepest gratefulness to my family and my brothers **Lecturer Dr. Hayder R. Abdulbaqi** and **Dr. Ahmed R. Abdulbaqi** for their valuable help and support.

Mustafa

Content

List of tables

List of figures

Abbreviations

AFM	Atomic force microscopy
ANOVA	Analysis of variance
BCS	Biopharmaceutical classification system
°C	Celsius degree
Caco	Colorectal adenocarcinoma cells
CLA	Clarithromycin
COPD	Chronic obstructive pulmonary
DMEM	Dulbecco modified Eagle's medium
DMSO	Dimethyl sulfoxide
DSC	Differential scanning calorimetric
e.e	Entrapment effiency
FDA	Food and drug administration
FTIR	Fourier transform infra-red spectroscopy
log	Logarithm
MCF-7	Michigan cancer foundation-7
MCF-10A	Michigan cancer foundation-10A
MNPs	Magnetic nanoparticles

m.p	Melting point
MRI	Magnetic resonance imaging
MTT	(3-(4,5 Dimethylthiazol-2-yl)-2,5-Diphenyltetrazolium Bromide)
NIR	Near Infrared Radiation
o/w	Oil-in-water
PAMAM	Polyamidoamine
pH	Negative logarithm of hydrogen ion concentration
PTX	Paclitaxel
RES	Reticulo-endothelial system
SEM	Scanning electron microscopy
siRNA	Small interfering ribonucleic acid
SLN	Solid lipid nanocarriers
TEM	Transmission electron microscopy
TGA	Thermal gravimetric analysis
U/mL	Unit/milliliter
US	United states
USP	United states pharmacopeia
USP-NF	United states pharmacopeia-National formulary

UV	Ultraviolet
w/o	water-in-oil
XRD	X-ray diffraction
λ max	Wave length with maximum absorbance
ξ	Zeta potential

ABSTRACT

Nanotechnology is the understanding and control of matter at dimensions of roughly 1 to 100 nm while nanocarriers are nanomaterials being used as a transport modules for another substances such as drugs.

Clarithromycin (CLA) is a macrolide antibiotic that have a dissolution rate-limited absorption and low bioavailability after oral administration due to its low solubility in which CLA belongs to the class II of biopharmaceutical classification system (BCS) with low solubility and good permeability, while paclitaxel (taxol) is a widely used chemotherapeutic drug and belong to class IV drug of BCS with poor solubility and poor permeability, in which the high lipophilicity with very poor aqueous solubility as well as lack of ionizable functional groups are the major challenges in the paclitaxel dissolution and delivery from its dosage form.

[illegible] and NiO nanoparticles were prepared and applied successfully as drug nanocarriers for clarithromycin and anticancer drug paclitaxel by simple one step reaction to improve their pharmaceutical properties and / or their biological activities. The yield and drug content percentages for CLA were 66.34%, 56.66% using CdS nanoparticles while they were 64.1%, 86.6% using NiO nanoparticles, while for PTX they were 62.9%, 76.65% using CdS nanoparticles and 95.04%, 95.67% using NiO nanoparticles.

The Fourier Transform Infra-Red (FTIR), Scanning Electron Microscopy (SEM), Atomic Force Microscopy (AFM), X-Ray Diffraction (XRD), Differential Scanning Calorimetric (DSC), Thermo-Gravimetric Analysis (TGA) and zeta potential measures were applied for drugs-nanocarriers complexes in comparison with the pure drugs and blank CdS and NiO

nanoparticles. These measures revealed that the reaction was by physical complex formation rather than chemical modification for surface loading of the drugs on the nano-sized prepared CdS and NiO nanoparticles. The solubility/dissolution study was applied and revealed that it had been significantly ($p < 0.05$) improved for CLA after loading on CdS and NiO nanoparticles, knowing that the improvement using NiO nanoparticles was much more higher than on CdS nanoparticles. While the antibacterial activity test for CLA was non-significantly improved after loading with the nanocarriers.

For PTX loaded on CdS and NiO nanoparticles showed non-significant change in its solubility, but significant ($p < 0.05$) increase in its antitumor activity on MCF-7 cell line accompanied with significant ($p < 0.05$) reduction in its undesirable cytotoxic effect on normal mammary cell line MCF-10A indicating the selectivity and targeting action of the prepared PTX-CdS/NiO nanocarriers with reduced cytotoxicity and [illegible] the drug by the nanocarriers.

Chapter One

1. Introduction:

1.1 Nanomedicine:

Nanomedicine is the application of nanotechnology to medicine[1] or it is the science and technology of preserving and improving human health, and of diagnosing, treating and preventing disease and traumatic injury of relieving pain using molecular tools and molecular knowledge of the human body[2].

Nanotechnology is the understanding and control of matter at dimensions of roughly 1 to 100 nm, where unique phenomena enable novel applications including the forming and use of structures, materials, devices and systems that have unique properties because of their small size[3].

The prefix 'Nano-' is derived from the Greek word Nanos that means "very short man", nano is used in sc[illegible] [illegible]0.000,000,001) of the base unit[4].

1.1.1 Advantages of nanotechnology:

1. Nanotechnology-based drug delivery systems can protect drugs from degradation by coating the drug[5].

2. It may reduce number of doses and increases efficacy of active ingredient leading to decreased risk of side effect and toxicity[6].

3. Nanotechnology-based systems permit delivery of water insoluble or poorly soluble drugs[7].

4. Tumors vasculature allows an enhanced permeability and retention effect of nanoparticles[8].

5. Nanotechnology gives a solution for using numerous chemical entities for treating brain disorders that are not clinically useful due to the presence of

the blood-brain barrier[9], for example nanoparticle-conjugated small-molecule activator of an epigenetic enzyme in the brain[10].

6. Improve the oral bioavailability of the agents that are not effective orally for example Rapamune® (drug-sirolimus) which is an immune suppressant agent [11].

7. Nanoparticles can be administered by several routes of administration like parentally, orally, nasally and by ocular route[12].

8. Nanotechnology based drug delivery systems can lead to controlled release over short or long durations, improved half-life, and highly specific site-targeted drug delivery of therapeutic compounds[13].

1.1.2 Disadvantages of nanotechnology:

1. Difficulties in implementation.
2. Expensive (high cost technology) [14].
3. Nanoparticles can result in [illegible]
4. Because of its small size, it can acc[illegible] harmful consequences, e.g. it can cross the nuclear envelope of a cell and cause unintended genetic mutations and damage[16].

1.1.3 Applications of nanomedicine:

- **Drug delivery and targeting:** Nanoparticles as carriers for drug can be designed to improve the therapeutic and pharmacological properties of conventional drugs, additionally the method of incorporation of drug molecules into nanocarrier offer possibilities of targeting and controlled release as well as protect the drug from premature degradation resulting in more effective and selective therapy than traditional form of drugs[17].

  The use of nanoparticles can overcome the limitations accompanied with conventional cancer chemotherapy including drug resistance, lack of

solubility and lack of selectivity[18], where many functional groups are allowed to be attached to nanoparticle due to their high surface area to volume ratio that can seek out and bind to certain tumor cells and preferentially accumulate at tumor sites because of the small size of nanoparticles[19].

Drug delivery from nanocarriers can be classified into[20]:

1. Sustained and controlled delivery system.
2. Site-specific targeting (tissue, cellular, intracellular).
3. Functional system for bioactives delivery.
4. Multi-functional system for combined delivery of therapeutic, diagnostic and biosensing.
5. Stimuli sensitive delivery system.

- **Nano-engineered devices:** Maximizing bioavailability of injected drugs to the body and over needed periods of time can be achieved by molecular engineering. Nanoengineered [illegible] technologies are smallest devices, less than the body as well as these devices are faster and more sensitive than ordinary regular size drug delivery[21].

- **Diagnosis:** Diagnosis of cancer in the early stages from a few drops of a patient's blood can be done by the use of sensor test chips which contain thousands of nanowires to detect proteins and other biomarkers of cancer cells left behind[19].
- **Blood purification:** Purification with nanoparticles allow specific targeting of substances and depend on functionalized carbon coated metal or iron oxide nanoparticles with ferromagnetic or super paramagnetic properties in contrast to dialysis which depend on ultrafiltration of fluid across a semi-permeable membrane and size related diffusion of solutes[22]. Binding agents such as antibodies, proteins or antibiotics are linked covalently to the particle surface forming an agglomerate and then particles can be separated from the

bulk fluid by applying an external magnetic field gradient resulting in cleaning it from the contaminants[23].

- ***In-vivo* imaging:** Quantum dots are attached to proteins that penetrate cell membranes, these dots can be random in size and made up of bio-inert material with a nanoscale property that its color is size-dependent and therefore sizes are selected so that to make a group of quantum dots fluoresce, the frequency of light used is an even multiple of the frequency required to make another group glow and then both groups can be lit with a single light source[24].
- **Tissue engineering:** To fabricate mechanically strong biodegradable polymeric nanocomposites for bone tissue engineering nanoparticles such as carbon nanotubes, graphene, molybdenum disulfide and tungsten disulfide are being used as reinforcing agents in which significant improvements in the compressive and flexural mechanical properties of polymeric [illegible] achieved by [illegible] concentrations of 0.2 weight %)[25].

1.2 Nanocarriers:

Nanocarriers are nanomaterials being used as a transport modules for another substances, such as drugs [26], with sizes of diameter range from 1-100 nm[27]. Optimized biological and physicochemical properties of nanocarriers make them taken up by cells more easily than larger molecules, so they can be successfully used as delivery tools for currently available bioactive compounds[28]. For a targeted therapy the way of conjugation of the drug to the nanocarrier and the strategy of its targeting is important. A drug may be encapsulated into nanocarrier or else it can be adsorbed or covalently attached to the nanocarrier's surface. Covalent linking has the advantage over other ways of attachment as the number of drug molecules connected

to the nanocarrier can be controlled, i.e., a precise control of the amount of therapeutic compound delivered[29].

1.2.1 Ideal nanocarrier properties necessary for drug delivery:

Stable in blood, non-toxic, non-inflammatory, non-immunogenic, non-thrombogenic, no activation of neutrophils, biodegradable, avoidance of the reticuloendothelial system, applicable to different molecules (such as small molecules, peptides, proteins and nucleic acids), inexpensive manufacturing process and scalable[30].

1.2.2 Physiochemical properties of nanoparticles and their effect on the efficacy of drug delivery:

1. Particle size: Nanoparticles offers a number of distinct advantages over [illegible] delivery, [illegible] penetrating virtually all tissues in the body [illegible] uptake compared with microparticles, in which 100nm size nanoparticles showed 2.5 fold greater up-take [illegible] higher uptake compared to 10 µm microparticles in Caco-2 cell line[32].

2. Surface charge: The nanoparticles surface charge reflects the electrical potential of particles and it is affected by the medium at which it is dispersed and by the chemical composition of the particles, where nanoparticles with a high positive or negative zeta potential would be stable in suspension, as the surface charge prevents aggregation of the particles[33]. In drug delivery, opsonisation (a process that involves the adsorption of proteins especially of the complement system, to any foreign material) is also affected by zeta potential. These proteins make the nanoparticles more susceptible to phagocytosis leading to their clearance from the body[34].

3. Hydrophobicity: By changing the hydrophobicity of a nanocarrier, the structure and composition of the polymer / copolymer or the molecular weight, the polymer degradation and hence the drug release mechanism and/ or duration is changed[35, 36].

4. Surface area: The decreased particle size to nano-scale would result in an increased surface-to-volume ratio and that size is inversely proportional to the specific surface area[37]. During formulation the drug would be adsorbed onto the outer layer of the nanoparticles, particularly in emulsion based techniques of preparation, resulting in an initial burst release because of the large surface area, hence affecting the drug release kinetics[38].

5. Crystallinity: Crystallinity is important during development process of nanoparticles formulation that greatly affects the solubility and dissolution behavior of the drug. Generally, amorphous (non-crystalline) drug particles have faster dissolution rate compared to crystalline forms and the [illegible] in the crystall[illegible]

1.2.3 Methods of drug loading:

Two methods are available for drug loading as follow:

- **Incorporation method:** Involve incorporation of the drug at the time of nanoparticles production.
- **(Adsorption /Absorption) method:** Involve incubation of the carrier with a concentrated drug solution resulting in absorption of the drug by nanoparticles after their formation[40].

1.2.4 Types of nanocarriers:

Organic Nanocarriers

- **Nanocrystals and nanosuspensions:** Nanocrystals are aggregates consisting of several hundred to tens of thousands of atoms that are clustered with typical sizes of these aggregates between 10-400 nm and exhibit physical and chemical properties between bulk solids and molecules[41]. Nanocrystallisation advantages include enhancement of saturation solubility, dissolution velocity and adhesiveness to surface/cell membranes[42]. A nanosuspension is a submicron colloidal dispersion of drug particles and pharmaceutical nanosuspension is defined as very finely colloid, dispersed, biphasic and solid drug particles in an aqueous vehicle with size below 1 µm and without matrix material that stabilized by polymers and surfactant. Nanosuspension solves the problem of poor solubility and bioavailability as well as the [illegible].

- **Polymeric nanocarriers and dendrimers:** Polymeric nanoparticles are colloid solid particles with a size range (10 to 1000nm) with different shapes like spherical, branched or shell structures. Their first fabrication was about 35 years ago as carriers for cancer chemotherapeutics and vaccines[44]. They are produced from biodegradable and non- biodegradable polymers. Drugs are incorporated into nanoparticles by dissolution, adsorption entrapment, attachment or by encapsulation, and the nanoparticles provide a sustained release of the drugs for longer periods of time, e.g., days and weeks[45]. Dendrimers are highly branched nano sized polymer mainly polyamidoamine (PAMAM), which are three dimensional, monodisperse, globular macromolecules with high number of surface functional groups. Their unique properties like different functional end groups, lesser viscosity and higher density make them applicable in different fields like as drug

delivery, dendrimer based nanomedicine, light harvesting, dendritic nanomaterials, gene delivery, electrode design, solubility enhancers and for various biotech applications[46].

- **Protein nanoparticles:** proteins are a class of natural molecules which are ideal for nanoparticle preparation due to its amphiphilicity that allow them to interact well with both the drug and solvent. Nanoparticles derived from natural proteins are metabolizable, biodegradable and easily subject to surface modifications to allow drugs and targeting ligands attachment[47]. For example Albumin–paclitaxel nanoparticle (Abraxane®) which has been approved for the treatment of lung, breast, small cell lung and pancreatic cancers [48] as well as bovine serum albumin nanoparticles loaded with sodium ferulate to target the liver[49].

- **Liposomes and niosomes:** Liposomes were defined as [illegible] vesicles which consist of an aqueous core surrounded by one or more [illegible] due to their ability to incorporate [illegible] compartment, hydrophobic drugs within lipidic membrane and amphiphilic substances in the lipid aqueous interface as well as they are non-toxic and biodegradable[50]. Its bioapplication include intracellular delivery systems for anti-sense molecules, proteins/peptides, ribosomes, and DNA[51]. While niosomes are hydrated non-ionic surfactant vesicles with unique structure make them capable of encapsulating both hydrophilic and lipophilic substances. They are very useful drug delivery system in which niosomes have the ability of entrapping different types of drugs, proteins, gene and vaccines[52].
- **Nanoemulsions and solid lipid nanocarriers (SLN):** Nanoemulsions are novel drug delivery systems that consist of emulsified oil and water systems with average droplet diameters ranging from 50 to 1000 nm and can exist as water-in-oil (w/o) or oil-in-water (o/w) form[53]. Their pharmaceutical

application include ocular delivery, topical delivery, in cell culture technology, antimicrobial, in cancer treatment and cosmetics[54]. While Solid lipid nanocarriers (SLN) are produced by replacing the oil in an emulsion by a solid lipid resulting in lipid nanoparticles being solid at both body and room temperature. SLN advantages include protection of sensitive molecules from the environment, use of physiological lipids, avoidance of organic solvents in preparation process, and controlled release characteristics[55]. They have wide biomedical applications [56].

- **Nanocapsules:** Nanocapsules are capsules in which drug particles are surrounded within a layer of polymers[57]. They are nano-vesicular systems that exhibit a typical core-shell structure in which the drug is confined within a cavity surrounded by a polymer membrane or coating. The active substance can be contained within the cavity in liquid or solid form as an oily core dispersion as well as the active substance can be imbibed in the polymeric matrix in nanocapsule surface[58].
- **Nanogels and Nanosponges:** Nanogels are nanoscale hydrogels composed of three-dimensional networks of water soluble/swellable polymers with high water content, biocompatibility and desirable chemical and mechanical properties. Their application include drug delivery, bioimaging, sensing, antifouling, DNA or siRNA delivery and tissue engineering[59]. While nanosponges are hyper-crosslinked polymer colloidal structures that consist of solid nanoparticles with colloidal sizes and nanosized cavities [60]. Nanosponges pharmaceutical applications include drug targeting, controlled and sustained drug release, topical and pulmonary drug delivery system, blood purification and protein ultrafiltration[61].
- **Implantable thin films carrying drug:** These defined as nanoscaled thin films that can control chemical agents release precisely by applying an electrostatic field. Their advantages include versatility, ease of preparation and high loading incorporation of biomolecules into films. The implanted

film can carry discrete packets of drugs that can be released separately thereby useful for chemotherapy particularly[62].

- **Carbon nanomaterials:** Nanocarbon materials including fullerenes, carbon nanotubes, carbon nanohorns and grapheme are extremely useful in various biological applications such as drug delivery, nanomedicine and biolabeling. Fullerenes are novel agents for gene therapy. Carbon nanotubes and carbon nanohorns show high drug-loading capacity and extended blood circulation times. Nanodiamonds have recently emerged as a novel platform for imaging, sensing and drug delivery[63].

Inorganic Nanocarriers

- **Ceramic and silica nanoparticles:** Ceramic nanoparticles such as alumina, silica, and titania are [illegible] in nature and easily engineered to a desired size and porosity. They protect doped molecules (drugs, enzymes, etc.) from denaturation by external pH and [illegible] used to e[illegible] of the body, delivery of insulin by oral administration and delivering proteins and genes[64]. Silica materials are attractive for several important biological applications, such as imaging, drug delivery, controlled release and oxygen carrier[65]. Nanoporous silica materials have high surface areas and large pore volumes, allowing the absorption of drugs in large amounts providing enough concentrations for local treatment. Silica materials surface is reactive due to the presence of silanol groups thereby allow facile modification by silanization reactions and therefore enhance the drug loading and for controlling the drug release[66].

- **Quantum dots Magnetic nanoparticles (MNPs):** Quantum dots (QDs) are pellucid semiconductors nanoparticles (group III-V and II-VI elements of periodic table) that have physical dimensions of 1–10 nm and under a light source like laser evident as fluorescence. Their inherent photophysical

properties made them attractive for the purposes imaging and targeted drug delivery[67]. Their biomedical application include labeling cells, tracking different particles, drug delivery system as well as used as biomarkers for cancer cells detection for diagnosis, forecasting of disease stage and clinical management[68]. While Magnetic nanoparticles (MNPs) are particulate materials that engineered to less than 100 nm and can be manipulated under the effect of an external magnetic field. Commonly used magnetic elements like iron, cobalt, nickel and their oxides[69]. Biomedical applications involve targeted drug and gene delivery, magnetic resonance imaging, protein bioseparation and magnetic hyperthermia[70].

1.3 Metallic nanocarriers:

Metallic nanocarriers are metallic nanoparticles for drug delivery which are nanosized metals with dimensions (width, length or thickness) within the size range of 1–100 nm, [illegible] existence was first recognized in 185[illegible] explanation was given by Mie in 1908[71]. Among nanoparticles with biomedical advantages are inorganic nanoparticles which include metals (gold, copper, silver, magnesium and iron), metal oxides (iron oxide, zinc oxide, titanium dioxide and cerium oxide) and quantum dots (cadmium selenide and cadmium sulfide) [72]. Metal NPs are unique with various biomedical applications involving drug and gene delivery, highly sensitive diagnostic assays, radiotherapy enhancement and thermal ablation[73].

1.4 The model drugs:

1.4.1 Clarithromycin (CLA):

The molecular formula of clarithromycin is ($C_{38}H_{69}NO_{13}$) and its molecular weight is 747.953 g/mol[74, 75]. Figure (1-1) shows the chemical structure of clarithromycin.

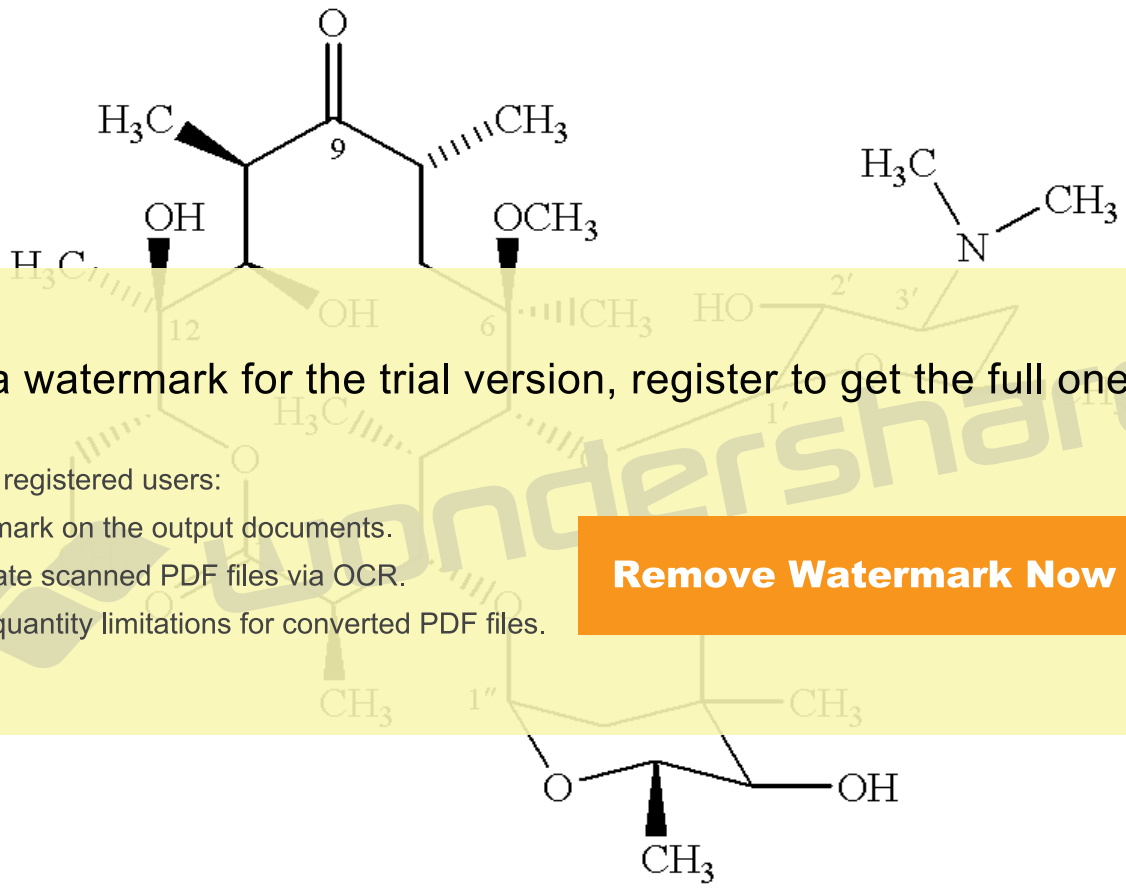

Figure (1-1): Structure of clarithromycin

1.4.1.1 Properties of clarithromycin:

Clarithromycin belongs to class II of BCS with low solubility that result in an absorption limited by dissolution rate leading to low bioavailability[76]. It is soluble in acetone, slightly soluble in ethanol, methanol and acetonitrile and practically insoluble in water[77].

Clarithromycin has high melting point (m.p 220 °C) and aqueous solubility of (0.342 µg/mL H_2O at 25 °C) [78] i.e., very slightly soluble. Its solubility is pH dependent which is sparingly soluble at stomach (pH 1.2) and very slightly soluble in the upper region of the small intestine (pH 5.0) where CLA absorbed, CLA solubility at pH 2.4 as 9.22 mg/mL and less than 1mg/mL at pH 6.8 and this decrease in CLA solubility in small intestine pH may contribute to its limited oral bioavailability which is not more than 50%, where CLA degrades quickly in acidic conditions obeying pseudo first-order kinetics with a degradation half-lives of 10.2 min at pH 1.2 and 17 min at pH 1.39[79]. The non-ionized form of clarithromycin had partition coefficient (log P) was 3.24[80]. It has a biological half-life of about 3-5 h[81].

1.4.1.2 Mode of action of clarithromycin:

Clarithromycin is a semisynthetic macrolide antibiotic which inhibit [illegible] by binding [illegible] susceptible organisms and thereby inhibiting protein synthesis through translocation of aminoacyl transfer RNA[82].

1.4.1.3 Pharmacokinetic of clarithromycin:

Clarithromycin undergoes first pass metabolism in which 25% of the parent drug converted to the active metabolite14-hydroxy clarithromycin.

Food slightly delays the onset of absorption for single 500 mg dose of CLR thereby increase the peak plasma concentration by about 24% and the peak time from approximately 2 to 2.5 hours, without change in the drug bioavailability extent. The absolute bioavailability of 250 mg CLR tablets was approximately 50%. CLR over a concentration range from 0.25 to 5 µg/L has serum protein binding ranging from 42 to 50% to the albumin fraction predominantly and high affinity for α1-acid glycoprotein[83].

1.4.1.4 Indications of clarithromycin:

Clarithromycin used for respiratory tract infection, Chlamydia infection, skin soft tissue infection, helicobacter pylori infection, acute maxillary sinusitis, pharyngitis, tonsillitis, acute bacterial exacerbation of chronic bronchitis and pneumonia[84]. Macrolides, like clarithromycin (CLA) and azithromycin, are the drugs of choice for the treatment of community acquired pneumonia due to their activity that is combined against pneumococcus and atypical bacteria, especially in areas with low macrolide resistance[85]. It is also used as prophylactic antibiotic for patients with mild to moderate chronic obstructive pulmonary disease (COPD)[86].

1.4.1.5 Marketed dosage forms of clarithromycin:

- Oral tablet (250 and 500 mg), twice a day.
- Modified release tablet 500 mg, once a day.
- Oral suspension (125 mg/5 mL), according to child under 8 kg, 62.5 mg for 8-11 kg, 125 mg for 12-19 kg, 187.5 mg for 20-29 kg and 250 mg for 30-40 kg child body-weight twice a day for child from 1 month - 12 years.
- Powder for solution Injectable infusion vial powder for solution (500 mg), twice a day given through a large proximal vein[87, 88].

1.4.2 Paclitaxel (PTX):

The chemical name of paclitaxel is:
(2α,4α,5β,7β,10β,13α)-4,10-Bis(acetyloxy)-13-{[(2*R*,3*S*)-3-(benzoylamino)-2-hydroxy-3-phenylpropanoyl]oxy}-1,7-dihydroxy-9-oxo-5,20-epoxytax-11-en-2-yl benzoate.

Its molecular formula is ($C_{47}H_{51}NO_{14}$) and its molecular weight is 853.93 g/mol[89, 90]. Figure (1-2) shows the structure of paclitaxel.

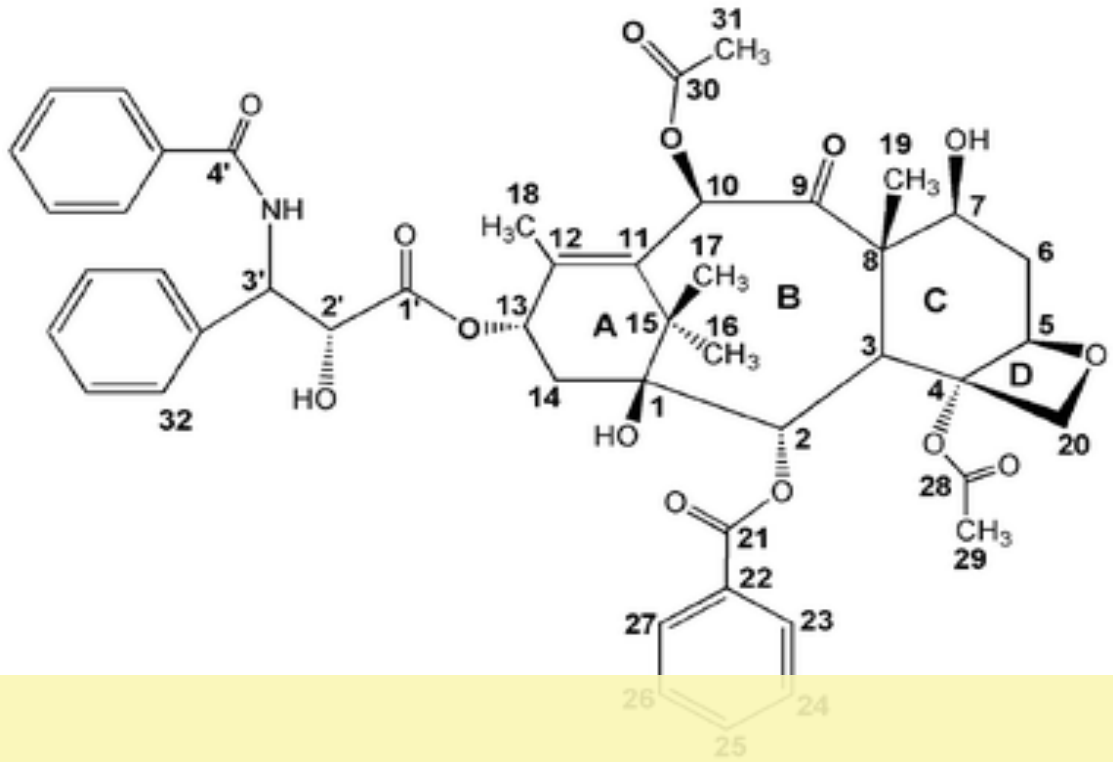

Figure (1-2): Structure of paclitaxel

1.4 Properties of Paclitaxel:

Paclitaxel is a mitotic inhibitor that was first isolated from the bark of Taxus brevifolia (northwest Pacific Yew Tree) in 1967. It is a white to off-white crystalline powder that is highly lipophilic, insoluble in water, and melts at around 216° to 217°C[91].

Paclitaxel is a diterpenoid centered around a complex, bulky and fused taxane ring that composed of hydrophobic substituents and therefore has very poor aqueous solubility of less than 0.01 mg/mL and log P value of 3.96. Paclitaxel lacks ionizable functional groups which might potentially lead to an increase in its solubility with pH alteration. PTX nonaqueous solvents solubility is found to be ~20 mM in methylene chloride or acetonitrile, ~46 mM in ethanol and ~14 mM in isopropanol as well as it is soluble in methanol, , dimethyl sulfoxide and tertiary-butanol[92, 93]. Paclitaxel belong to Class IV of BCS (low solubility and low permeability)[94].

1.4.2.2 Mode of action of paclitaxel:

Paclitaxel acts primarily as anticancer by suppression of microtubule spindle dynamics resulting in the blockage of metaphase-anaphase transitions, thereby inhibit mitosis and induction of apoptosis, in which paclitaxel binds to the polymeric tubulin and specifically stabilizes microtubules, thereby preventing tubulin disassembly[95].

1.4.2.3 Pharmacokinetic of paclitaxel:

Paclitaxel Pharmacokinetics shows a wide variability. The volume of distribution (steady-state) was found to be ~87.1 $L.m^{-2}$ and terminal half-life was found to be in range 1.3-8.6 h. The drug undergoes an extensive hepatic metabolism mediated by P-450 and less than 10% of drug excreted in the urine and most drug is eliminated in feces. Paclitaxel plasma protein binding [illegible] 90% and it's rapid as well as extensive[96, 97].

1.4.2.4 Indications and side effects:

Paclitaxel is U.S. Food and Drug Administration (FDA) approved for the treatment of several carcinomas including breast, advanced ovarian, non-small cell lung, head and neck, colon, and AIDS-related Kaposi′s sarcoma[98]. Paclitaxel showed serious adverse effects including; pain, redness and swelling at the injection site, unusual bruising or bleeding, , Hand-foot syndrome, fever, chills, cough, sore throat, change in normal bowel habits for more than two days, swallowing difficulty, dizziness, severe exhaustion, shortness of breath, skin rash, facial flushing, female infertility by ovarian damage. Common side effects include loss of appetite, nausea and vomiting, change in taste, thinned or brittle hair, changes in the color of the nails, pain in the joints of the arms or legs lasting two to three days, and tingling in the hands or toes[99].

1.4.2.5 Marketed dosage forms and doses of paclitaxel:

Paclitaxel FDA approved formulations include:

- TAXOL (Bristol-Myers Squibb); paclitaxel is dissolved in Cremophor EL and ethanol, as a delivery agent.
- ABRAXANE or nab-paclitaxel (American Bioscience, Inc.); paclitaxel is bound to albumin[100].

TAXOL is usually given slowly through an IV infusion up to 24 hours to complete every 3 weeks. The recommended ABRAXANE regimen for Injectable Suspension (paclitaxel protein-bound particles for injectable suspension) is 260 mg/m^2 that administered intravenously over 30 minutes every 3 weeks[101].

1.5 Literature survey:

In 2011, Thagele and et al prepared nanoparticles of CLA) containing [illegible] effect and reducing dosing frequency and was evaluated by transmission electron microscopy (TEM) and zeta potential sensitizer for particle size and morphology as well as by fourier transform infra-red (FTIR), differential scanning calorimetric (DSC) and UV-Visible spectroscopy[102]. In 2012, Lotfipour and et al prepare CLA nanoparticles by Modified Quasi Emulsion Solvent Diffusion (MQESD) method and loaded with PLGA (poly lactic-co-glycolic acid) nanoparticles as nanosuspension with improved antibacterial activity against *Staphylococcus aureus* in comparison with the pure drug[103]. Particle size and morphology of loaded drug was evaluated using SEM. In 2014, Esfandi and the other co-workers prepare aqueous nanosuspension of CLA by sonoprecipitation technique with enhanced antibacterial and dissolution rate in comparison with course powder of CLA[104]. The prepared nanosuspension particle size was measured using SEM, while thermal

behavior was studied using DSC. In 2016, Oktay and et al prepare nanocomposite hydrogel containing surface modified Fe_3O_4 nanoparticles and loaded with CLA for prolonged sustain release of the drug which was approved by *in-vitro* release study. The morphological and structural characterizations of loaded CLA were performed by FTIR, SEM and TEM[105].

In 2002, Fonseca and et al prepare paclitaxel (PTX) loaded poly(lactic-co-glycolic acid) (PLGA) nanoparticles with enhanced cytotoxicity of PTX against lung cancer cell line[106]. In 2005, the U.S. Food and Drug Administration (FDA) approved PTX bound protein (albumin) nanoparticles for injectable suspension (ABRAXANE) for the treatment of several carcinomas including breast, advanced ovarian, non- small cell lung, head and neck, colon, and AIDS-related Kaposi's sarcoma[98]. In 2009, Li and et al prepare paclitaxel loaded chitosan nanoparticles by solvent evaporation and ionotropic gelation cross-linking method. PTX loaded chitosan nanoparticles and loaded drug morphology and particle size were characterized by TEM and AFM microscopy[107]. In 2013, Aygul and et al prepare PTX loaded PLGA and polyvinyl alcohol (PVA) nanoparticles by emulsification solvent diffusion method and evaluated for particle size and particle size distribution using zeta potential with enhanced cytotoxicity of loaded PTX against human colon cancer cell line[108]. In 2014, J. Lu and et al prepare PTX loaded poly ethylene glycogylated nanoparticles (PEGylated-paclitaxel nanoparticles) with increased cellular uptake of breast cancer cell line (MCF-7), higher stability and enhanced cytotoxicity than unloaded PTX[109]. In 2015, Yang and et al prepare PTX loaded glycyrrhizic acid (GA) micelles to improve the oral bioavailability of PTX using ultrasonic dispersion method. DSC thermograms was applied and indicated that PTX was entrapped in the GA micelles and existed as an amorphous state, while zeta

potential sensitizer was applied to measure particle size and particle size distribution. PTX-loaded GA micelles displayed a delayed drug release compared to Taxol in the in vitro release experiment[92]. In 2015, Bayindir and et al prepare PTX-loaded Span 40 niosomes using thin-film method with higher area under curve and improved volume of tissue distribution than Taxol (FDA approved PTX with cremophor el and ethanol) after intravenous injection to rats[110].

In 2013, M. Ahamed and et al study the effect of nickel oxide (NiO) nanoparticles on human liver (HepG2) cells and revealed that NiO nanoparticles exert cytotoxicity via reactive oxygen species (ROS) and induce apoptosis to human liver (HepG2) cells in dose-dependent manner causing DNA damage, chromatin condensation, and micronuclei induction as well as altered mRNA levels of apoptotic genes[111]. In 2015, Rajput et al assess the cytotoxicity of synthesized NiO (by sol-gel solution method) [illegible] MCF7 AND A-[illegible] found that the synthesized NiO nanoparticles were more active towards the cancer cells with less toxicity toward normal cells[112]. In 2015, Vinardell and et al study the anticancer activity of metal oxides (CeO, CuO, Fe_3O_4, TiO_2, CoO and ZnO) and conclude that these metal oxides have cytotoxic effect on a variety of cancer cell lines (Squamous carcinoma, breast cancer, non-small cell lung, human myeloid, HeLa, .. etc cell lines) by the generation of reactive oxygen species or apoptosis and necrosis[113]. In 2015, Rashid and et al prepare metal oxides (NiO, Fe_3O_4, SnO and CoO) and loaded with the anticancer drug doxorubicin (DOX) that characterized by SEM, XRD and UV-Vis spectroscopy[114]. In 2015, Adhikary and et al prepare NiO nanoparticles varieties [NiO(I), NiO(Br) and NiO(Cl)] and conjugated with erythromycin (broad spectrum antibiotic) to develop NiO(I)-Ery, NiO(Br)-Ery and NiO(Cl)-Ery that show effective antimicrobial activity against

erythromycin resistant *Staphylococcus aureus* and *Escherichia coli*. These conjugated NiO varieties were characterized by FTIR, UV-Vis, XRD, DLS, SEM, and TEM methods[115].

In 2014, Hayder J. Essa prepare cadmium sulfide (CdS) nanoparticles loaded with the widely used anticancer drug 5-fluorouracil (5-FU) and then functionalized with iron oxide (Fe_2Cl_3) nanoparticles. The prepared CdS nanoparticles loaded drug were characterized using FTIR and UV-Visible spectroscopy. The anticancer activity of CdS loaded 5-FU against cervical carcinoma cell line revealed an enhanced anticancer activity after loading of 5-fluorouracil with CdS nanoparticles[116]. In 2014, Malarkodi and et al prepare cadmium sulfide (CdS) and zinc sulfide (ZnS) nanoparticles by green method and characterize them using FTIR, UV-Vis spectrophotometer, TEM and XRD spectra. The bacterial (*Bacillus subtilis*) activity of the prepared CdS and ZnO nanoparticles against oral pathogens (*Streptococcus mutans*, *Streptococcus sanguinis*, *Lactobacillus casei* and *Candida albicans*) was successfully demonstrated by well diffusion method on the agar plate[117]. In 2015, Shivashankarappa and et al prepare CdS nanoparticles by green synthesis using *Bacillus licheniformis* bacteria and characterized using FTIR, UV-Vis, XRD and SEM methods. They revealed that the prepared CdS nanoparticles possess significant antimicrobial activity against different food borne bacteria (*E coli*, *Bacillus licheniformis*, *Pseudomonas aeruginosa*, *Bacillus cereus* and *Staphylococcus aureus*) and fungi (*Fusarium oxysporum*, *Aspergillus flavus* and *Penicillium expansum*) which was successfully demonstrated by well diffusion method[118]. In 2015, Grinyte and et al study the catalytic role of CdS nanoparticles and found that the colorimetric sensitive assays for glucose oxidase and glutathione reductase based on enzymatic generation of CdS nanoparticles acting as light-powered catalysts by photo-oxidation of the chromogenic enzymatic substrate 3,3′,5,5′-tetramethylbenzidine by oxygen[119].

Aim of the study

The aim of this work involves preparation of cadmium sulfide (CdS) and nickel oxide (NiO) nanoparticles and incorporation (loading) of clarithromycin (class II) and paclitaxel (class IV) as model drugs and to characterize them as a promising nanocarriers that may improve physiochemical properties and/or biological activity of the drugs as well as may contribute to reducing the adverse effect of both drugs and applied metals.

Chapter Two

2. Materials and Methods:

2.1 Materials:

The following table summarizes the materials used and their manufacturer.

Table (2-1): Materials

Materials	Formula	Molecular Weight	Manufacture
Clarithromycin	$C_{38}H_{69}NO_{13}$	747.957 g/mol	Jiangsu Yew Pharmaceutical Co., Limited (China)
Paclitaxel	$C_{47}H_{51}NO_{14}$	853.93 g/mol	
Acetone	C_3H_6O	58.08 g/mol	
Ethanol	C_2H_6O	46.068 g/mol	Sigma Chemical Co., Limited (USA)
Methanol	CH_3OH	32.04 g/mol	
Acetonitrile	C_2H_3N	41.05 g/mol	Sinopharm Chemical Reagent Co., Limited (China)
Ammonia solution	$NH_4(OH)$	35.04 g/mol	

Cadmium acetate dihydrate	$(CH_3COO)_2Cd.2H_2O$	266.53 g/mol	Qualikems Fine Chem Co., Limited (India)
Nickel nitrate	$Ni(NO_3)_2 .6H_2O$	290.76 g/mol	Barcelona Co., Limited (Spain)
Sodium sulfide	$Na_2S.10H_2O$	258.04 g/mol	Thomas Baker Co., Limited (India)
Dimethylsulfoxide (DMSO)	C_2H_6OS	78.13 g/mol	Loba Chemie Pvt. Ltd (India)

Atomic Force Microscopy (AFM)	Augestrom advance inc.	USA
Differential Scanning Calorimetric (DSC)	Linsies	Germany
USP Dissolution Apparatus Type 2	Copley	UK
Fourier Transform Infra-Red Spectroscopy (FTIR)	8400S	Shimadzu Japan

Melting Point Apparatus	Stuart SMP 30	UK
pH Meter	WTW-INO LAB	Switzerland
X-Ray Diffraction (XRD)	220V/50Hz	Shimadzu Japan
Scanning Electron Microscopy (SEM)	FET company	Netherlands
Sonicator	Elma	Germany
UV-Visible Spectrometer	1800	Shimadzu Japan
Thermal Gravimetric Analyzer (TGA)	Linsies	Germany
Zeta Potential Analyzer	Brook	

2.3 Methods:

2.3.1 Melting point (m.p) determination method:

Melting point of clarithromycin and paclitaxel was achieved using capillary method, by taking a small amount of the drug through tipping the powdered drug in a capillary tube closed at one end then it was placed in melting point apparatus and the temperature at which the drug melts was noted to be compared with the standards reported in USP-NF[120].

2.3.2 Preparation of metallic nanoparticles:

2.3.2.1 Preparation of cadmium sulfide (CdS) nanoparticles:

Cadmium sulfide (CdS) nanoparticles were prepared by chemical co-precipitation technique by drop wise titration of 0.1M of $Na_2S.10H_2O$ aqueous solution (by dissolving 1.29g in 50 mL of deionized water) using 50 mL burette with a rate of (1 drop/minutes) to 0.1M of $(CH_3COO)_2Cd.2H_2O$ aqueous solution [illegible] heating at 50°C. While dropping and stirring, the solution color change from yellow to orange then red and finally return back to orange color, after dropping was finished, stirring was continued for 4 hours and then filtered and washed with deionized water three times to remove impurities. The residue was then left in desiccator containing silica gel for three days to be dried and finally, the product (orange nanoparticles) was collected, grinded by mortar and pestle and placed in a preweighed plastic container to be weighed and characterized[121, 122].

2.3.2.2 Preparation of nickel oxide (NiO) nanoparticles:

Nickel oxide (NiO) nanoparticles were prepared by thermochemical processing by drop wise titration of 100 mL of $NH_4(OH)$ solution using 100 mL burrete with a rate of (10 drops/minutes) to the preheated 0.5M of $Ni(NO_3)_2$.$6H_2O$ (by dissolving 7.269g in 50 mL of deionized water and heated to 70°C with stirring at 1000 rpm) with increased stirring to 1500 rpm. After dropping has been finished, stirring was continued for 4 hours and then filtered and washed with 1:1 (v/v) of deionized water and ethanol five times to remove impurities. The resulted light green residue was then placed in the oven at 70°C for 24 hours, then the temperature was raised to 220°C for 2 hours to dry the product and finally, the product (black nanoparticles) was grinded with mortar and pestle and placed in a preweighed plastic container to be weighed and characterized [ ].

2.3.3 Loading of two drugs (clarithromycin and paclitaxel) on metallic nanoparticles (CdS and NiO nanoparticles) by two different methods (incorporation) method and (adsorption/absorption) method, respectively.

2.3.3.1 Loading of clarithromycin and paclitaxel on CdS nanoparticles:

Clarithromycin and Paclitaxel each one separately was loaded to CdS nanoparticles by incorporation method which involves the addition of the drug in the last step of nanoparticles synthesis, where 0.1M of clarithromycin using acetone as a solvent (by dissolving 3.739g in 50mL of acetone) and 0.1M of paclitaxel using acetonitrile as a solvent (by dissolving 2.134g in 25mL of acetonitrile) was added (each one separately) by fast dropping to

the mixture of cadmium acetate and disodium sulfide while it is vigorously stirred(1500 rpm) at 50°C and just before dropping of disodium sulfide has been finished. After finishing the disodium sulfide dropping, the stirring was continued for 4 h and then filtered, washed with ethanol, desiccated and finally collected as light yellow powder to be characterized and evaluated[40].

2.3.3.2 Loading of clarithromycin and paclitaxel on NiO nanoparticles:

Loading of clarithromycin and Paclitaxel each one separately on NiO nanoparticles was done by (Adsorption/Absorption) method that involves addition of 0.1M of each drug by fast dropping to the preheated solution of NH_4OH containing NiO nanoparticles at 60°C with vigorous stirring (1500rpm) that continued for 2 h after drug addition has been completed. Then the mixture is filtered, washed with ethanol, desiccated and finally collected as a yellow powder to be characterized.

2.3.4 Determination of calibration curve of drugs method:

Clarithromycin stock solution was prepared by dissolving 100 mg of clarithromycin in 6mL of acetonitrile and then complete the volume to 100 mL by phosphate buffer (pH 7.4). The stock solution was then scanned by UV-Visible spectrophotometer at the range of 200-400 nm using 6mL acetonitrile completed to 100mL phosphate buffer pH 7.4 as a blank and the λ max of the drug was determined. Calibration curve of clarithromycin in phosphate buffer pH 7.4 was done by preparing serial dilutions from the prepared stock solution (1mg/1mL) including 1, 0.9, 0.8, 0.7, 0.6, 0.5, 0.4, 0.3, 0.2 and 0.1mg/mL and the samples were scanned spectrophotometrically at 210 nm (λ max of CLA) and then the measured absorbance values of the

samples were plotted versus related concentrations to obtain the standard calibration curve[126-128].

While paclitaxel stock solution was prepared by dissolving 4.5 mg of Paclitaxel in 50 mL methanol then the volume was completed to 100 mL by phosphate buffer (pH 7.4). The stock solution was scanned by UV-Visible spectrophotometer at the range of 200-400 nm using 50:50(v/v) of methanol and phosphate buffer (pH 7.4) as a blank and the λ max of the drug was determined. Calibration Curve of Paclitaxel in phosphate buffer pH 7.4 was done by preparing serial dilutions from the prepared stock (45µg/mL) including 45, 40.5, 36, 31.5, 27, 22.5, 18, 13.5, 9 and 4.5µg/mL and the samples were scanned spectrophotometrically at 230 nm (λ max of PTX), then the measured absorbance values of samples were plotted versus related concentrations to obtain the standard calibration curve

2.3.5.1 Fourier Transform Infra-Red (FTIR) measurement:

Characterization by FTIR spectroscopy (4000-500 cm^{-1}) using potassium bromide disc was performed for pure clarithromycin, CLA loaded on CdS and NiO nanoparticles each separately, pure paclitaxel and paclitaxel loaded CdS and NiO nanoparticles each separately[132].

2.3.5.2 Scanning Electron Microscopy (SEM) measurement:

Scanning Electron Microscope (SEM) was applied for the prepared metallic nanoparticles before and after drug loading as well as for pure drugs (each separately). It was done by taking 1-2 mg of powdered material and mounted on a sample small aluminum holder followed by coating with gold (conductive metal) and remove large molecules by nitrogen gas, then the

sample is scanned with a focused fine beam of electrons in SEM machine to take images[133].

2.3.5.3 Zeta Potential (ξ) measurement:

Zeta potential (ξ) analysis for CdS and NiO nanoparticles before and after loading with Clarithromycin and Paclitaxel was achieved by dissolving 2mg of each sample separately in 10mL of phosphate buffer pH 7.4 with sonication, then filtered using 0.2µl filter syringe and finally introduced to the zeta potential analyzer to read the zeta potential data for each sample[134].

2.3.5.4 X-Ray Diffraction (XRD) measurement:

The X-ray diffraction XRD was achieved for pure drugs, blank CdS and NiO nanoparticles alone and drugs loaded nanoparticles to determine their crystalinity in which the XRD system was equipped with Cu-Ka radiation (1.54 Å), voltage 40 [illegible] were analyzed at scanning speed of (5 [illegible] to 60 degrees [135].

2.3.5.5 Thermal Gravimetric Analysis (TGA) measurement:

Powder samples of pure drug, blank CdS and NiO nanoparticles and nanoparticles loaded drugs were analyzed by TGA during heating process (0-400 °C), where each sample was located separately in TG instrument pan to record the weight loss with increase temperature by subjecting them to a constant heating rate of 5 C°/min and air atmosphere with a gas (nitrogen) flow of 50 mL/min. As a result, thermal scan was recorded as plot of heat flow versus temperature[136].

2.3.5.6 Differential Scanning Calorimetric (DSC) measurement:

Differential Scanning Calorimetric (DSC) analysis was performed for pure drugs, blank CdS and NiO nanoparticles and drugs loaded nanoparticles by taking 1-2 mg of each sample and dispersed in 5mL of phosphate buffer PH 7.4, then take 1mL of the dispersed sample and heated from 25°C to 300°C at the rate of 10°C per minute under nitrogen gas carrier supplied at 10 mL/min[137].

2.3.5.7 Atomic Force Microscopy (AFM) measurement:

Atomic Force Microscopy (AFM) was performed for pure drugs (clarithromycin and paclitaxel), blank nanoparticles (CdS and NiO) and drugs loaded nanoparticles. Powder sample was dissolved by methanol and few drops of each sample was dropped separately on a silica glass plate and allowed to dry at room temperature to be deposited on the plate. The deposited plate was scanned [illegible] instrument[138].

2.3.6 *In-vitro* drug release study:

Clarithromycin *in-vitro* release study was achieved for CLA loaded on CdS and NiO nanoparticles each one separately as well as for pure CLA as control using a USP type II rotating paddle apparatus at 37± 0.5°C and rotating speed of 100 rpm in 500 mL of phosphate buffer solution (pH 7.4). Equivalent to 100mg CLA of the prepared drug loaded CdS and NiO nanoparticles as well as 100mg of pure CLA were dispersed in the dissolution medium and samples of 5 mL were withdrawn at predetermined time intervals and replaced with the same volume of fresh media after each withdrawal, then the withdrawn samples were filtered and the content of CLA was determined spectrophotometrically by using UV-Visible

spectrophotometer at 210 nm, each experiment was analyzed in triplicate [139, 140].

The same was applied to paclitaxel by dispersing 10 mg of the standard PTX as well as equivalent to 10 mg PTX of the prepared drug loaded CdS and NiO nanoparticles in 500mL of phosphate buffer solution pH 7.4 using USP type II rotating paddle apparatus at 37± 0.5°C and rotating speed of 100 rpm. The withdrawn samples was determined spectrophotometrically by using UV-Visible spectrophotometer at 230 nm, each sample was analyzed in triplicate[141, 142].

2.3.7 Calculation of yield, drug loading and entrapment efficiency percentages methods[143, 144]:

The percentage yield (% yield) was calculated as a percentage ratio of the weight of nanoparticles (or materials forming it) after incorporation of the drug with nanoparticles to the weight of nanoparticles and drug initially in the reaction before incorporation.

$$\%\text{Yield} = \frac{\text{weight of nanoparticles after drug incorporation}}{\text{weight of nanoparticles and drug before incorporation}} \times 100\%$$

The percentage of drug loading (% drug loading) was calculated as a percentage ratio of the weight of drug in nanoparticles alone to the weight of nanoparticles loaded with the drug, as follow:

$$\%\ \text{Drug loading} = \frac{\text{weight of drug in nanoparticles}}{\text{weight of nanoparticles loaded with the drug}} \times 100\%$$

The weight of clarithromycin loaded on CdS and NiO nanoparticles was determined by dissolving 20mg of drug loaded CdS and NiO nanoparticles each one separately in 3mL of acetonitrile and then complete the volume to 50mL with phosphate buffer pH 7.4 and scanned spectrophotometrically at λ max 210 nm by UV spectrophotometer. While the weight of paclitaxel in nanoparticles was determined by dissolving 5mg of CdS and NiO nanoparticles loaded drug each separately in 50mL of methanol and then complete the volume to 100mL with phosphate buffer pH 7.4 and scanned spectrophotometrically at λ max 230 nm by UV spectrophotometer.

The percentage of entrapment efficiency (% e.e) of the drug was calculated as a percentage ratio of the weight of drug in nanoparticles after incorporation to the weight of drug fed initially in the reaction before incorporation, as follows:

$$\%\ e.e = \frac{\text{weight of drug in nanoparticles after incorporation}}{\text{weight of drug fed initially before incorporation}} \times 100\%$$

2.3.8 Solubility determination of drugs before (pure drug) and after loading on CdS and NiO nanoparticles method:

A widely spread method to determine the equilibrium solubility of drug molecules is saturation shake-flask method. An excess amount of pure CLA (10 mg/mL), pure PTX (0.1 mg/mL) and an equivalent amount of each drug loaded CdS and NiO nanoparticles were dispersed separately in phosphate buffer pH 7.4 containing stoppered flask in water bath at 37°C and stirred for 48 hours. After 48 hours the undissolved material was filtered and the concentration of dissolved drug was quantified using UV-Visible spectrophotometer at the specified λ max of each drug in triplicate [145, 146].

2.3.9 Antibacterial activity test of clarithromycin loaded on CdS and NiO nanoparticles method:

The antibacterial activity of clarithromycin loaded CdS and NiO nanoparticles each separately was compared with pure CLA as well as with blank CdS and NiO nanoparticles. Each sample was tested against two types of gram +ve bacteria (*Staphylococcus aureus* and *Streptococcus pyogen*) and two types of gram –ve bacteria (*Serratia marcescens* and *Klebsiella oxytoca*) using a concentration of 100 µg/mL of pure CLA and an equivalent concentration of CLA loaded with CdS and NiO nanoparticles as well as blank CdS and NiO nanoparticles. The samples were dissolved using dimethylsulfoxide (DMSO) as a solvent and cultured in Muller Hinton agar for 24 h at 37°C[104, 147].

2.3.10 Cytotoxic activity of paclitaxel loaded on CdS and NiO nanoparticles method:

The cytotoxic activity of paclitaxel loaded on CdS and NiO nanoparticles, as well as the blank CdS and NiO nanoparticles was perform by Centre for Natural Product Research and Drug Discovery in the University of Malaya in Malaysia country using the following procedures:

- **Cell culture:**

The human cancer breast cell line (MCF-7) and human normal mammary epithelial cell line (MCF-10A) were grown each separately in Dulbecco modified Eagle's medium (DMEM) with 10% (v/v) heat-inactivated newborn calf serum and antibiotics (100 mg/mL of streptomycin and 100 U/mL of penicillin) at 37°C in a humidified atmosphere containing 5% CO_2 [148].

- **MTT assay:**

MCF-7 cells and MCF-10A cells were seeded separately in 96-well plate (0.8×10^4 cells/well) in triplicate and incubated for 24 h to be attached to the plates. After incubation for 24 h, cells were treated with increasing concentrations (2.5, 5, 10, 20 nM) of pure paclitaxel, paclitaxel loaded CdS and NiO nanoparticles and blank CdS and NiO nanoparticles for 24, 48 and 72 h, respectively. After respective incubation periods, 20 µL (5 mg/mL) of MTT (3-(4,5 Dimethylthiazol-2-yl)-2,5-Diphenyltetrazolium Bromide) was added to each well and incubated for 4 h at 37°C. Then the formazan crystals formed by the viable cells were dissolved by the addition of 200 µL from DMSO to each well and the color intensity value of the processed cells was measured at 550 nm that present the cell survival percentage in corresponding wells in contrast with their respective control.

2.5. Statistical analysis:

All the experiments were conducted in triplicate. The results of quantitative data obtained from antibacterial and antitumor activity of clarithromycin and paclitaxel respectively were analyzed using one-way and two-way ANOVA tests as well as Student t-test was used for clarithromycin quantitative data comparison for *in-vitro* release, the results were expressed as mean ± standard deviation. Statistical analysis was performed using the statistical package SPSS for windows (version 13, SPSS Inc., Chicago, IL, USA). The statistical significance for each test a *P* value of less than 0.05 was adopted[153, 154].

Chapter Three

3. Results and Discussions:

3.1 Determination of drugs melting point (m.p):

Melting points of clarithromycin and paclitaxel were used to characterize drugs and determine their purity and they were 218-220°C for CLA and 215-217°C for PTX, which are consistent to the reported values (220°C for clarithromycin and 217C°for paclitaxel) in USP-NF indicating a high degree of purity of the drugs[120].

3.2 Preparation of cadmium sulfide (CdS) and nickel oxide (NiO) metallic nanoparticles:

Cadmium sulfide (CdS) nanoparticles precipitated as hexagonal orange-yellow powder as shown in equation (3-1)[156]:

$$Na_2S + Cd(CH_3COO)_2 \rightarrow CdS\ (NPs)\downarrow + 2CH_3COONa$$

Colorless crystals Orange precipitate

Equation (3-1): Preparation of cadmium sulfide (CdS) nanoparticles

While nickel oxide nanoparticles (NiO) were black, indicating NiO (which adopts the NaCl structure, with octahedral Ni(II) and O^{2-} sites) are non-stoichiometric , as displayed in equation (3-2)[156]:

$$Ni(NO_3)_2 + 2NH_4OH \rightarrow NiO\ (NPs)\downarrow + 2NH_4NO_3 + H_2O$$

Emerald green hygroscopic solid Black precipitate

Equation (3-2): Preparation of nickel oxide (NiO) nanoparticles

3.3 Loading of drugs on the prepared CdS and NiO nanoparticles:

Clarithromycin (white powder) and paclitaxel (white powder) are loaded on cadmium sulfide (orange powder) and nickel oxide (black powder) nanoparticles by physical complexation between them without any chemical reaction, in which a yellow powder was obtained for both CLA and PTX loaded on CdS nanoparticles as a new compound and grey powder was resulted due to the complexation of the drugs with NiO nanoparticles.

Furthermore loading of CLA and PTX on the prepared CdS/NiO nanoparticles was approved according to the characterization techniques used (FTIR, SEM, zeta potential, XRD, TGA, DSC and AFM).

3.4 Determination of calibration curve of drugs

The calibration curve of clarithromycin (figure 3- 1) was obtained from the plotting of absorbance versus concentration, where it is found to obey Beer's law within the used range of concentrations. The same result was obtained for paclitaxel (figure 3- 2) and it is also obeys Beer's law.

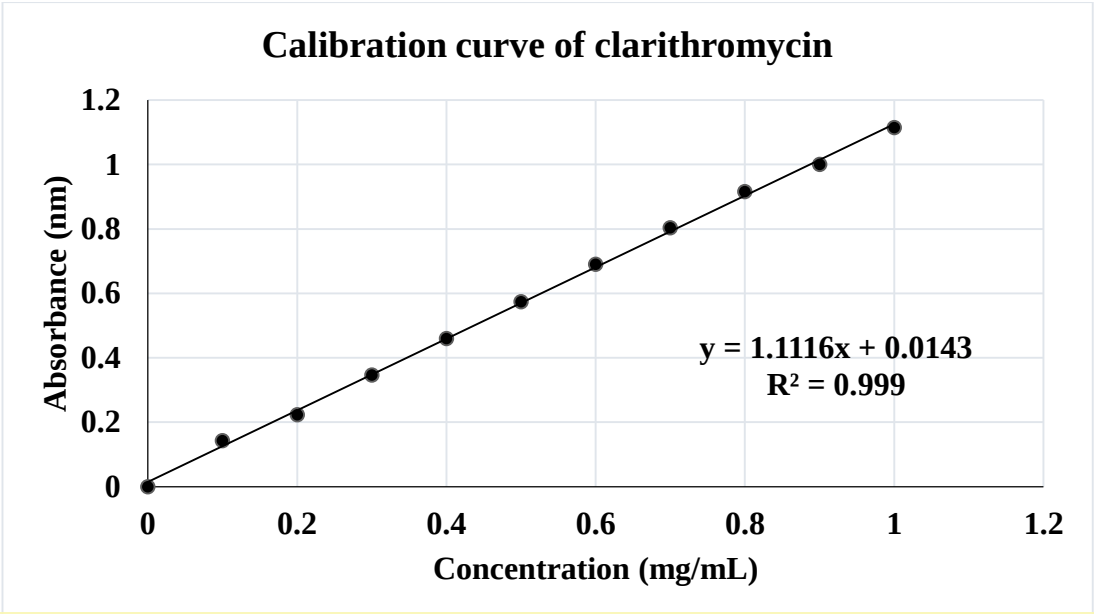

Figure (3-1): Calibration curve of clarithromycin in phosphate buffer (pH 7.4)

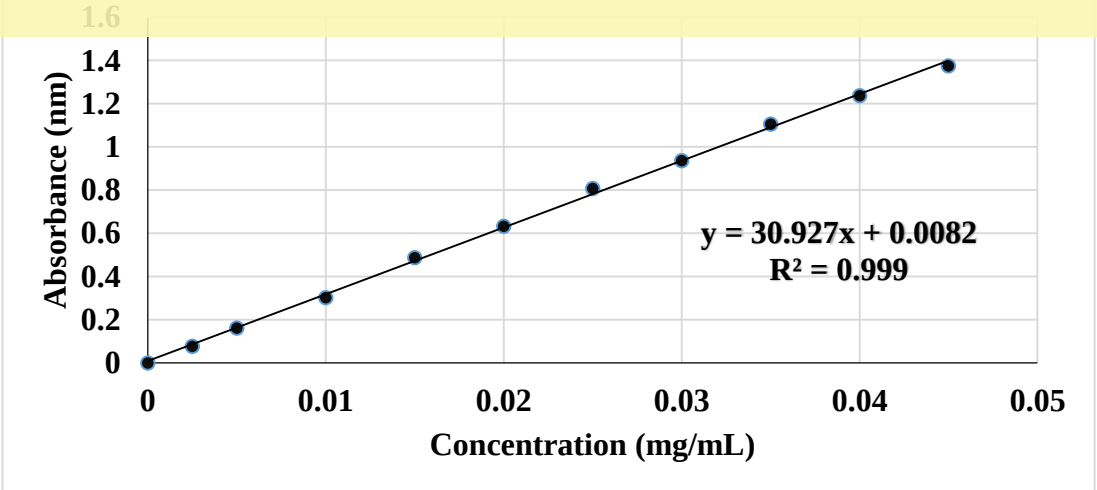

Figure (3-2): Calibration curve of paclitaxel in phosphate buffer (pH 7.4)

3.5 Characterization of clarithromycin and paclitaxel loaded on CdS and NiO nanoparticle:

3.5.1 Fourier Transform Infra-Red (FTIR):

The FTIR spectrum of pure clarithromycin (figure 3-3 A) displayed bands at the range (3618 – 3420 cm^{-1}) attributed to multiple hydroxyl groups (OH) in the backbone structure of CLA. The bands at 1722 cm^{-1} and 1697 cm^{-1} assign to the two carbonyl groups of ester and ketone respectively, while the aliphatic groups (CH_3 and CH_2) appeared in the expected area for the stretching (asymmetrical and symmetrical) in the range (2781-2840 cm^{-1}), while the finger prints area showed the bending bands of the drug. The FTIR spectra of CLA loaded CdS and NiO nanoparticles (figures 3-3 B and C) showed the same functional groups of pure CLA with small shifting.

The FTIR spectrum of pure paclitaxel (figure 3-4 A) showed peaks at 3510 cm^{-1} and 3439 cm^{-1} can be attributed to stretching of hydroxyl group (OH) in the PTX molecule. The bands at 3063 cm^{-1} and 3021 cm^{-1} assign to aromatic CH stretching, while the carbonyl groups appear as multiband due to the different environments of these groups at 1712, 1700 and 1647 cm^{-1}. The FTIR spectra of PTX loaded on CdS and NiO nanoparticles (figures 3-4 B and C) showed the same functional groups of pure PTX with small shifting.

The FTIR spectra showed the same main functional groups of CLA and PTX before and after loading on CdS and NiO nanoparticles (figures 3-3, 3-4) with small shifting, indicating physical complexes formation between drug and metal nanoparticles rather than chemical interaction [139, 157-159].

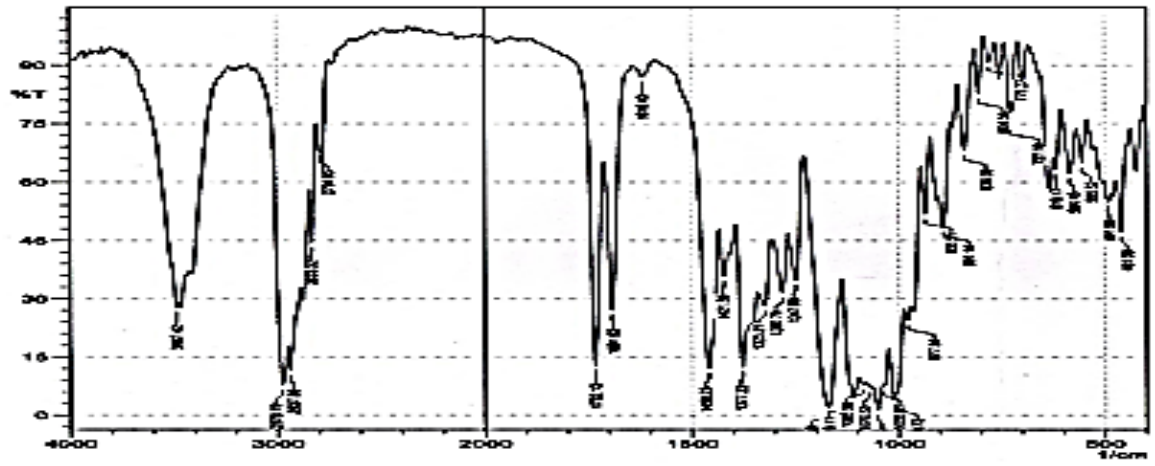

A

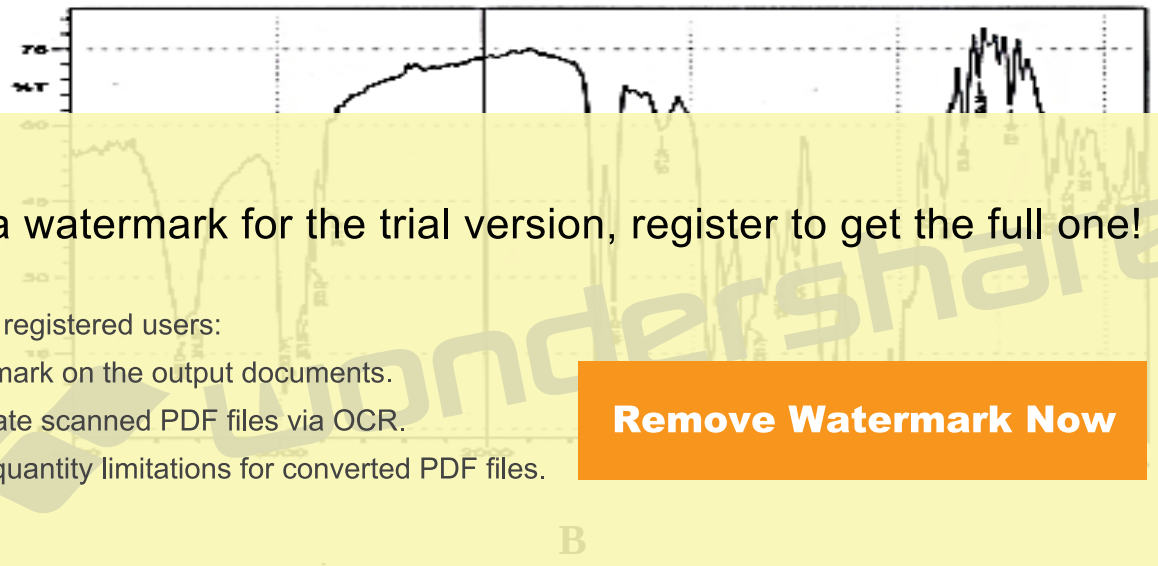

B

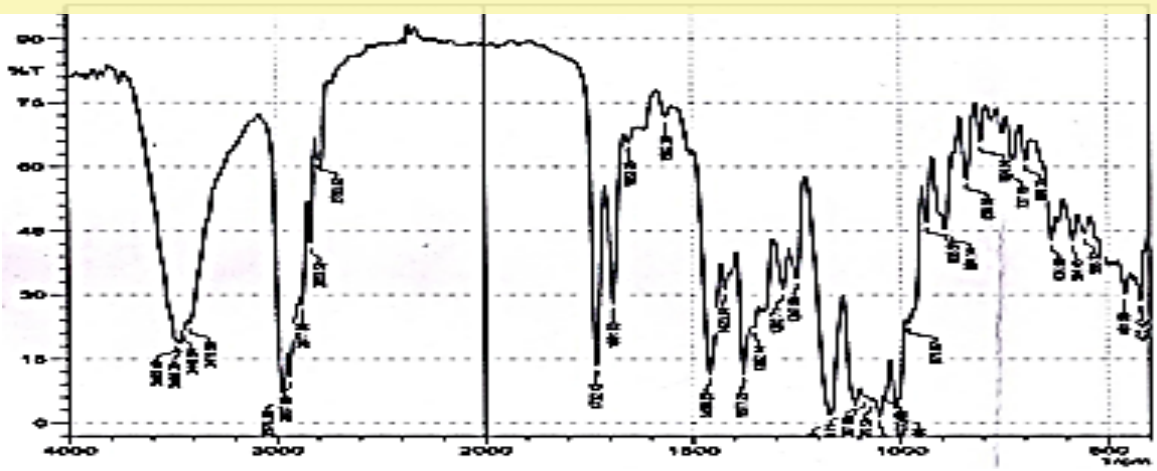

C

Figure (3-3): FTIR spectra of (A) pure clarithromycin, (B) CLA loaded CdS nanoparticles and (C) CLA loaded NiO nanoparticles.

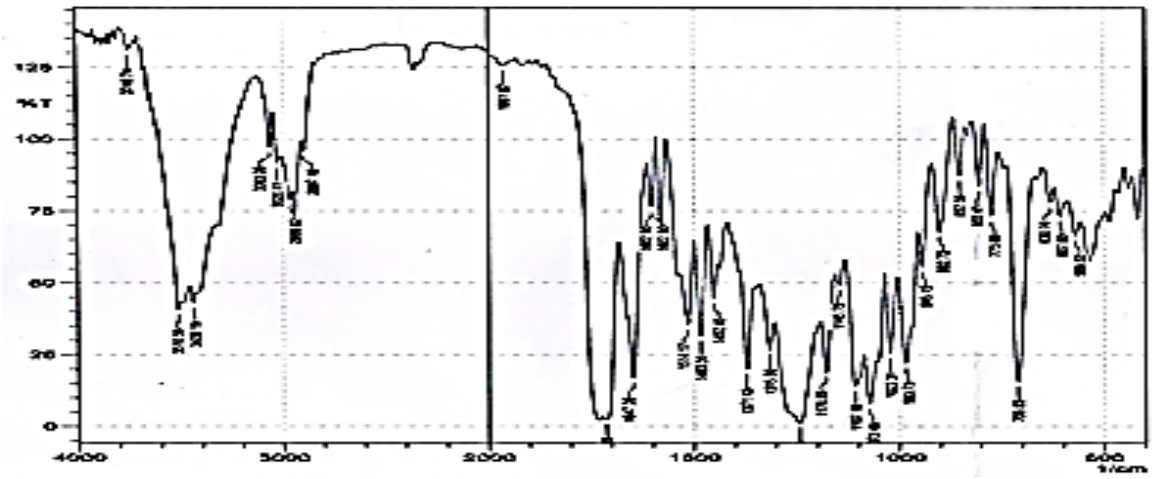

A

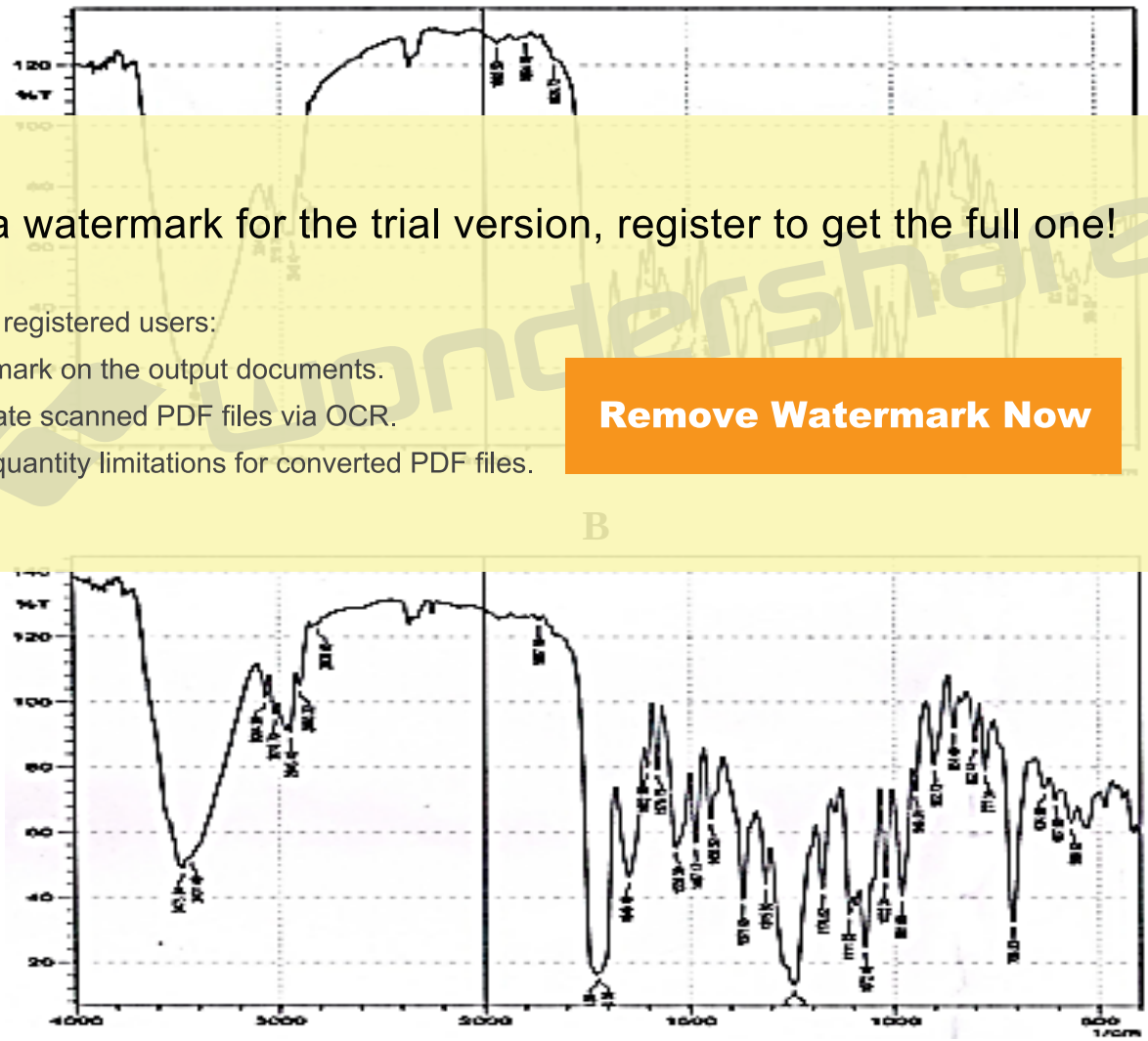

B

C

Figure (3-4): FTIR spectra of (A) pure paclitaxel, (B) PTX loaded CdS nanoparticles and (C) PTX loaded NiO nanoparticles.

3.5.2 Scanning Electron Microscopy (SEM):

Scanning electron microscope instrument is used to determine the shape, size and morphologies of formed nanoparticle to give high resolution images of the sample surface by magnifying images up to 200.000 times[160]. The scanned electronic microscope (SEM) images (figure 3-5) of blank CdS and NiO nanoparticles and pure drugs provide informations about their particle size and morphology. The images showed that blank CdS and NiO nanoparticles had fine particles and homogenous distribution more than the particles of pure drugs as well as more regular shape with sharp edges. The SEM images of clarithromycin loaded on CdS / NiO nanoparticles (figures 3-5 E and G) showed different shape and size in comparison with the pure CLA (figure 3-5 C) and blank CdS and NiO nanoparticles (figures 3-5 A and B) where they showed better distribution, more compact and higher particle size with smoother surfaces that indicate the loading of CLA on the surface of CdS and NiO nanoparticles [147, 161]. The same changes were observed on the morphology of ultrasonicated after loading PTX (figures 3-5 F and H), since they appeared more compact with smooth like surfaces and higher particle size than that of free PTX (figure 3-5 D) and blank nanoparticles (figures 3-5 A and B) with flakes like shape for PTX-NiO complex (figure 3-5 H) referring to surface loading of PTX with the nanocarriers [158, 162, 163].

3.5.3 Zeta Potential (ξ):

Zeta (ξ) potential is the electrostatic potential that exists at the particle shear plane and it is related to surface charge as well as the local environment of the particle[164]. Zeta potential measurement was performed for blank CdS and NiO nanoparticles (figure 3-6) as well as for pure clarithromycin and paclitaxel before and after loading on CdS and NiO nanoparticles(figures 3-7 and 3-8) as an indicator of their stability in suspension. The zeta potential values are summarized in table (3-1), indicating the good stability of CLA loaded on CdS and NiO nanoparticles (below -30 mV). The zeta potential of PTX loaded on CdS and NiO nanoparticles displayed excellent stability (below -60 mV). The higher electric surface charge will prevent the aggregation of drug loaded metal nanoparticles in buffer solution due to strong repellent forces between particles[33,165].

A B C D E F G H

Figure (3-5): SEM images of (A) blank CdS nanoparticles, (B) blank NiO nanoparticles, (C) pure clarithromycin, (D) pure paclitaxel, (E) CLA loaded CdS nanoparticles, (F) PTX loaded CdS nanoparticles, (G) CLA loaded NiO nanoparticles and (H) PTX loaded NiO nanoparticles.

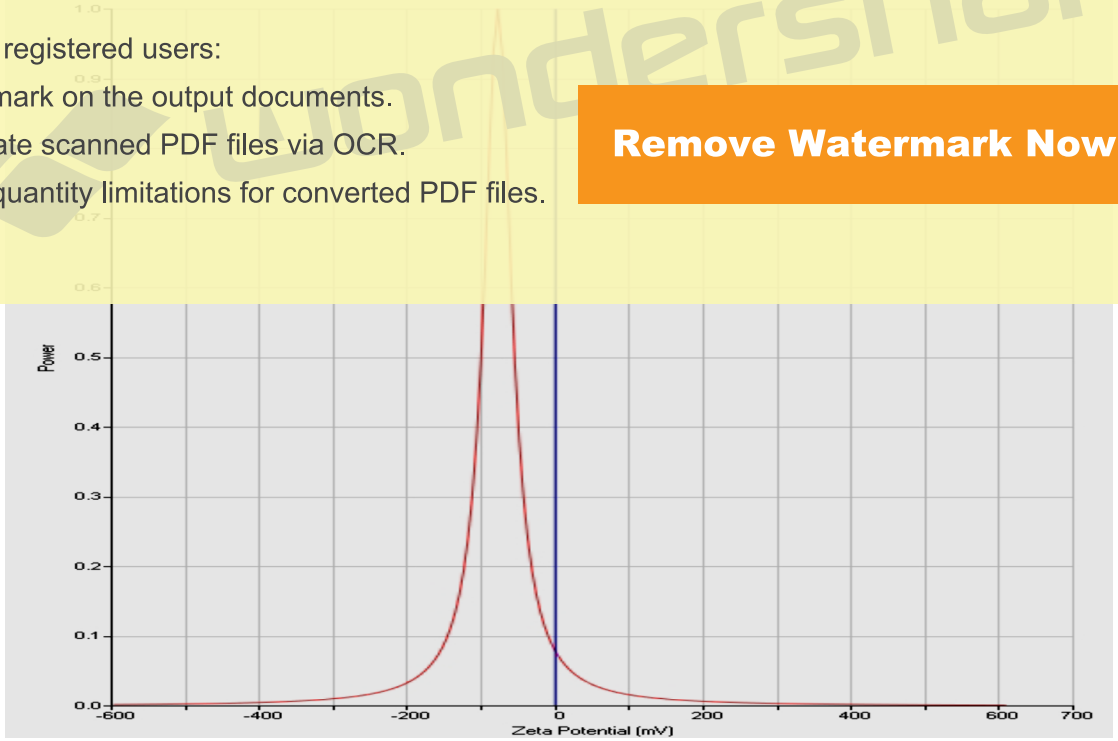

B

Figure (3-6): Zetapotential monographs of (A) blank CdS nanoparticles and (B) blank NiO nanoparticles.

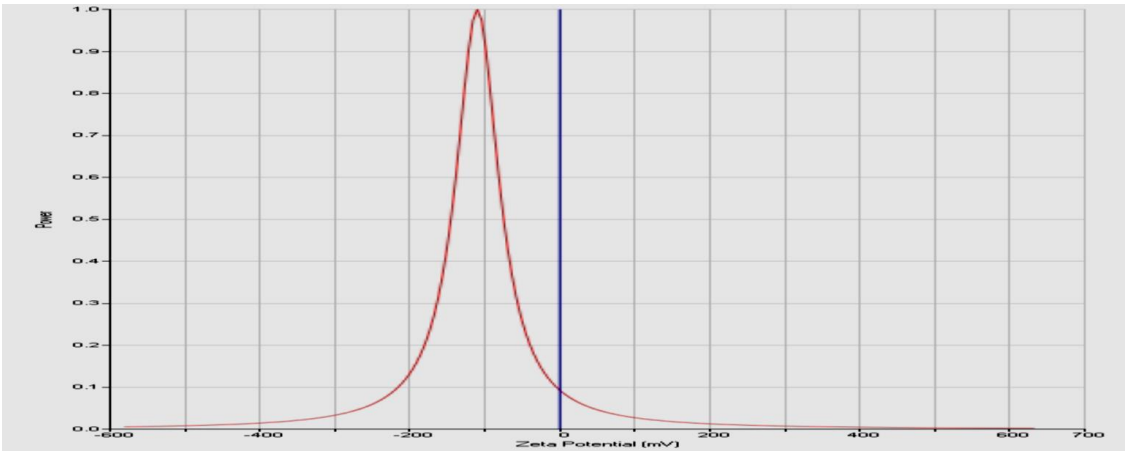

A

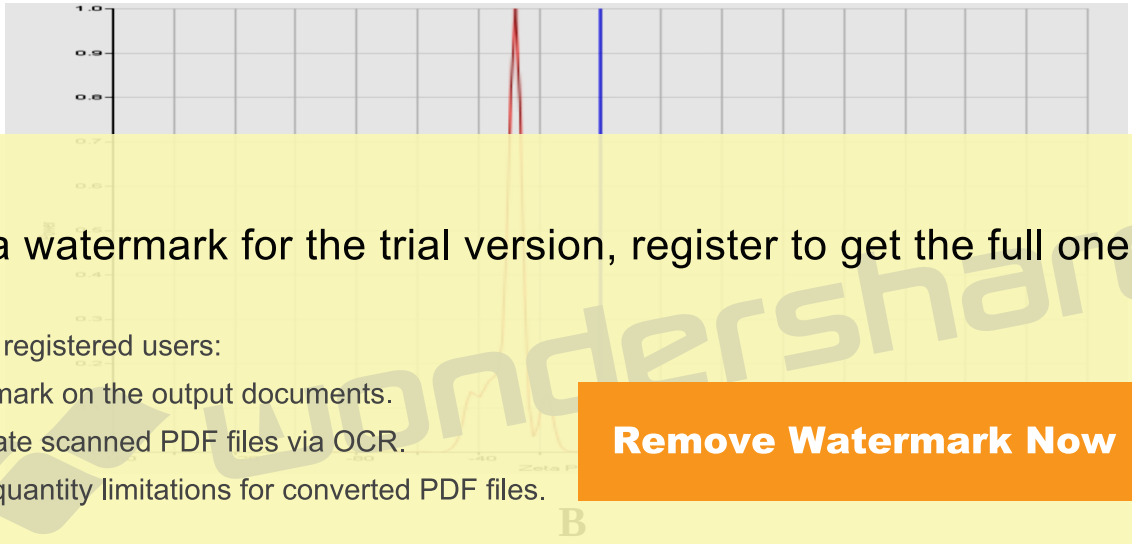

B

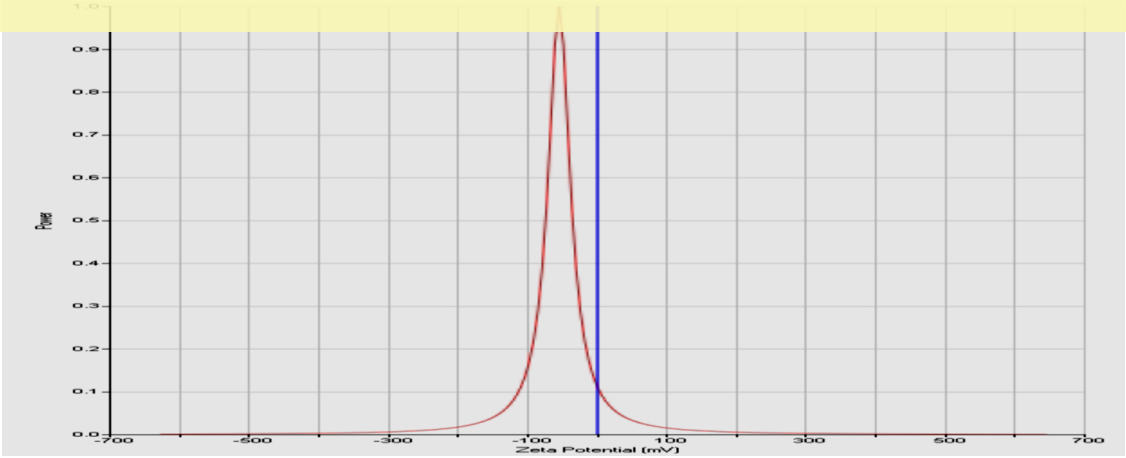

C

Figure (3-7): Zeta potential monographs of (A) pure clarithromycin, (B) CLA loaded CdS nanoparticles and (C) CLA loaded NiO nanoparticles.

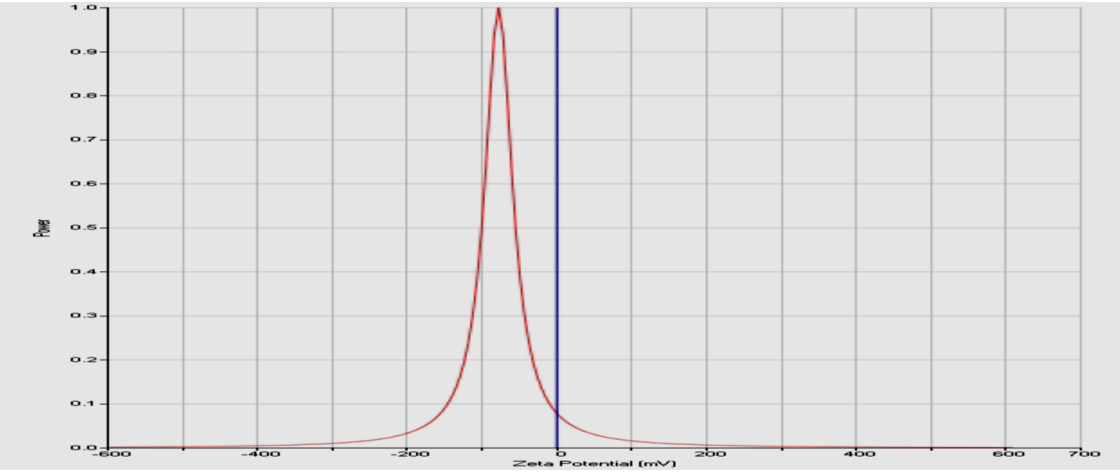

A

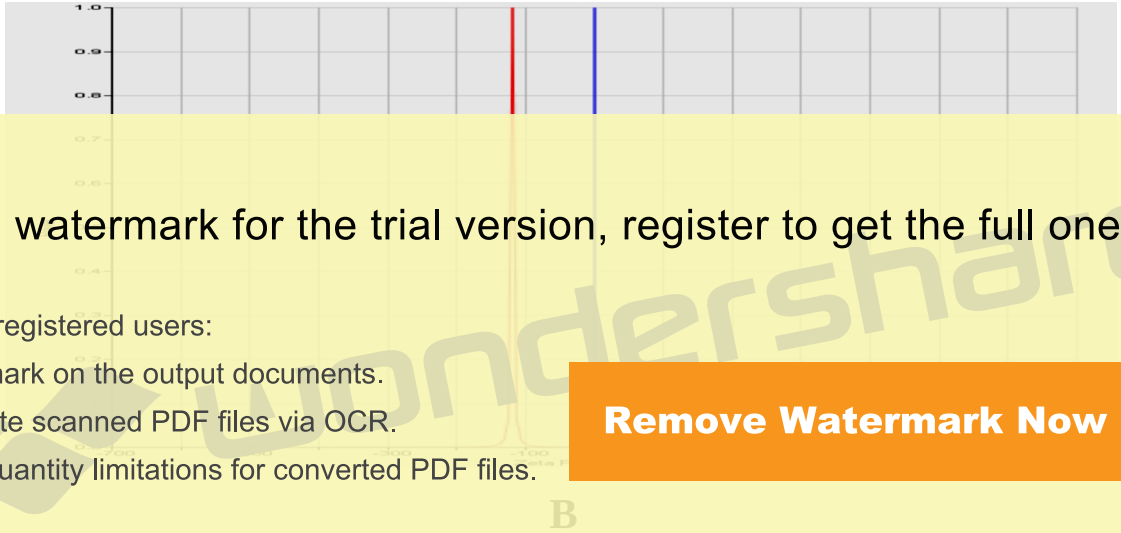

B

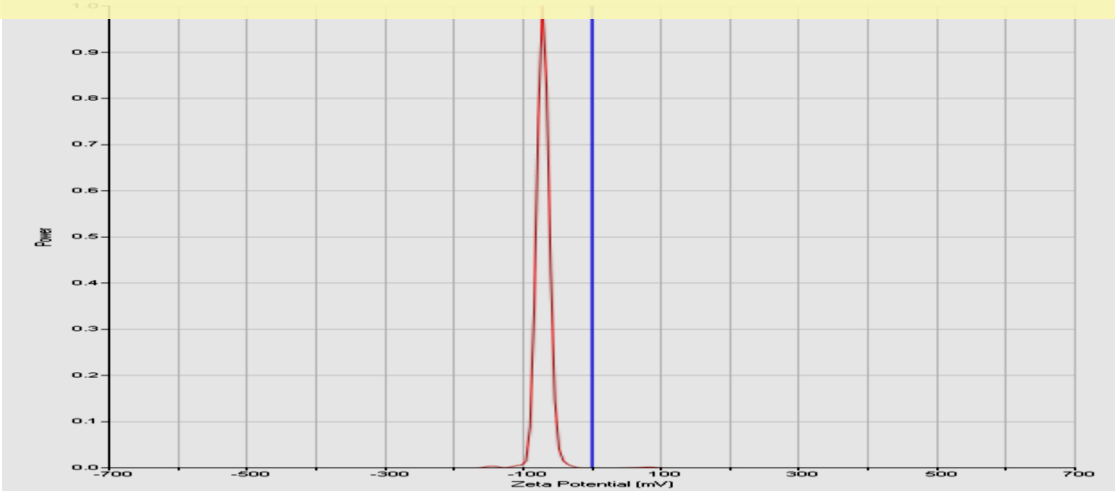

C

Figure (3-8): Zeta potential monographs of (A) pure paclitaxel, (B) PTX loaded CdS nanoparticles and (C) PTX loaded NiO nanoparticles.

Table (3-1): Zeta potential of CdS and NiO nanoparticles before and after loading with clarithromycin and paclitaxel as well as pure drugs in phosphate buffer (pH 7.4).

Sample	Zeta Potential (mV) ± SD	Mobility (μ/s)/(V/cm) ±SD	Frequency (Hz) ±SD	Frequency Shift (Hz) ±SD
Cds nanoparticles	-152.45 ± 4.8	- 3.03 ± 0.10	223.44 ± 0.62	- 27.04 ± 0.95
NiO nanoparticles	- 90.82 ± 4.1	-1.80 ± 0.08	235.03 ± 0.64	-16.84 ± 1.71
Pure clarithromycin	-119.67 ± 8.23	- 2.38 ± 0.16	230.45 ± 1.26	-19.25 ± 2.1
Clarithromycin loaded CdS nanoparticles	- 32.54 ± 2.21	-0.65 ± 0.04	232.04 ± 0.81	-16.70 ± 1.21
Clarithromycin loaded NiO nanoparticles	- 59.58 ± 6.94	-1.18 ± 0.14	240.65 ± 1.10	-7.68 ± 1.83
Pure paclitaxel	- 77.76 ± 4.08	-1.54 ± 0.08	237.13 ± 0.67	-13.98 ± 1.57
Paclitaxel loaded CdS nanoparticles	-117.90 ± 8.95	- 2.34 ± 0.18	231.57 ± 1.44	-18.84 ± 1.69
Paclitaxel loaded NiO nanoparticles	-72.93 ± 2.85	-1.45 ± 0.06	238.44 ± 0.46	-11.78 ± 1.65

Data represent mean ± SD (n=3).

3.5.4 X-Ray Diffraction (XRD):

The X-ray diffraction technique is the most important characterization tools used in solid state chemistry for the determination of shape, size and lattice parameter (crystalinity). The X-Ray Diffraction (XRD) spectrum of blank CdS nanoparticles (figure 3-9 A) displayed neither sharp nor intense peaks indicating highly amorphous property, while for blank NiO nanoparticles (figure 3-9 B) displayed highly crystalline multiple intense diffraction peaks. The XRD spectrum of pure clarithromycin (figure 3-10 A) displayed numerous narrow strongly intense diffraction peaks indicating its highly crystalline structure, while the XRD spectrum of CLA loaded CdS and NiO nanoparticles (figures 3-10 B and C) showed less intense and less characterized sharp diffraction peaks with decreased multiplicity in comparison with the XRD spectrum of pure CLA indicating a more amorphous compound. The highly stable crystalline structure requires higher [illegible] and will show [illegible]

The XRD spectrum of pure paclitaxel (figure 3-11 A) displayed many characterized intense multiple diffraction peaks indicating PTX crystalline structure, while the XRD spectrum after loading of PTX on CdS and NiO nanoparticles (figures 3-11 B and C) displayed decreased multiplicity of sharp diffraction peaks with lower intensities (except some characteristic diffraction peaks of pure PTX) referring to decreased crystalline property of PTX loaded nanocarriers in comparison with the pure PTX, although the PTX-CdS and PTX-NiO complexes showed decreased crystallinity this did not improve the solubility of the drug [157, 158, 168].

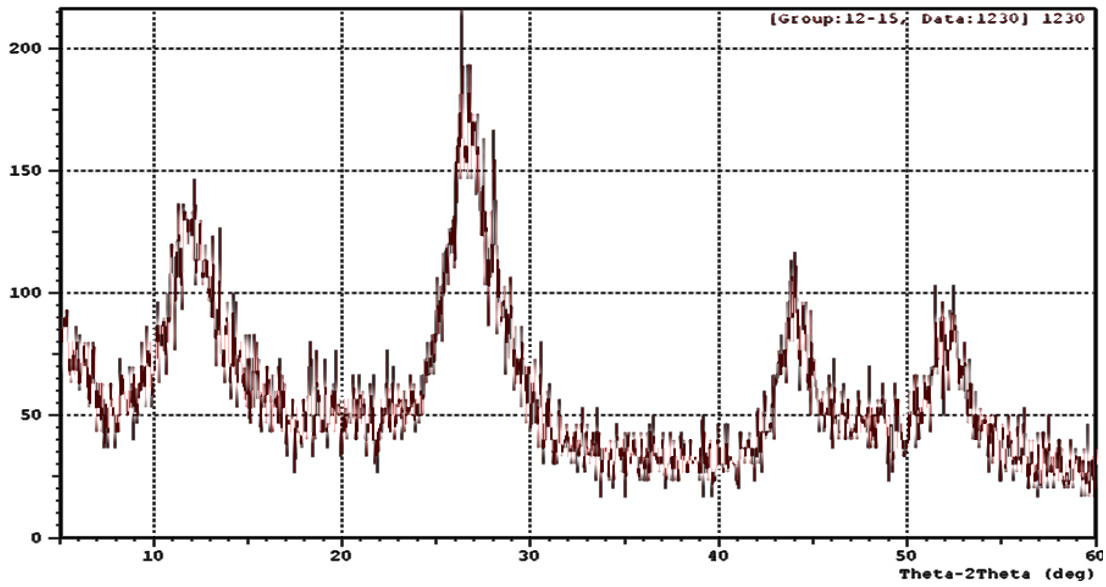

A

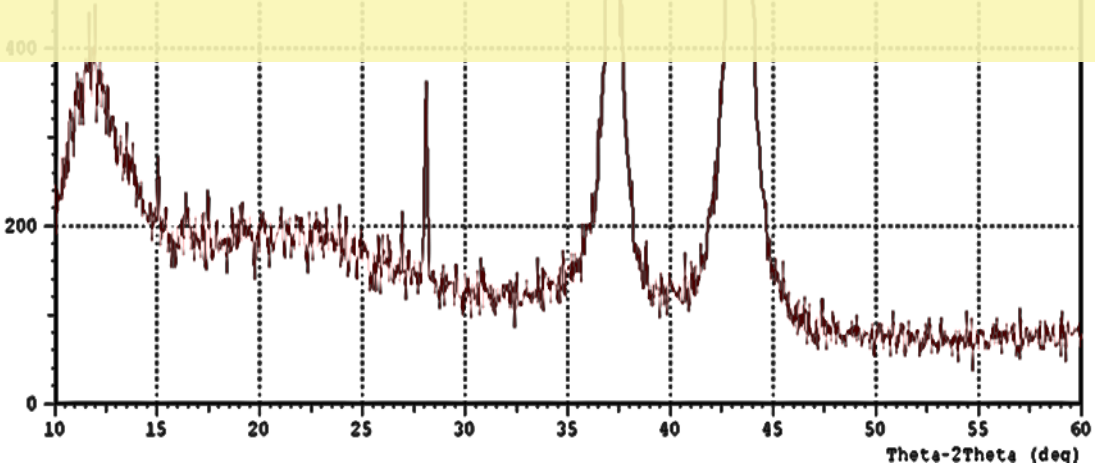

B

Figure (3-9): XRD spectra of (A) blank CdS nanoparticles and (B) blank NiO nanoparticles.

Figure (3-10): XRD spectra of (A) pure clarithromycin CLA, (B) CLA loaded CdS nanoparticles and (C) CLA loaded NiO nanoparticles.

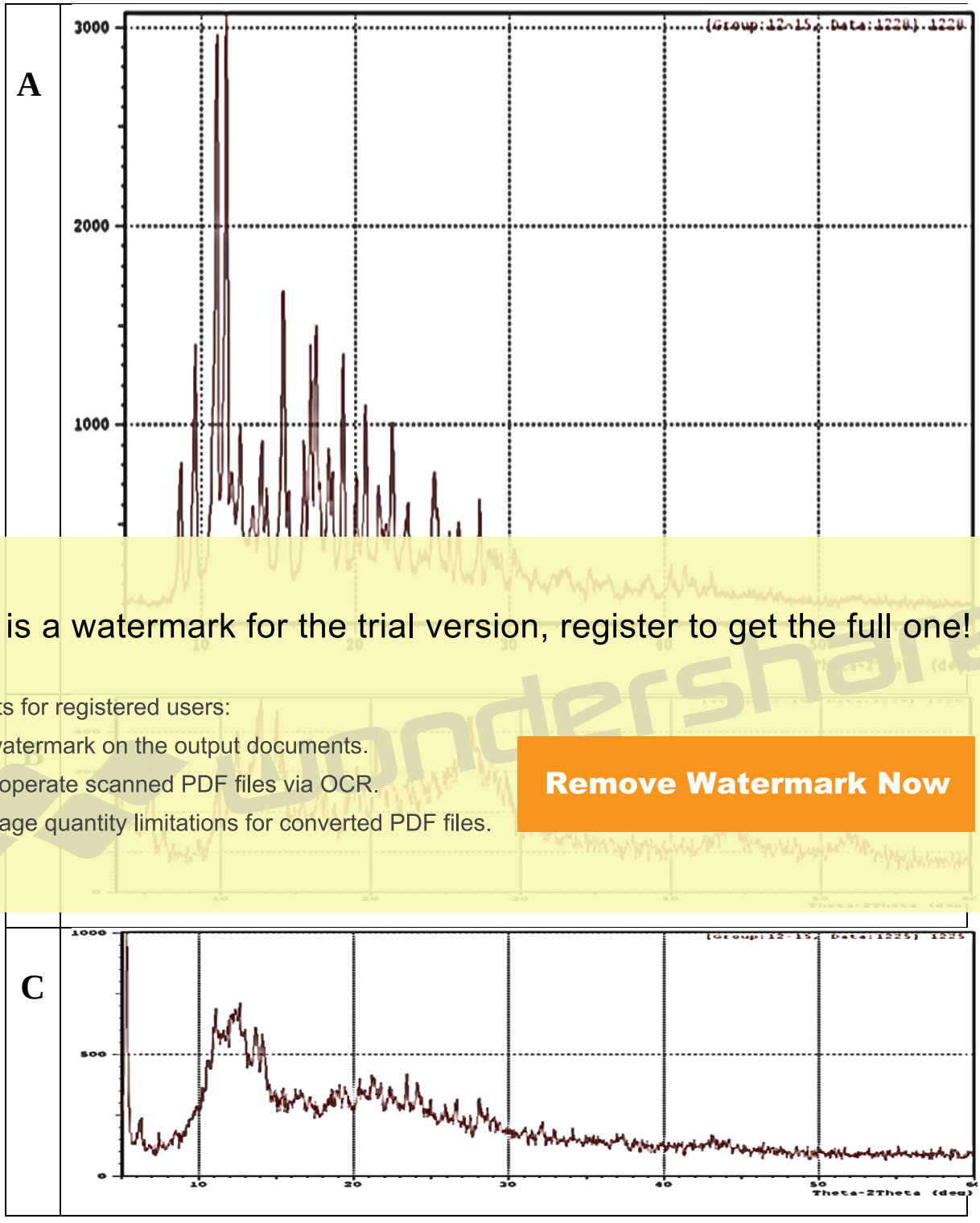

Figure (3-11): XRD spectra of (A) pure paclitaxel, (B) PTX loaded CdS nanoparticles and (C) PTX loaded NiO nanoparticles.

3.5.5 Thermo Gravimetric Analysis (TGA):

Thermal analysis measurement was carried out from (0 – 400 °C) with heating rate 5 °C/min to evaluate thermal behavior of blank CdS and NiO nanoparticles, pure drugs (pure clarithromycin and pure paclitaxel) and drugs loaded CdS and NiO nanoparticles. Thermal analysis of the prepared blank CdS nanoparticles (figure 3-12 A) showed a degradation weight loss peak at 398.8°C, while the TGA of blank NiO nanoparticles (figure 3-12 B) showed its degradation peak at 399°C. Thermal analysis of pure clarithromycin (figure 3-13 A) showed a peak at 279°C, while TGA spectra of CLA after loading with CdS and NiO nanoparticles (figures 3-13 B and C) showed thermal weight loss peaks at 255.5°C and 276°C respectively, that is close to the peak of pure CLA (279°C) indicating surface loading of CLA on CdS and NiO nanoparticles. The peak of CLA loaded CdS nanoparticles at 255.5°C referring to partial decomposition (weight loss) of the drug followed by CdS for its degradation above this temperature, while CLA loaded NiO nanoparticles showed thermal peak at 276°C indicating loss of drug by melting followed by its decomposition above this temperature [169, 170].

Thermal analysis of pure paclitaxel (figure 3-14 A) showed sharp thermal weight loss peak at 230.9°C, while TGA spectra of PTX loaded CdS and NiO nanoparticles (figures 3-14 B and C) showed thermal weight loss peaks at 213.8°C and 229.6°C respectively, that is also close to the peak of pure PTX (230.9°C) indicating surface loading of PTX on CdS and NiO nanoparticles. Where thermal analysis of PTX loaded CdS nanoparticles showed broad weight loss thermal peak at 213.8°C that result from partial drug decomposition at this peak followed by stationary thermal stability without degradation of PTX-CdS complex indicating its thermal stability in comparison to drug and nanoparticles each alone[171].

Paclitaxel loaded NiO thermal analysis displayed two steps of weight loss by thermal effect, first thermal peak appears at 229.6°C indicating the melting followed by decomposition of PTX, while the second thermal peak appears at 359.8°C that may be resulted from degradation of most NiO nanoparticles[172, 173].

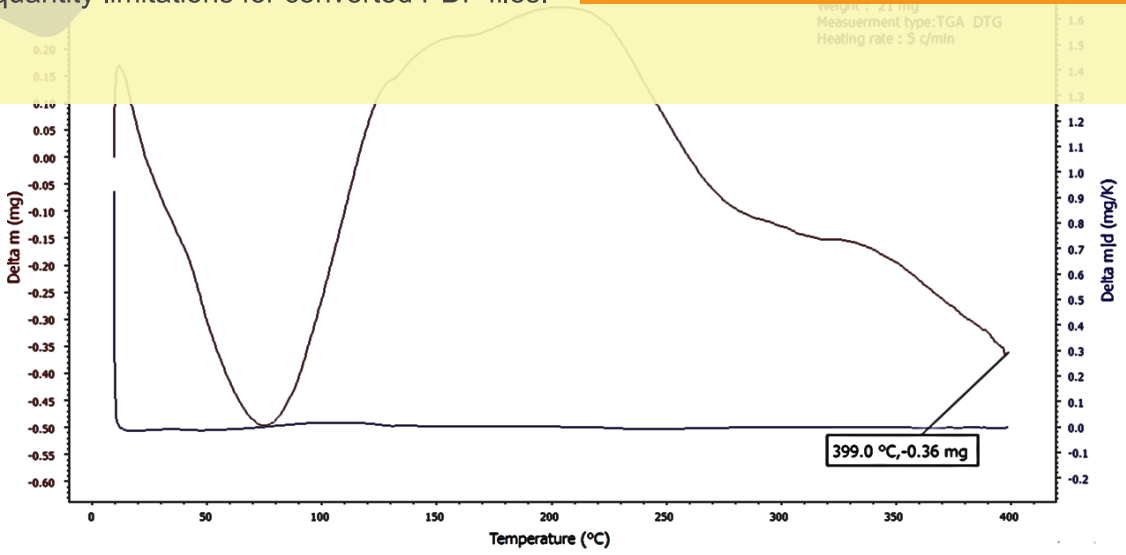

B

Figure (3-12): TGA spectra of (A) blank CdS nanoparticles and (B) blank NiO nanoparticles.

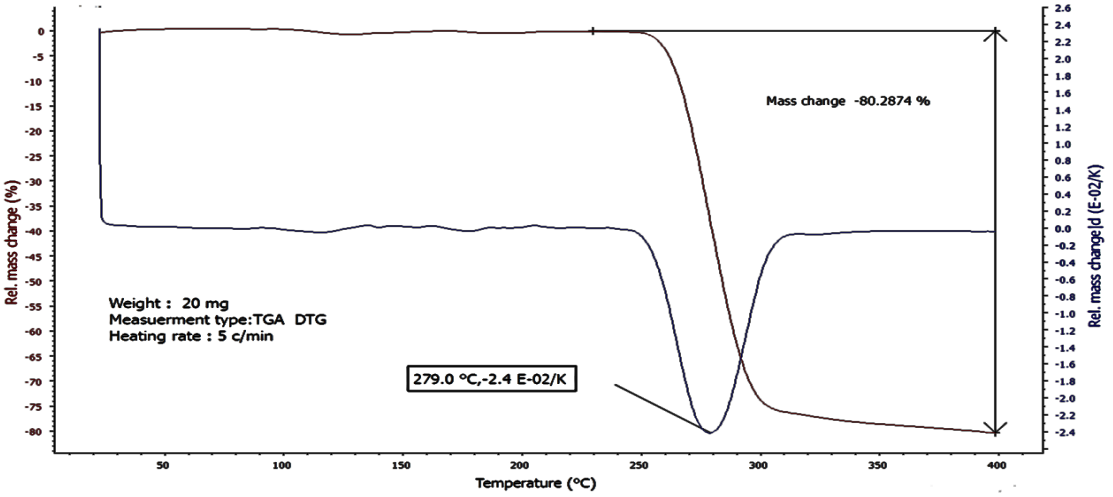

A

B

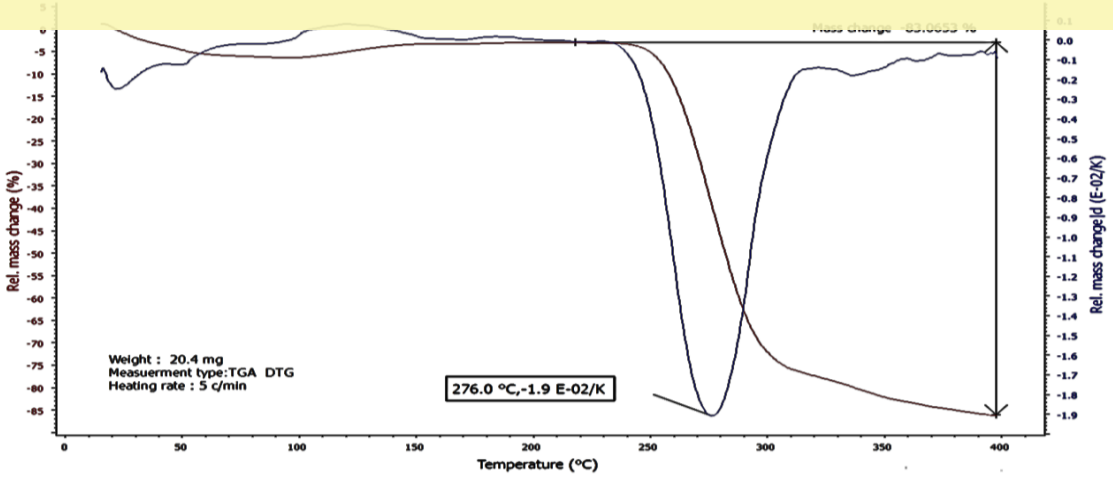

C

Figure (3-13): TGA spectra of (A) pure clarithromycin, (B) CLA loaded CdS nanoparticles and (C) CLA loaded NiO nanoparticles.

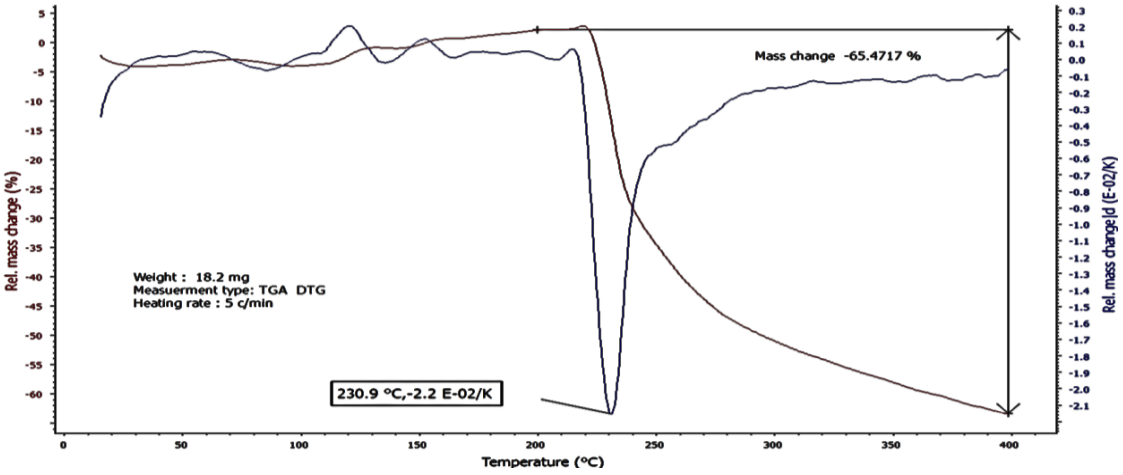

A

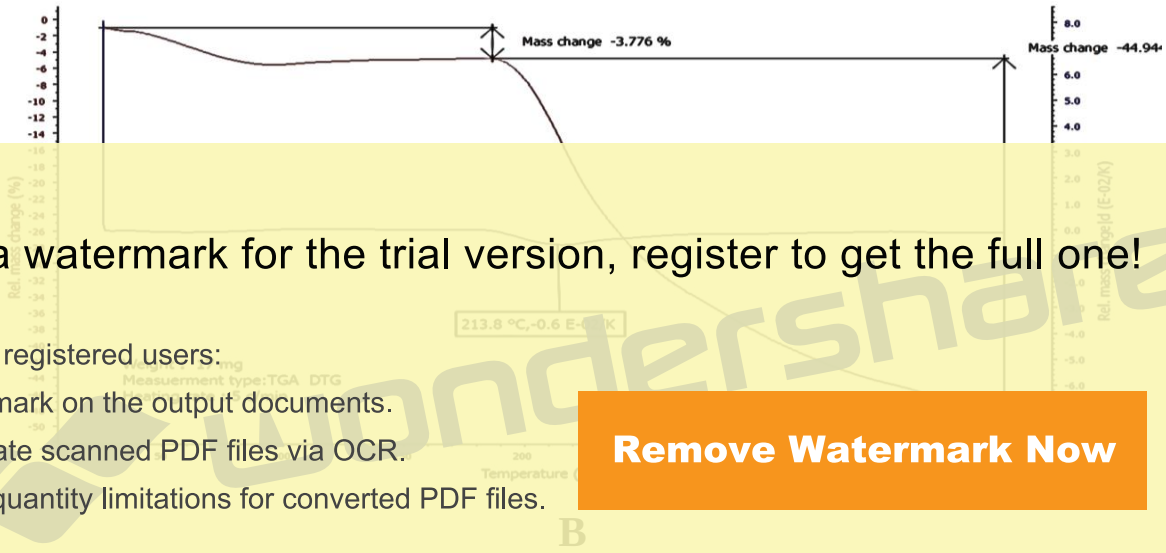

B

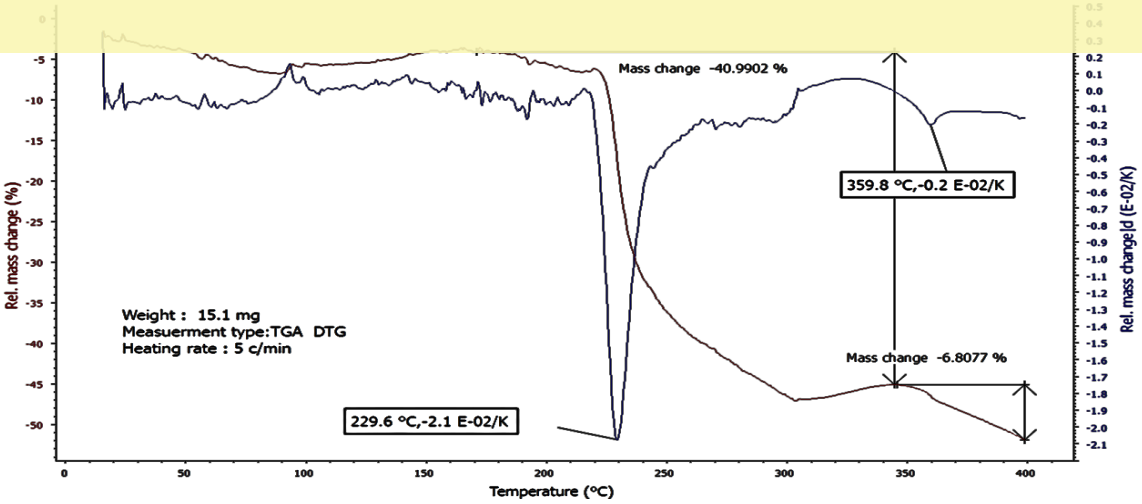

C

Figure (3-14): TGA spectra of (A) pure paclitaxel, (B) PTX loaded CdS nanoparticles and (C) PTX loaded NiO nanoparticles.

3.5.6 Differential Scanning Calorimetric (DSC):

Differential Scanning Calorimetric (DSC) analysis was carried out to characterize the physical state and phase transition of drugs[174]. Differential scanning calorimetric spectra of blank CdS and NiO nanoparticles (figure 3-15) displayed no sharp endothermic peak. The DSC spectrum of pure CLA (figure 3-16 A) displayed a sharp narrow intense endothermic peak at 228.58 °C that corresponds to the melting point of the drug indicating its crystallinity [161], while DSC spectrum of CLA loaded CdS nanoparticles (figure 3-16 B) showed small non-intense peak at 92.1°C that indicate the initiation of melting of the complex followed by a sharp intense endothermic peak at 223.07°C referring to melting of CLA. For CLA-NiO complex, DSC spectrum (figure 3-16 C) displayed sharp endothermic peak at 228.1°C that indicate melting and finally degradation of the compound. As a result, the DSC spectra of CLA loaded on CdS and NiO nanoparticles showed smaller [illegible] °C and 2[illegible] indication in its crystal[illegible] the drug loaded CdS / NiO nanoparticles were close to that of pure CLA, this may indicate surface loading of the drug[104, 161, 175, 176].

The DSC spectrum of pure paclitaxel (figure 3-17 A) showed sharp narrow endothermic peak at 217.65°C that is attributed to the melting of the drug indicating its crystallinity[177], while DSC spectrum for PTX-CdS complex (figure 3-17 B) showed wide broad non-sharp endothermic peak at 109°C that indicate the initiation of melting and another broad small endothermic peak at 165.04°C corresponding to further melting and degradation of PTX-CdS crystalline complex. The PTX-NiO complex (figure 3-17 C) showed DSC spectrum with multiple endothermic peaks that appeared as broad small peak at 163.8°C that indicate the initiation of melting, in addition to small intense peaks also appeared at 219.4, 245.54

and 256.68°C indicating a shifting of pure PTX melting peak within PTX-NiO complex. The DSC spectra of PTX loaded CdS and NiO nanoparticles showed more than one endothermic peak indicating more than one glass transmission temperature and altered lattice property [150, 178-180].

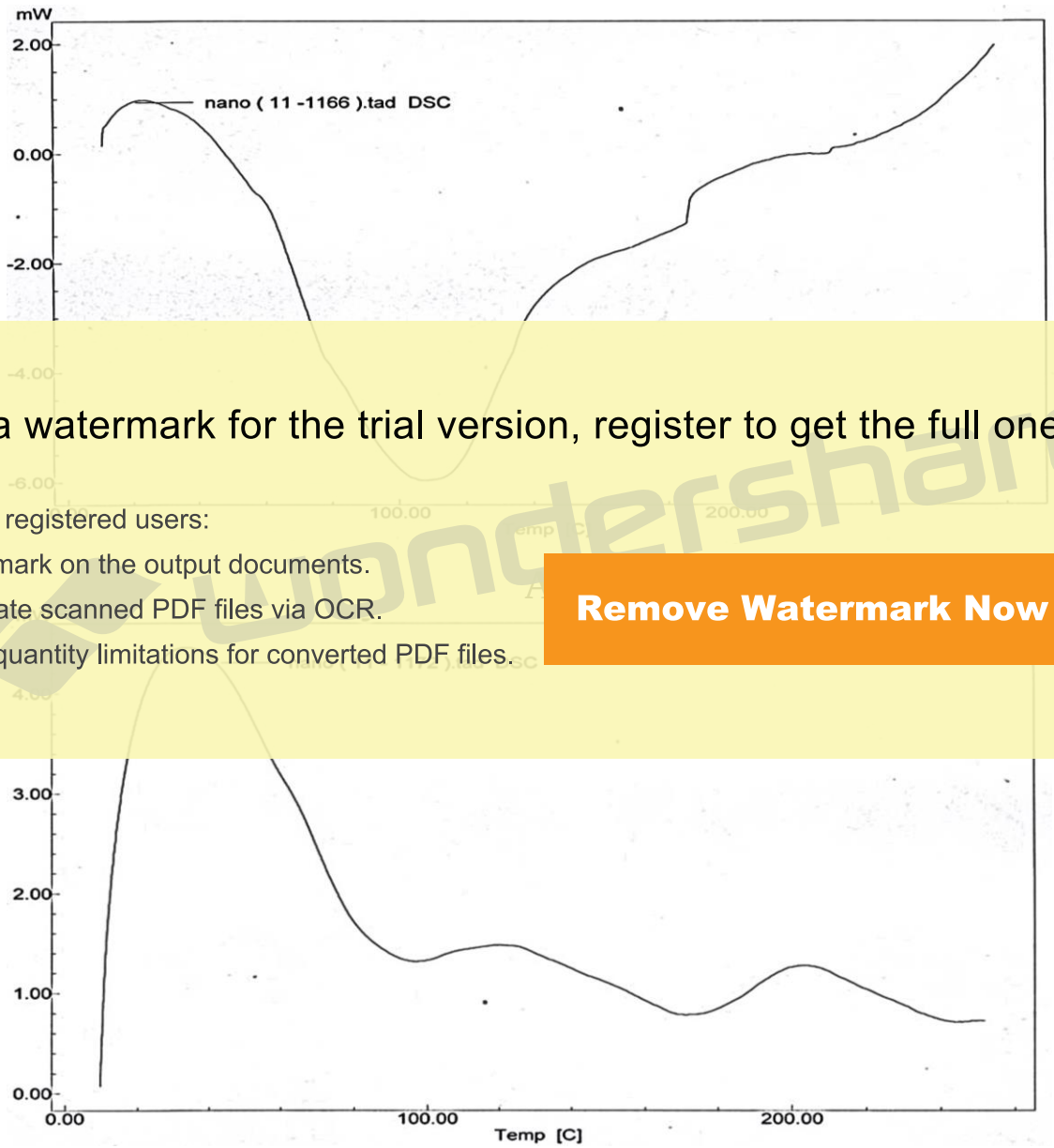

B

Figure (3-15): DSC spectra of (A) blank CdS nanoparticles and (B) blank NiO nanoparticles.

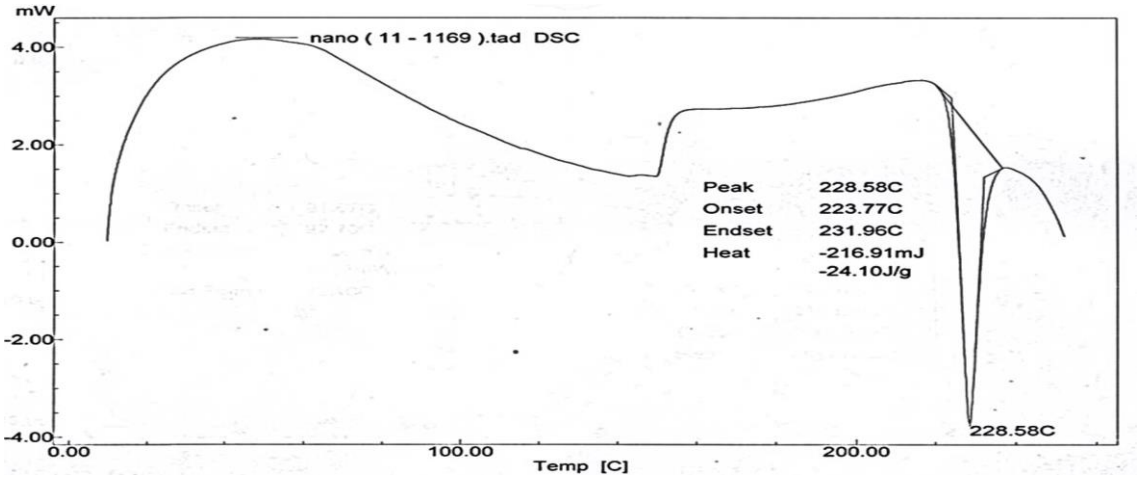

A

B

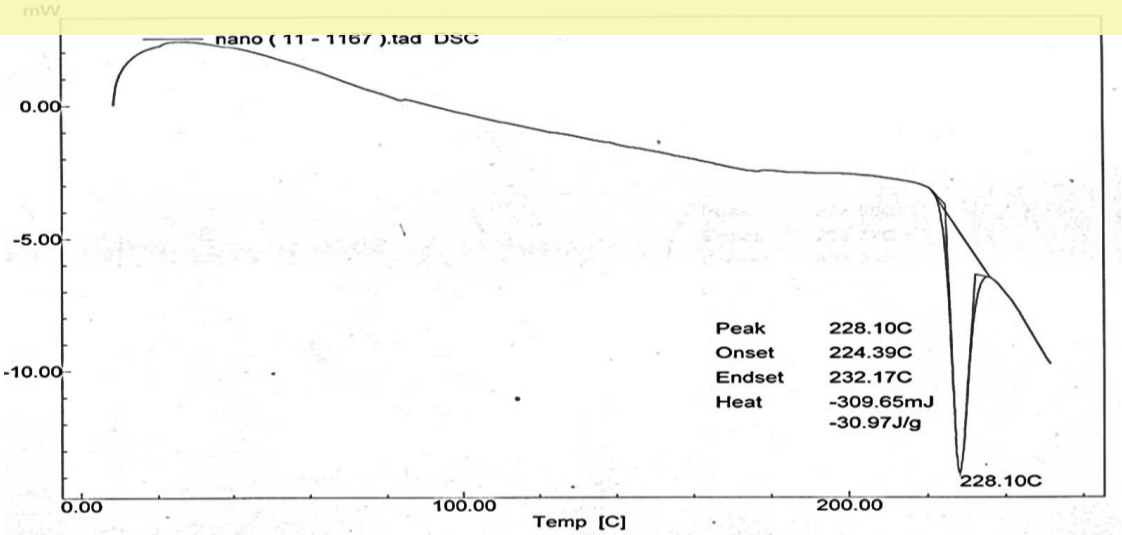

C

Figure (3-16): DSC spectra of (A) pure clarithromycin, (B) CLA loaded CdS nanoparticles and (C) CLA loaded NiO nanoparticles.

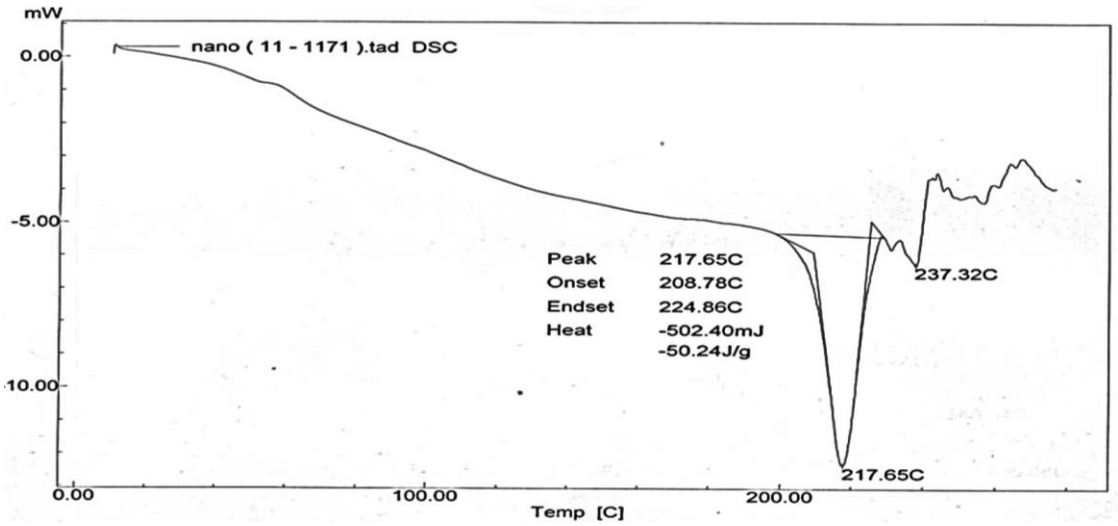

A

B

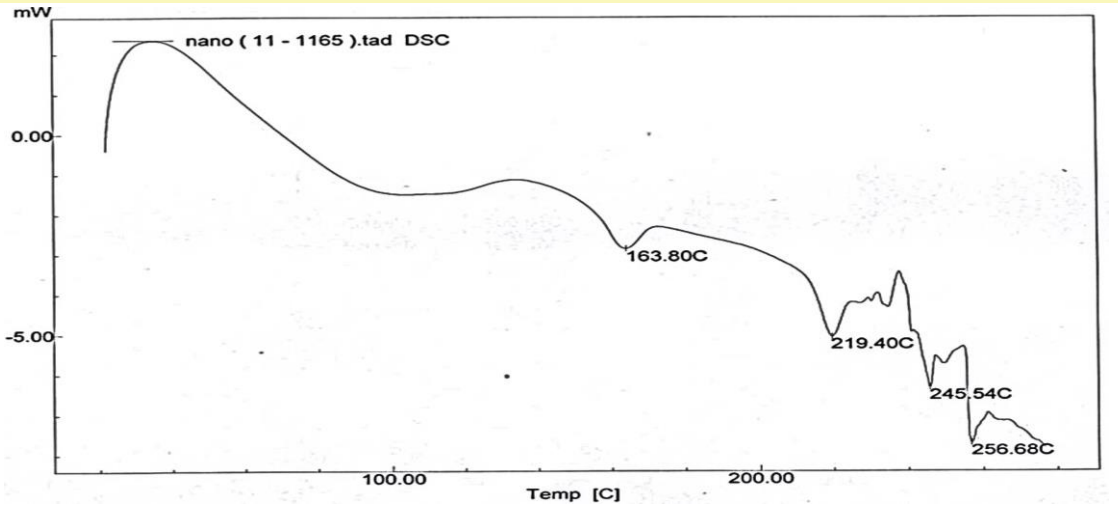

C

Figure (3-17): DSC spectra of (A) pure paclitaxel, (B) PTX loaded CdS nanoparticles and (C) PTX loaded NiO nanoparticles.

3.5.7 Atomic Force Microscopy (AFM):

Atomic Force Microscopy (AFM) was used to determine shape, particle size and particle size distribution of nanoparticles by resolving individual particles and groups of particles in three dimensions analysis[181, 182]. The AFM images and particle size distribution of clarithromycin loaded CdS and NiO nanoparticles showed smooth surfaces (figures 3-19 B and C) with fine distribution of particles (figures 3-22 B and C) in comparison with pure CLA (figures 3-19 A and 3-22 A) and blank CdS and NiO nanoparticles (figures 3-18 and 3-21). The same was observed in paclitaxel, in which AFM images of PTX loaded CdS and NiO nanoparticles showed rice shaped particles with smooth surfaces (figures 3-20 B and C) and fine distribution (figures 3-23 B and C) than that of pure PTX (figures 3-20 A and 3-23 A) [illegible]. The average particle size was also determined by [illegible] in which the average particle size of CLA loaded CdS and NiO nanoparticles [illegible] respectively [illegible] blank CdS nanoparticles (82.57 nm) indicating the loading of the drug. The same was observed for paclitaxel, in which the average size of PTX before loading was 95.28 nm while the average sizes after loading with CdS and NiO nanoparticles were 116.7 nm and 106.03 nm respectively indicating complex formation between the drug and the CdS / NiO nanoparticles[179, 186, 187].

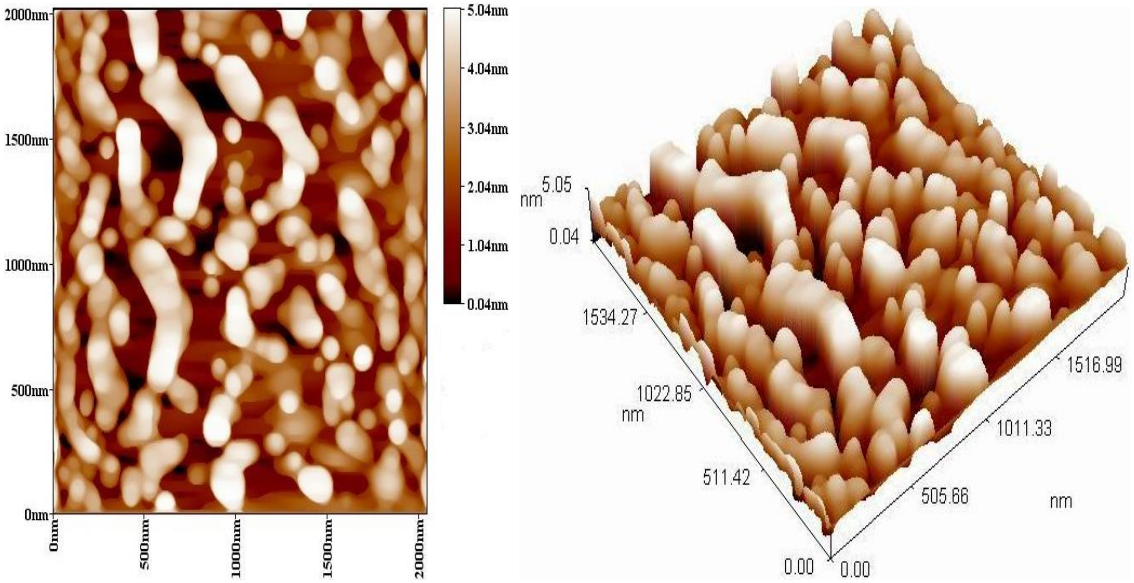

A

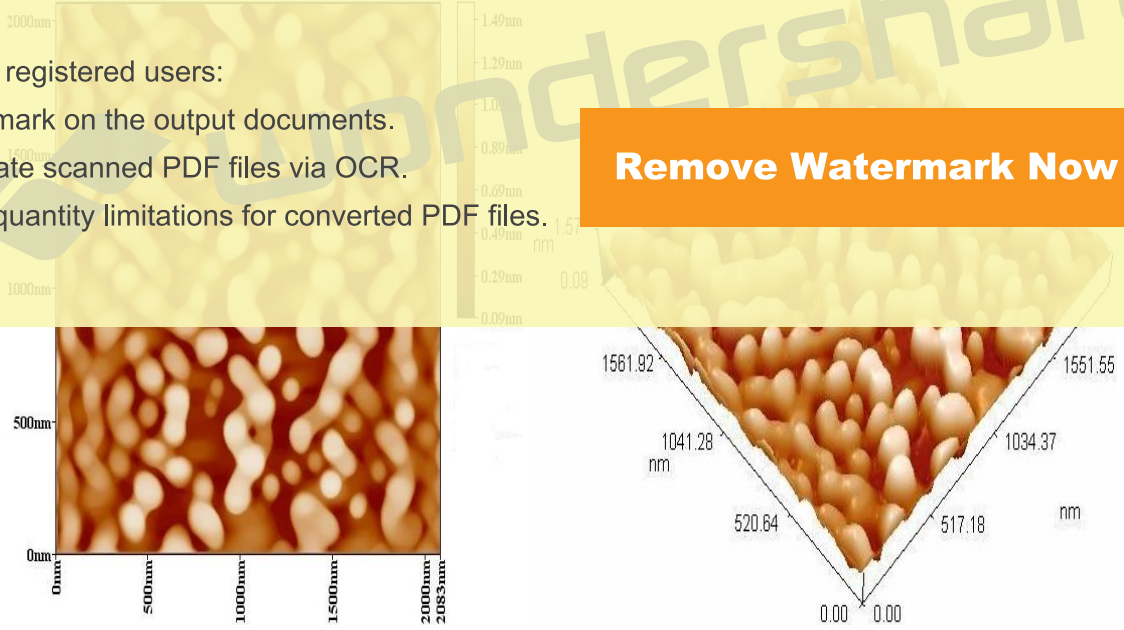

B

Figure (3-18): AFM two and three dimensional images of (A) blank CdS nanoparticles and (B) blank NiO nanoparticles.

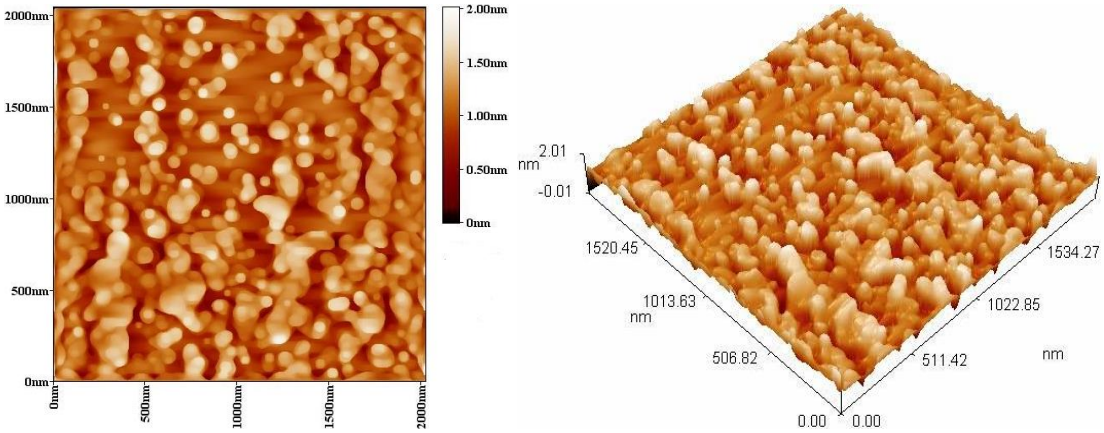

A

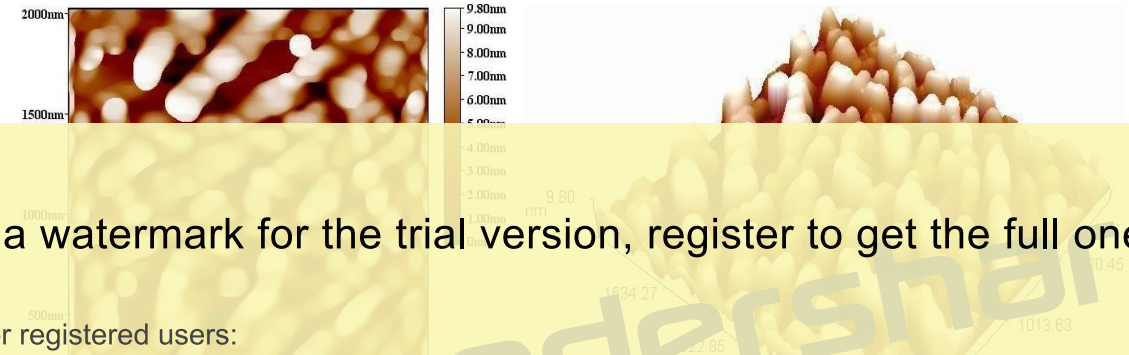

B

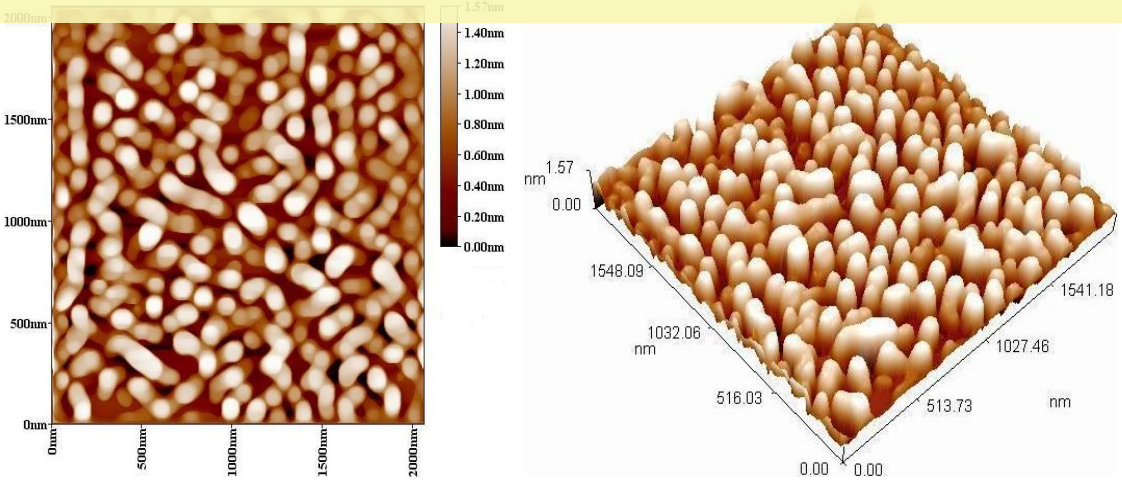

C

Figure (3-19): AFM two and three dimensional images of (A) pure clarithromycin, (B) CLA loaded CdS nanoparticles and (C) CLA loaded NiO nanoparticles.

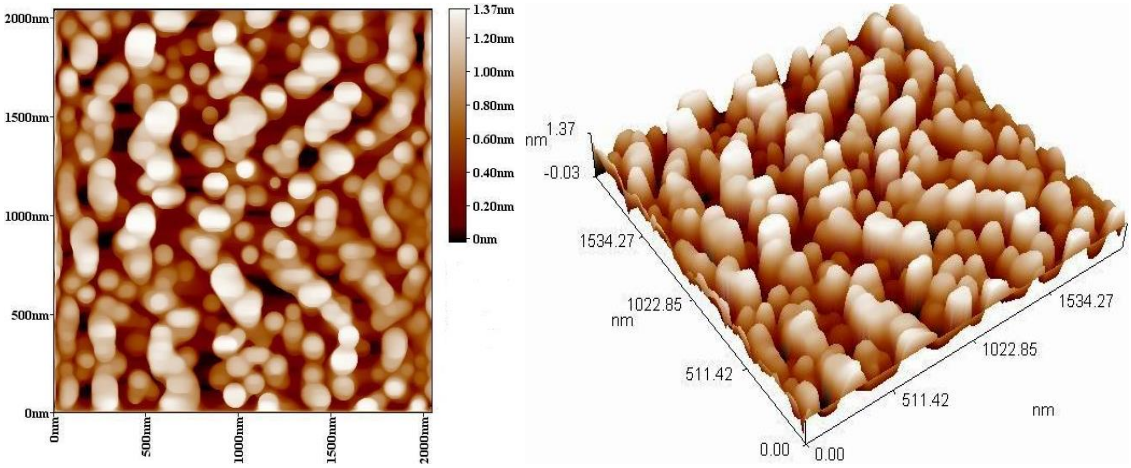

A

B

C

Figure (3-20): AFM two and three dimensional images of (A) pure paclitaxel, (B) PTX loaded CdS nanoparticles and (C) PTX loaded NiO nanoparticles.

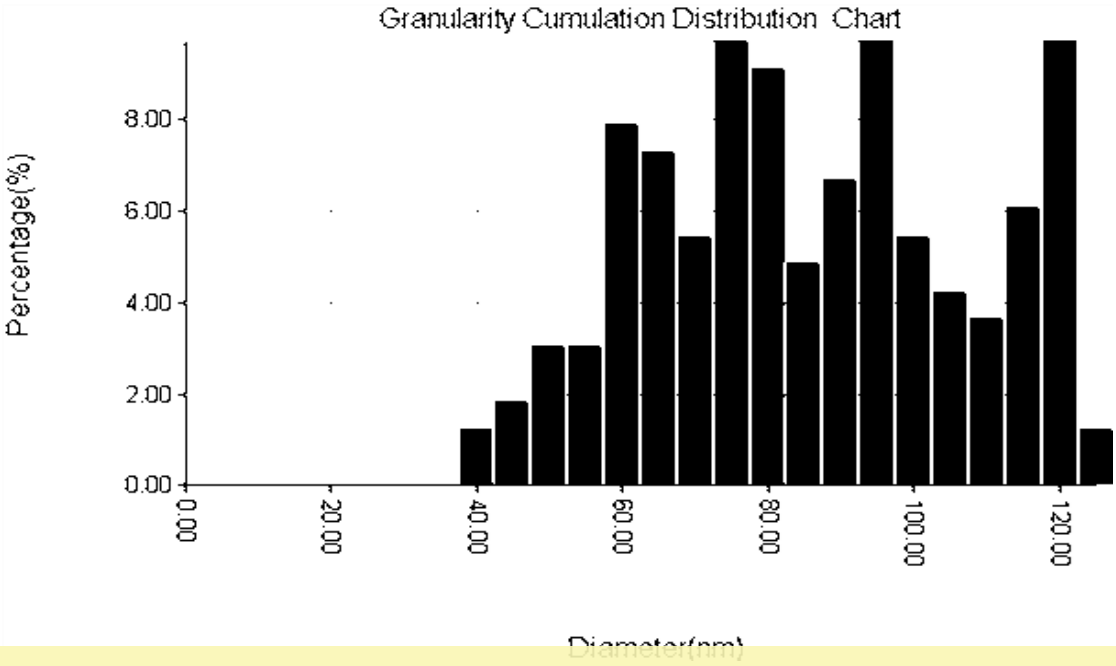

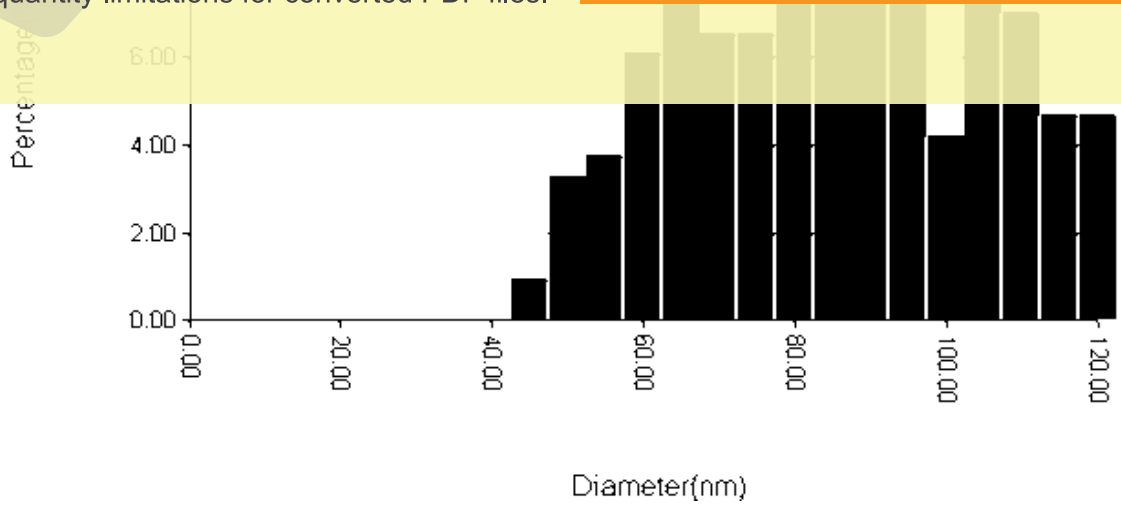

B

Figure (3-21): AFM particle size distribution of (A) blank CdS nanoparticles and (B) blank NiO nanoparticles.

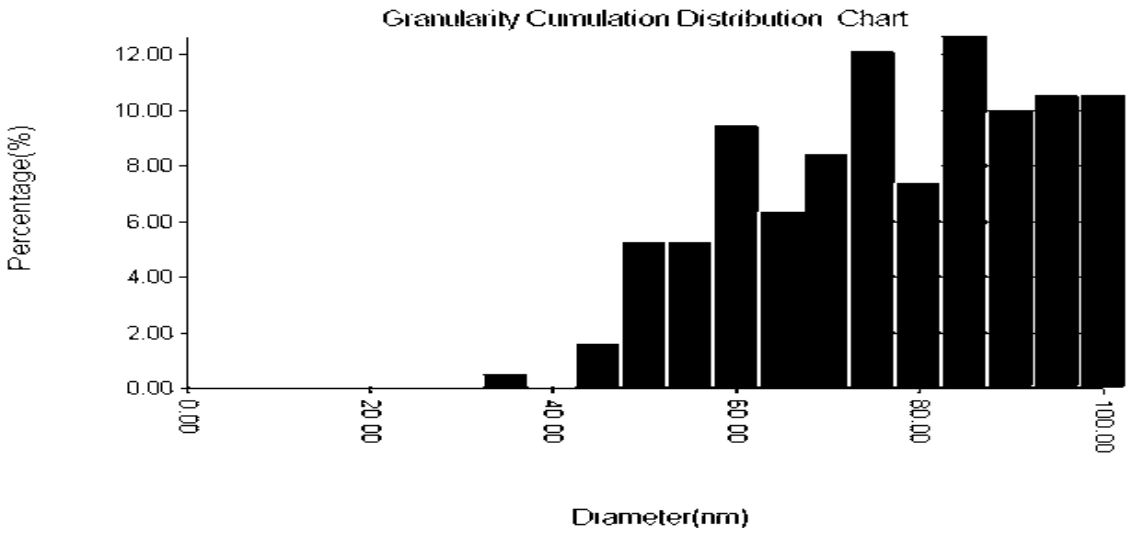

A

B

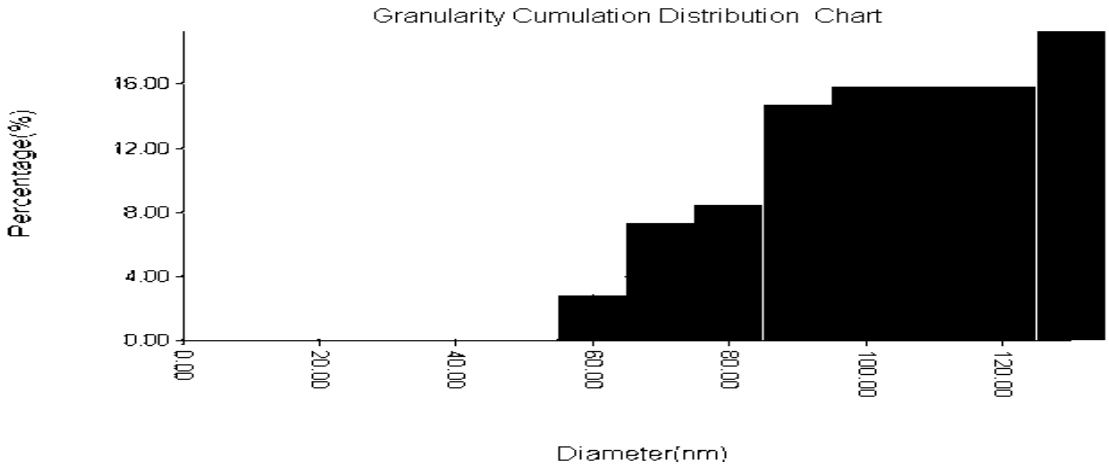

C

Figure (3-22): AFM particle size distribution of (A) pure CLA, (B) CLA loaded CdS nanoparticles and (C) CLA loaded NiO nanoparticles.

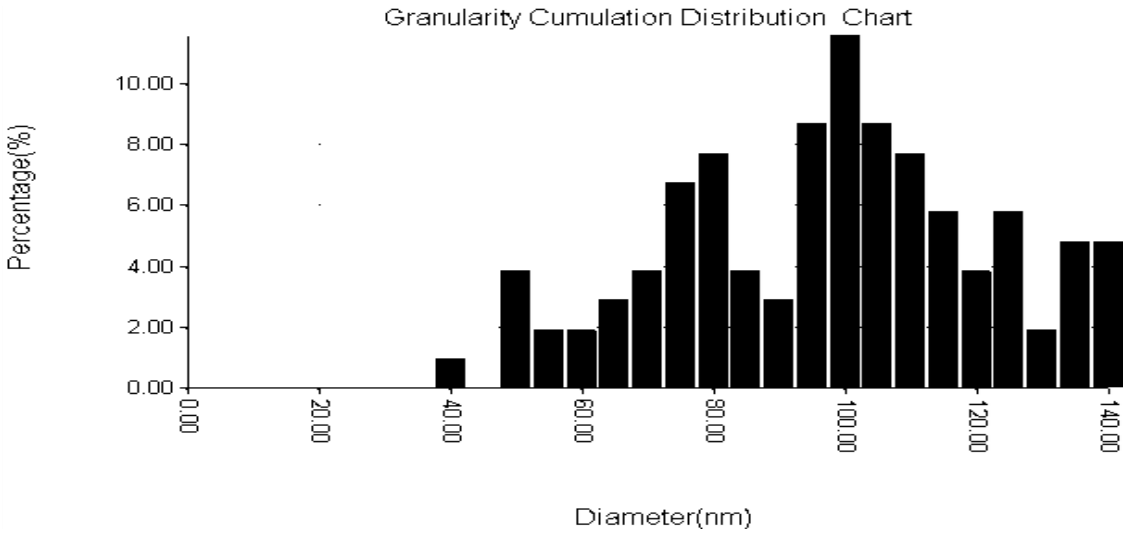

A

B

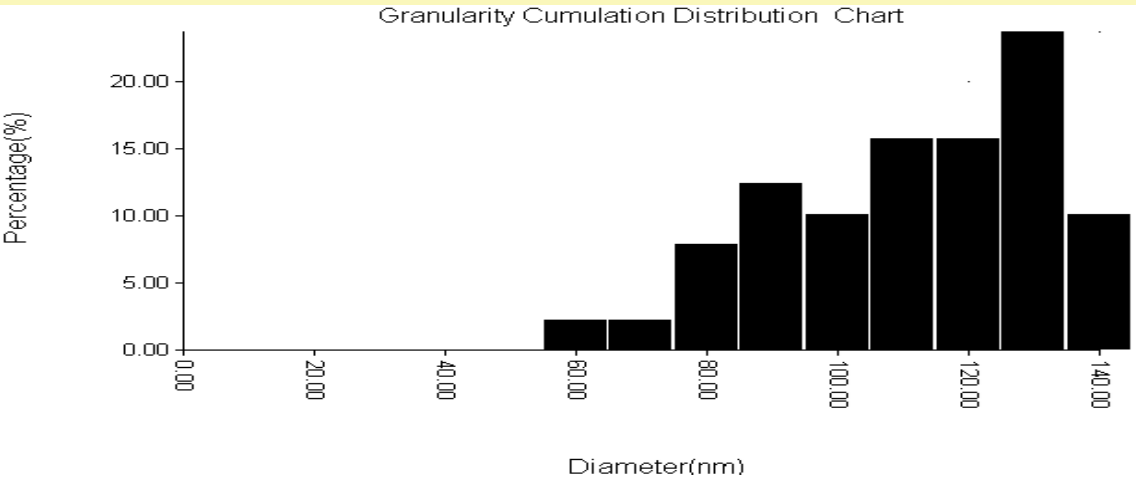

C

Figure (3-23): AFM particle size distribution of (A) pure Paclitaxel, (B) PTX loaded CdS nanoparticles and (G) PTX loaded NiO nanoparticles.

3.6 *In-vitro* release of drugs:

The *in-vitro* release of clarithromycin and paclitaxel from CdS and NiO nanocarriers was performed in phosphate buffer PH 7.4 to simulate the PH value of extracellular fluid in normal tissues according to USP pharmacopeia. The experiment was also performed for pure CLA and pure PTX and the results were drawn as cumulative % release versus time curve.

The *in-vitro* release profile (figure 3-11) of clarithromycin had been significantly ($p<0.05$) improved with about 1 fold increment for CLA loaded on CdS nanoparticles and 3 fold increment for CLA loaded on NiO nanoparticles in comparison with the dissolution of pure CLA, where the percentage release of CLA after 30 min equal 34.1% from pure CLA while the release after 30 min was found to be 49.86% and 88.95% from CLA - CdS and CLA - NiO complexes respectively. The release percentage of CLA reaches 100% from CdS and NiO nanocarriers within 150 and 45 min respectively, this fast CLA release could be due to phase transition from [illegible] indicated in XRD and DSC) as well as due to particle size reduction that was obviously observed from SEM and AFM study thereby increasing surface area of exposed drug to the dissolution medium [139, 188-190].

No release-profile was detected for paclitaxel from CdS and NiO nanocarriers as well as for pure PTX after 8 h due to its very low solubility of the drug.

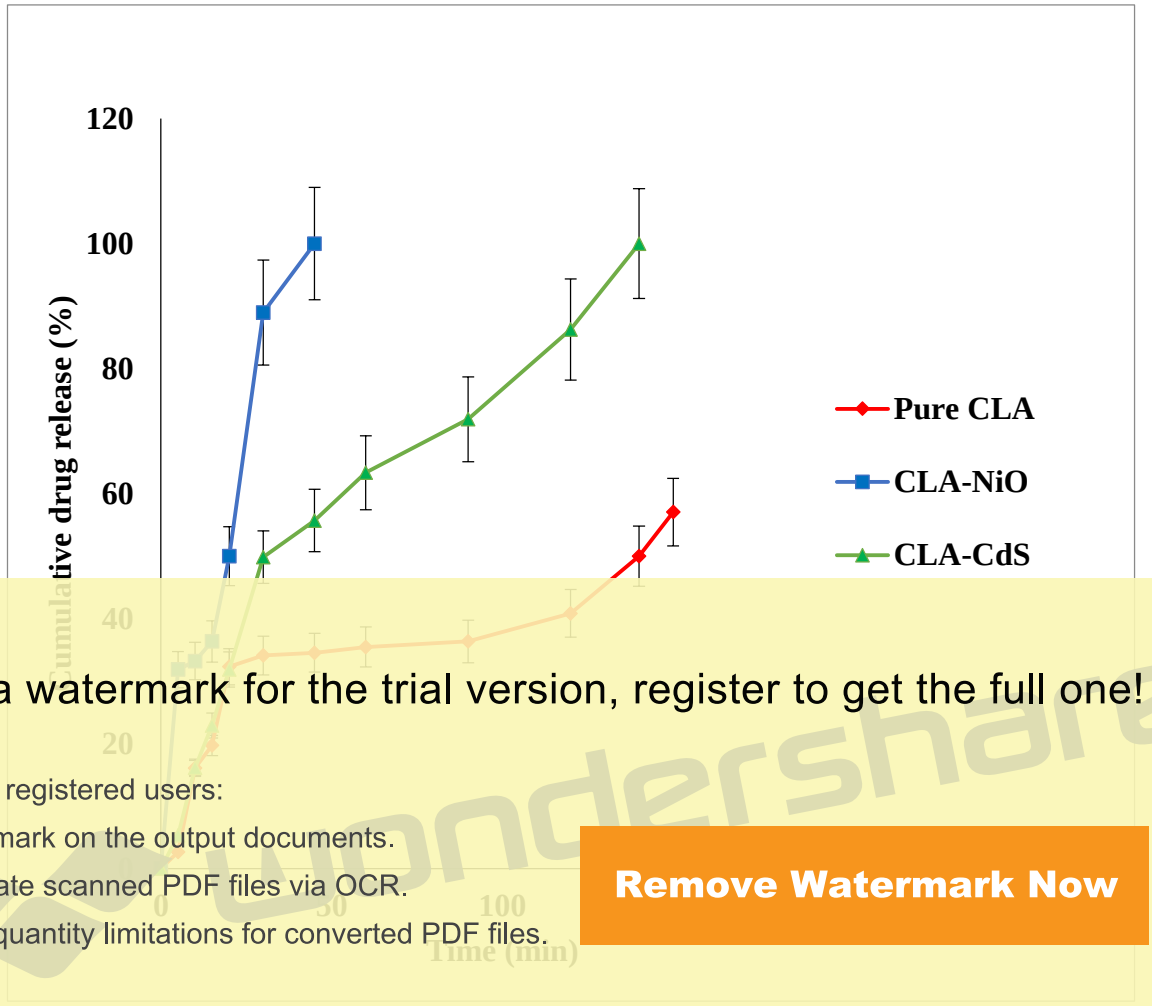

Figure (3-24): Comparative *in-vitro* release of pure clarithromycin, CLA loaded CdS nanoparticles and CLA loaded NiO nanoparticles in phosphate buffer (pH 7.4). Data points represent mean ± SD (n=3).

3.7 Calculation results of yield, drug loading and entrapment efficiency percentages:

The results are illustrated in table (3-2) and showed the yield percentage of the reaction involving clarithromycin with CdS and NiO nanoparticles after complexation was 66.34% and 64.1% respectively, while the yield percentage of the reaction involving paclitaxel loaded CdS and NiO nanoparticles was 62.9% and 95.04% respectively. The drug content of clarithromycin and paclitaxel that has been loaded on CdS and NiO nanocarriers was expressed as percentage of drug loading, in which for CLA loaded CdS and NiO nanoparticles was 56.66% and 86.6% respectively and for PTX loaded CdS and NiO nanoparticles was 76.65% and 95.67% respectively. The percentage of clarithromycin that has been efficiently entrapped with CdS and NiO nanoparticles was 92.5% and 91.6% respectively while the percentage of entrapment efficiency for paclitaxel with CdS and NiO nanoparticles was [illegible] % yield, drug loading and % applicability of CdS and NiO nanoparticles as drug nanocarriers due to their compatibility, uniformity and low drug loss, as well as carrying enough drug to the targeted area[191-193].

Table (3-2): Percentages of yield, drug loading and entrapment effiency for clarithromycin and paclitaxel loaded CdS / NiO nanoparticles.

Drugs / Percentages	Clarithromycin		Paclitaxel	
	CLA-CdS	CLA-NiO	PTX-CdS	PTX-NiO
% Yield	66.34%	64.1%	62.9%	95.04%
% Drug loading	56.66%	86.6%	76.65%	95.67%
% Entrapment efficiency	92.67%	94.6%	96.74%	98.66%

3.8 Solubility determination of drugs before and after loading with CdS and NiO nanoparticles

The results illustrated in table [illegible] clarithromycin loaded on CdS and NiO nanocarriers was significantly ($p < 0.05$) improved in comparison with the saturated solubility of pure CLA, this is may be due to their amorphous property in comparison with the highly stable crystalline structure of pure CLA (in consistence with the results obtained from X-ray diffraction; different study mentioned before), as well as could be attributed to the decreased particle size and thereby enhanced surface area exposed to the dissolution medium[194, 195],

While paclitaxel showed non-significant difference in its saturated solubility before and after loading due to enhanced crystalline property of PTX loaded CdS and NiO nanoparticles.

Table (3-3): Saturation solubility of clarithromycin and paclitaxel before and after loading with CdS and NiO nanoparticles in phosphate buffer (pH 7.4).

Sample	Solubility (mg/mL)
Pure clarithromycin	0.203 ± 0.017
Clarithromycin loaded CdS nanoparticles	0.397 ± 0.035
Clarithromycin loaded NiO nanoparticles	0.510 ± 0.048
Pure paclitaxel	0.0145 ± 0.0012
Paclitaxel loaded CdS nanoparticles	0.0127 ± 0.0011
Paclitaxel loaded NiO nanoparticles	0.0112 ± 0.0012

3.9 Antibacterial activity of clarithromycin loaded on CdS and NiO nanoparticles:

The antibacterial activity (figure 3-12) of clarithromycin loaded CdS and NiO nanoparticles in comparison with pure CLA and blank nanoparticles (CdS and NiO) was determined by measuring the zone of inhibition (ZOI) caused by each sample separately in Muller Hinton agar at 37°C after 24 h incubation. The results illustrated in table (3-3) where there was non-significant difference in the activity of CLA before and after loading with CdS and NiO nanoparticles on gram +ve bacteria *Staphylococcus aurous* and *Streptococcus pyogen* and on gram –ve bacteria *Serratia marcescens*, while there was no effect on gram-ve bacteria *Klebsiella oxytoca*. Blank CdS nanoparticles showed no activity against all

examined bacteria while NiO nanoparticles showed a little antibacterial activity against gram +ve bacteria. The solvent used (DMSO) showed no effect in all samples. Therefore, loading of clarithromycin on metal nanoparticles showed no further improvement in its antibacterial activity in comparison with the pure drug.

Table (3-4): Antibacterial activity of pure clarithromycin, clarithromycin loaded on CdS and NiO nanoparticles and blank CdS and NiO nanoparticles represented by zone of inhibition in (mm).

Sample	*Staphylo-coccus aurous*	*Strepto-coccus pyogen*	*Serratia marcescens*	*Klebsiella oxytoca*
Control dimethylsulfoxide (DMSO)	–	–	–	–
Pure Clarithromycin	31 ± 3.1	32 ± 2.8	21 ± 1.8	–
Clarithromycin loaded CdS nanoparticles	32 ± 3	34 ± 3.1	20 ± 1.5	–
Clarithromycin loaded NiO nanoparticles	32 ± 2.8	35 ± 3.3	22 ± 2	–
CdS nanoparticles	–	–	–	–
NiO nanoparticles	20 ± 1.7	16 ± 1.2	–	–

Data represent mean ± SD (n=3).

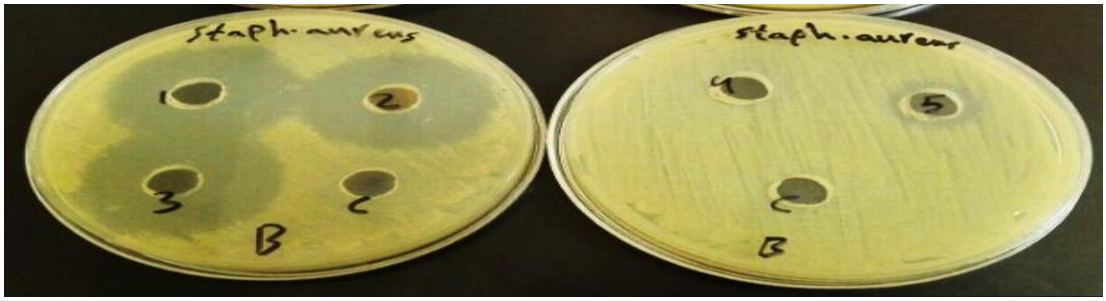

A

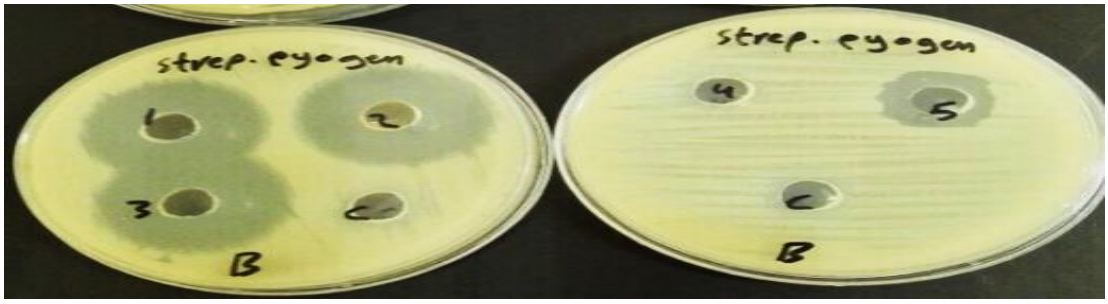

B

C

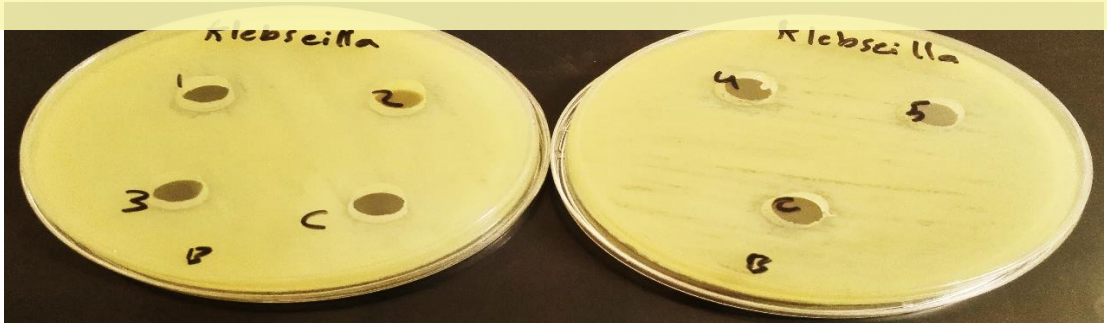

D

Figure (3-25): Zone of inhibition (ZOI) images of (1) pure clarithromycin, (2) CLA loaded CdS nanoparticles, (3) CLA loaded NiO nanoparticles, (4) CdS nanoparticles and (5) NiO nanoparticles on (A) *Staphylococcus aurous*, (B) *Streptococcus pyogen*, (C) *Serratia marcescens* and (D) *Klebsiella oxytoca*.

3.10 Cytotoxic activity of paclitaxel loaded on CdS and NiO nanoparticles:

MCF-7 and MCF-10A cells were treated with increasing concentrations of paclitaxel before and after loading with CdS and NiO nanoparticles as well as with blank CdS and NiO nanoparticles, where each sample was dissolved (separately) in dimethylsulfoxide (DMSO), knowing that DMSO showed no or negligible cytotoxic activity (inhibition rate percent IR %) on both tumor and normal cells.

The anticancer activity (figures 3-26 and 3-27) of paclitaxel against breast cancer cells (MCF-7) for PTX loaded CdS and NiO nanocarriers showed significantly ($p < 0.05$) higher cytotoxic effect (high IR %) than that of pure PTX and blank CdS and NiO nanoparticles in all concentrations used (2.5-20 nM) at different times of exposure (24, 48 and 72 h). The IR % for all concentrations for same sample was almost the same indicating dose-independent kinetics. In addition, there

The results also showed that loading of PTX on the metal nanoparticles led to significantly ($p < 0.05$) increase in its anticancer activity (using MCF-7 breast cancer cell line) in comparison with the pure drug. This could be due to the formation of stable PTX loaded CdS / NiO complexes [150, 162, 196, 197] that may release the drug in slow and continuous (sustained) manner [198, 199], in addition to the synergistic effect of CdS and NiO nanoparticles [113] although these metals showed limited anticancer activities.

To evaluate the undesirable cytotoxic effect (figures 3-28 and 3-29) of paclitaxel loaded CdS and NiO nanoparticles on MCF-10A human normal mammary epithelial cell line, the same concentrations and times of

exposure were applied. It was found that the undesirable cytotoxic effect of PTX from PTX loaded CdS and NiO nanoparticles on MCF-10A cell line was significantly ($p < 0.05$) lower than that of pure PTX and the blank CdS and NiO nanoparticles from all used concentrations and at different times of exposure. The undesirable cytotoxicity of all examined samples on MCF-10A normal cell line had variable dose-dependent kinetics, where above 2.5 nM concentration PTX from PTX loaded CdS and NiO nanoparticles showed steep decline after 48 h (for all concentrations). While after 72 h, the steep decline in drug cytotoxic effect on MCF-10A cell line was observed until 10 nM. In all cases, the loading of PTX on metal nanoparticles led to significantly ($p < 0.05$) reduced the undesirable cytotoxic effect of the drug on normal cell line. This could be attributed to the decreased permeability or increased resistance of normal cells toward the drug in its complex form with CdS and NiO nanoparticles [200, 201]

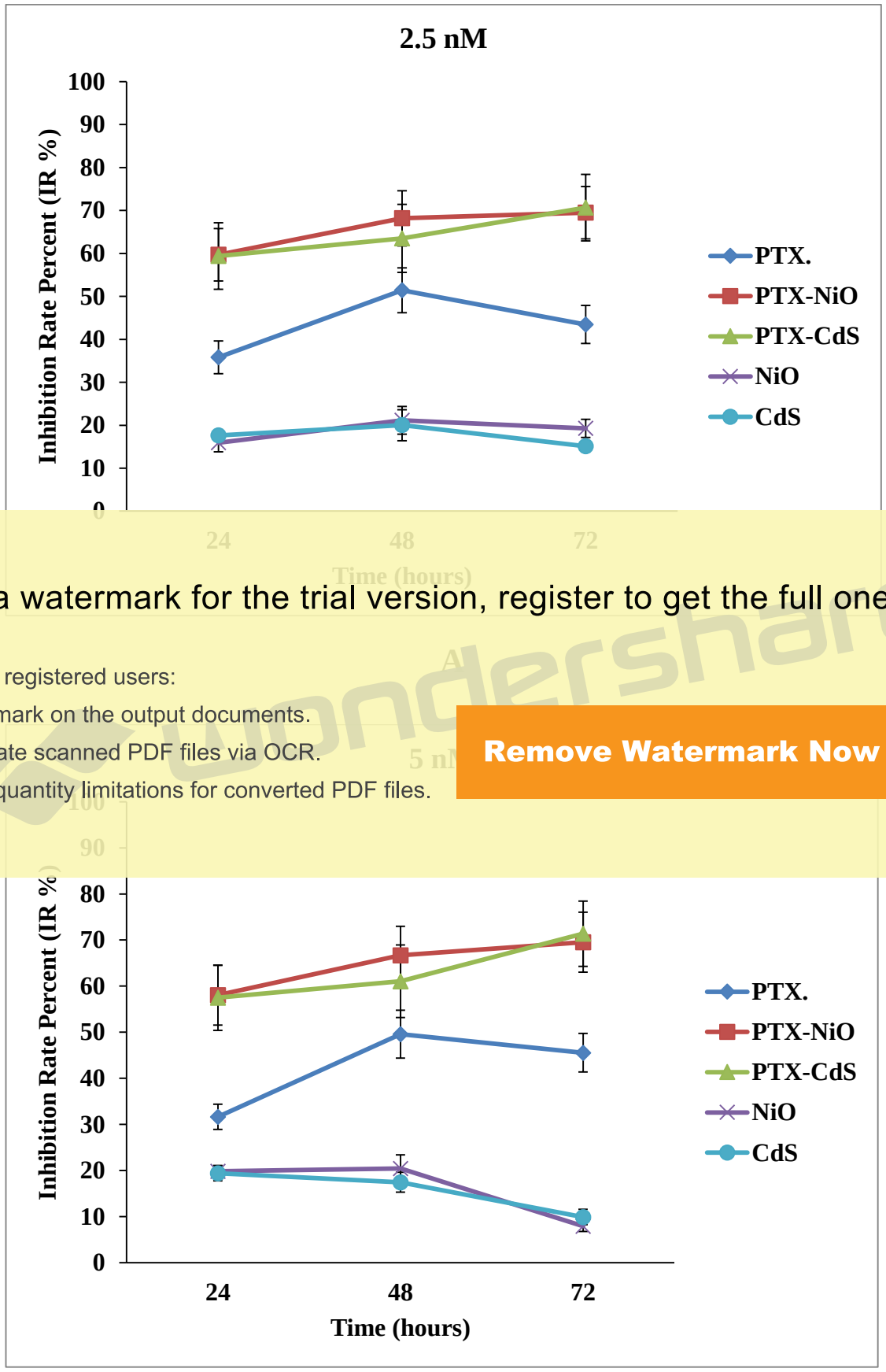

B

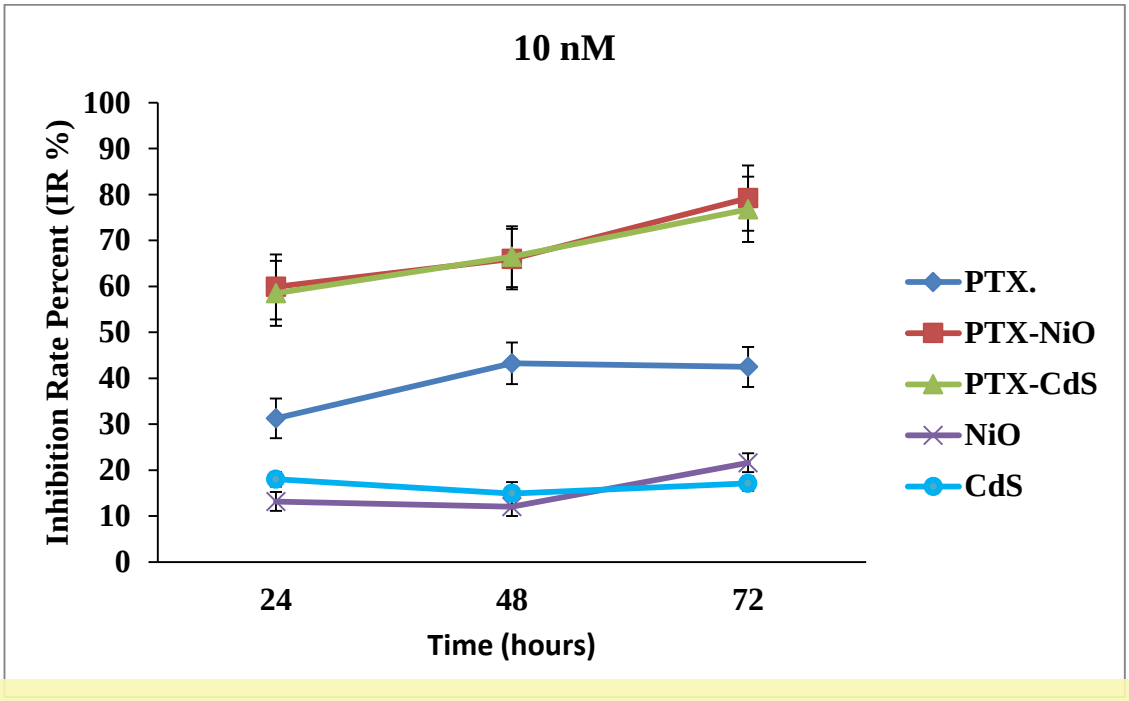

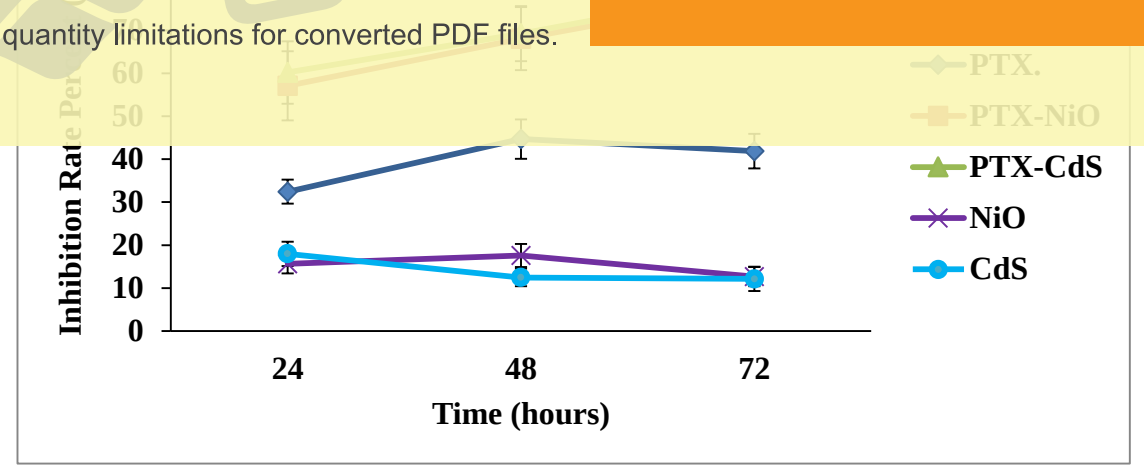

D

Figure (3-26): Time-response curves for comparative *in-vitro* cytotoxicity of pure paclitaxel, PTX loaded CdS nanoparticles, PTX loaded NiO nanoparticles, blank CdS nanoparticles and blank NiO nanoparticles on MCF-7 cancer cell line using (A) 2.5 nM, (B) 5 nM, (C) 10 nM and (D) 20 nM. Data points represent mean ± SD (n=3).

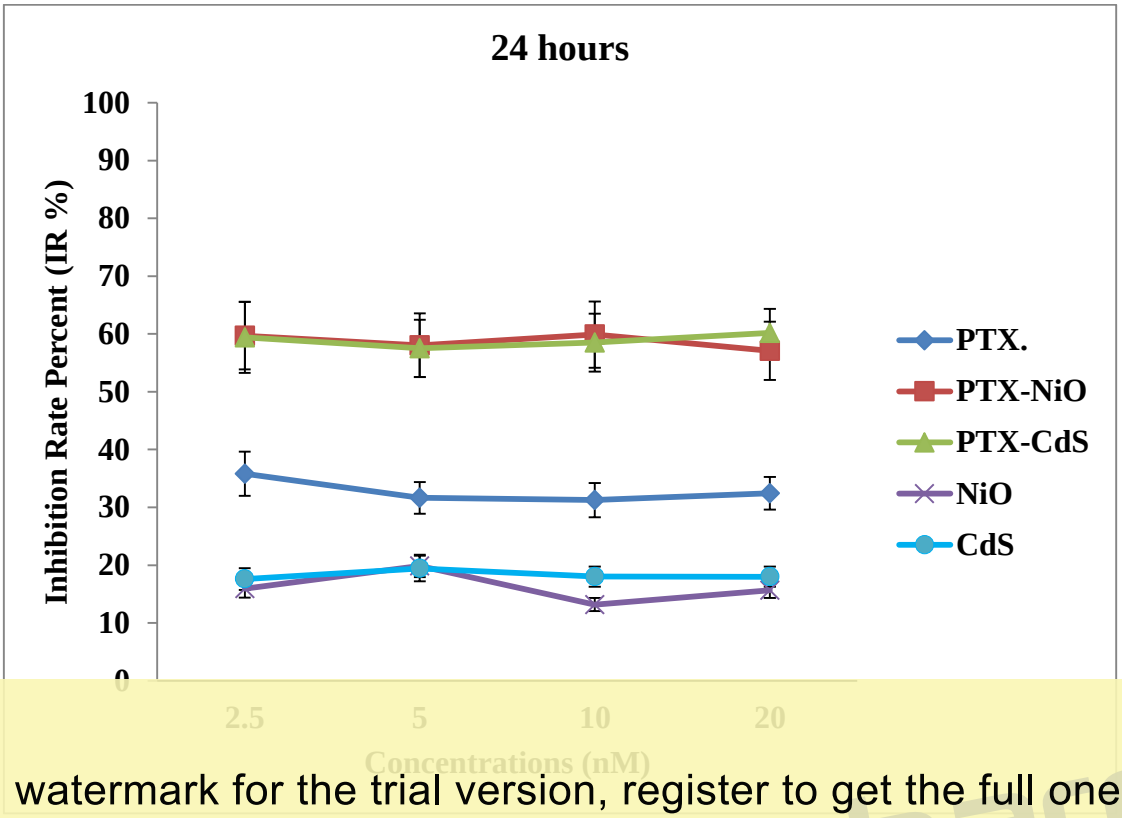

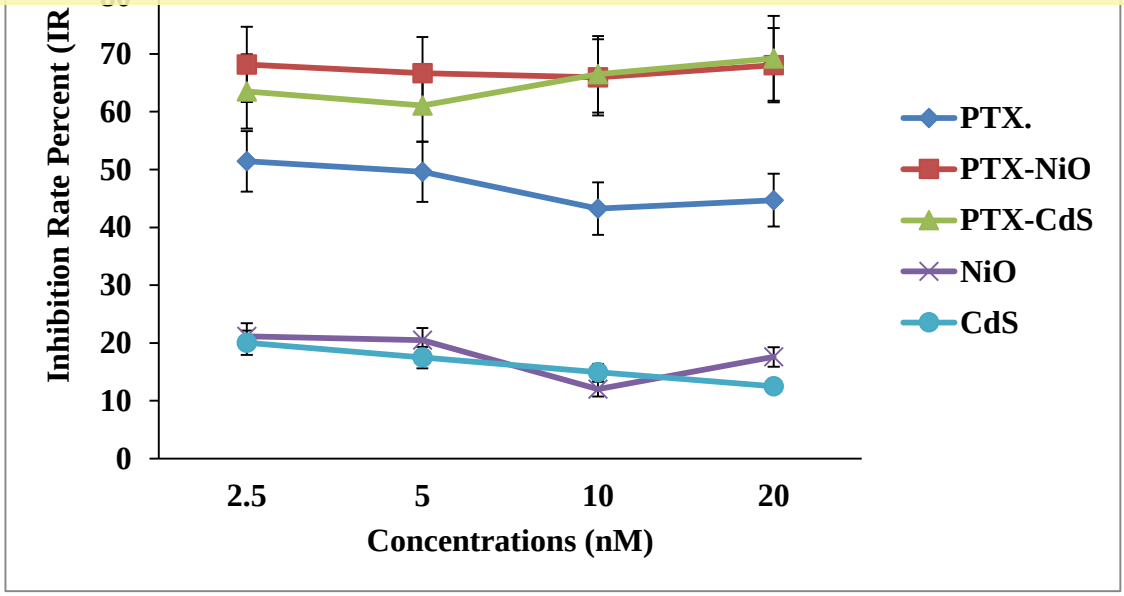

B

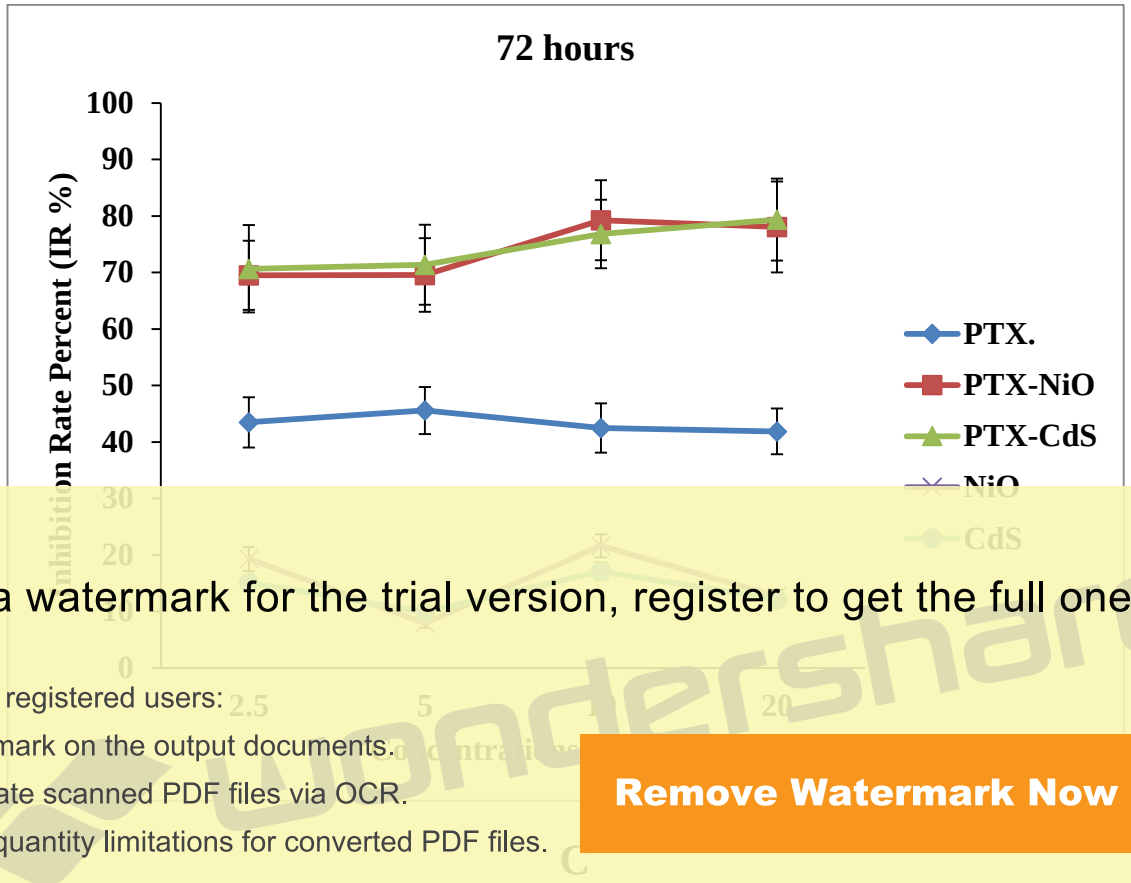

Figure (3-27): Comparative *in-vitro* cytotoxicity of pure paclitaxel, PTX loaded CdS nanoparticles, PTX loaded NiO nanoparticles, blank CdS nanoparticles and blank NiO nanoparticles showing the effect of concentration on their anticancer activity on MCF-7 cell line after (A) 24, (B) 48 and 72 h of exposure. Data points represent mean ± SD (n=3).

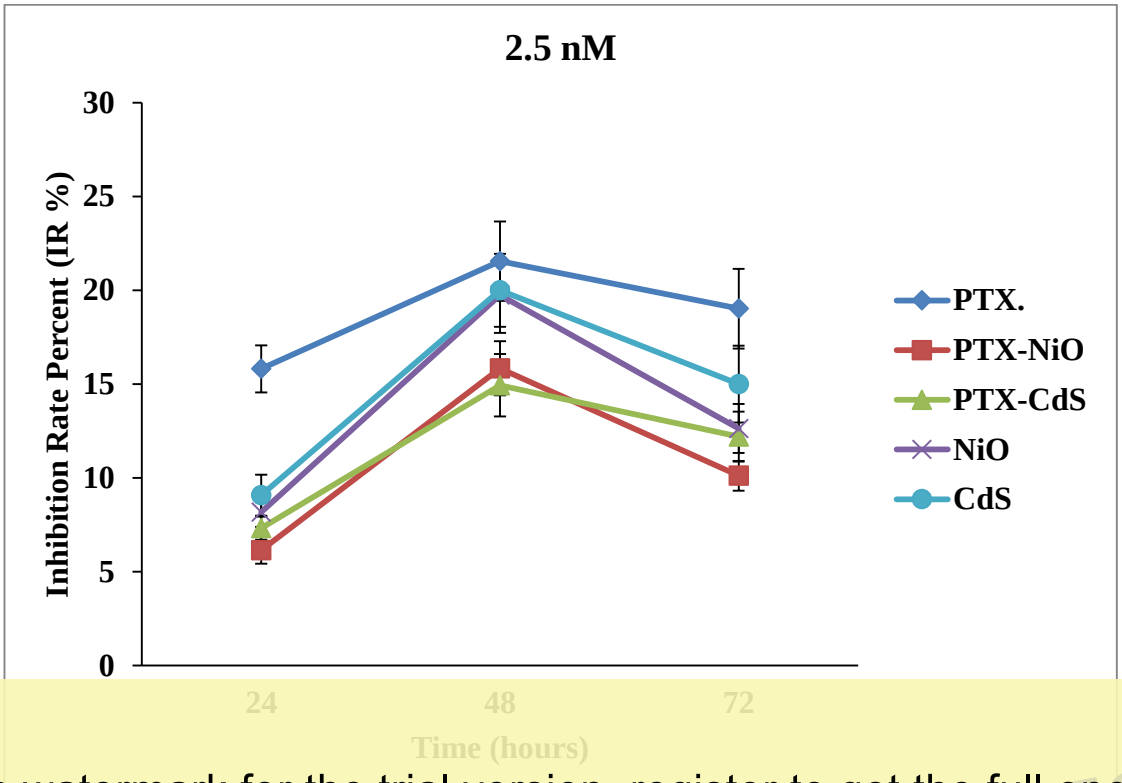

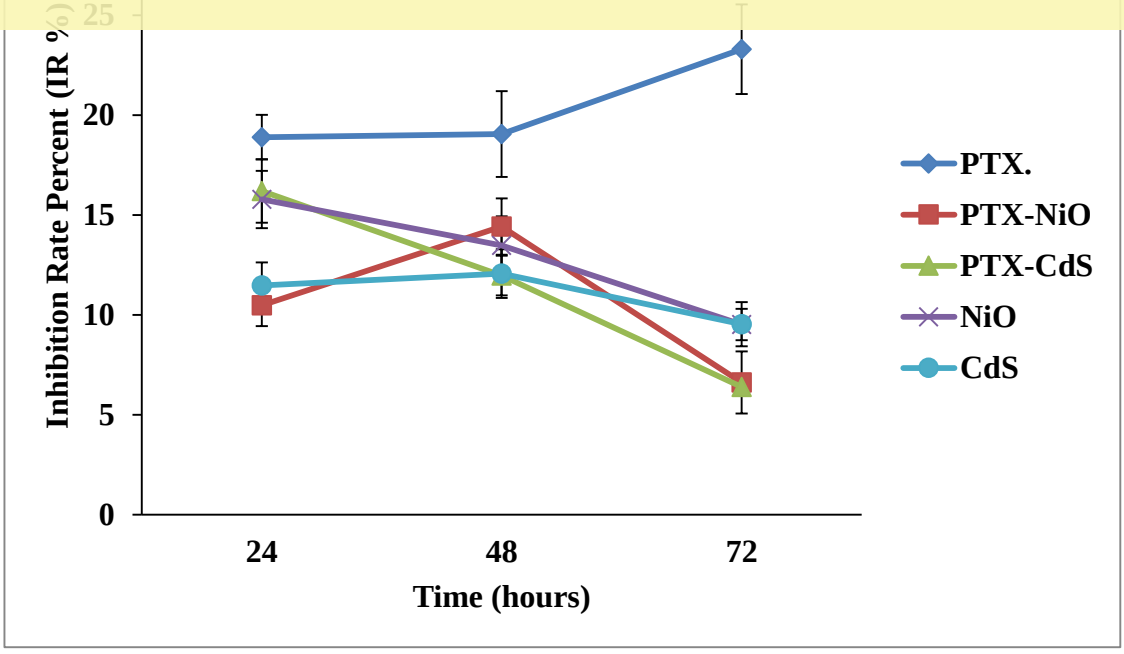

B

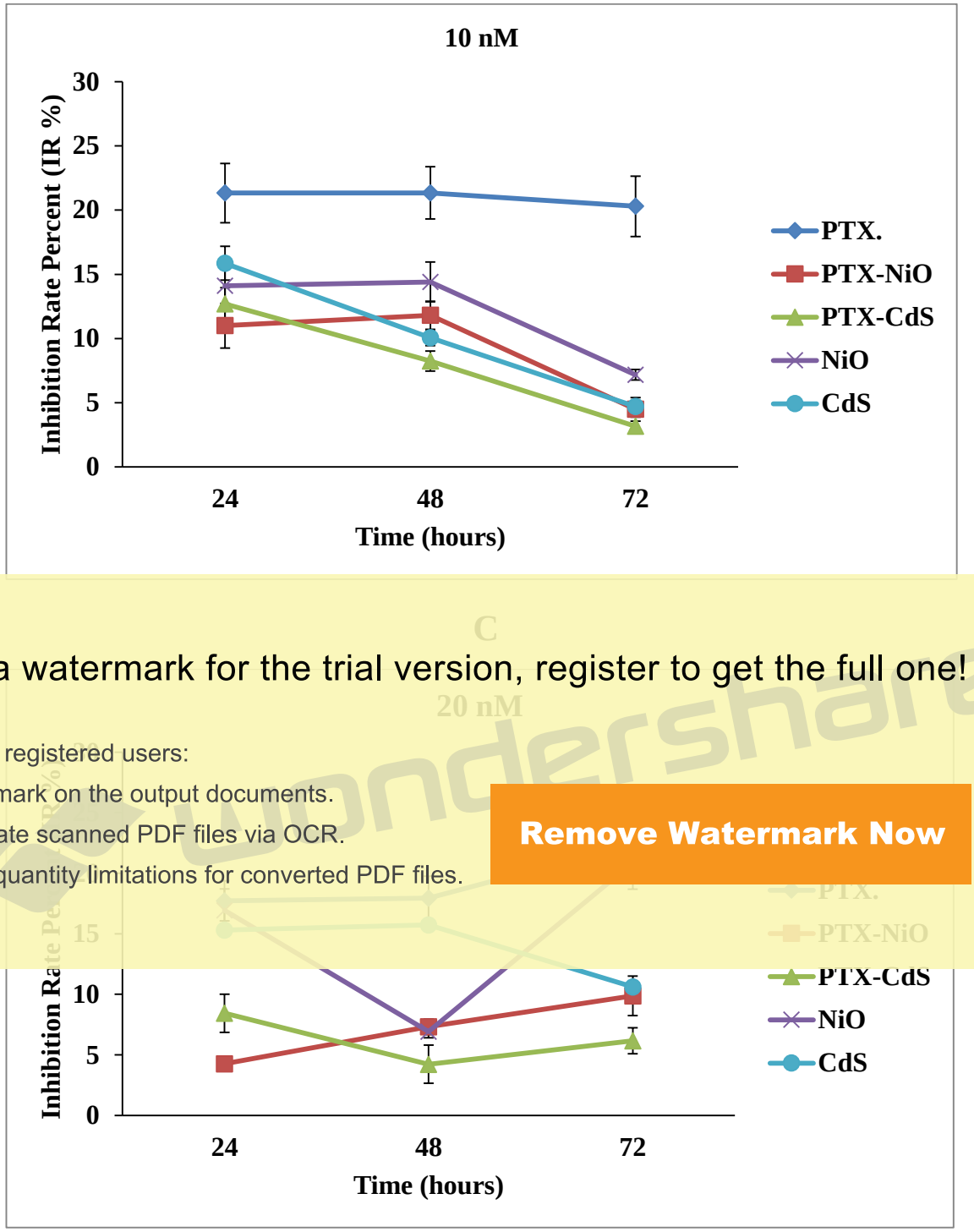

D

Figure (3-28): Time-response curves for comparative *in-vitro* cytotoxicity of pure paclitaxel, PTX loaded CdS nanoparticles, PTX loaded NiO nanoparticles, blank CdS nanoparticles and blank NiO nanoparticles on MCF-10A normal cell line using (A) 2.5 nM, (B) 5 nM, (C) 10 nM and (D) 20 nM. Data points represent mean ± SD (n=3).

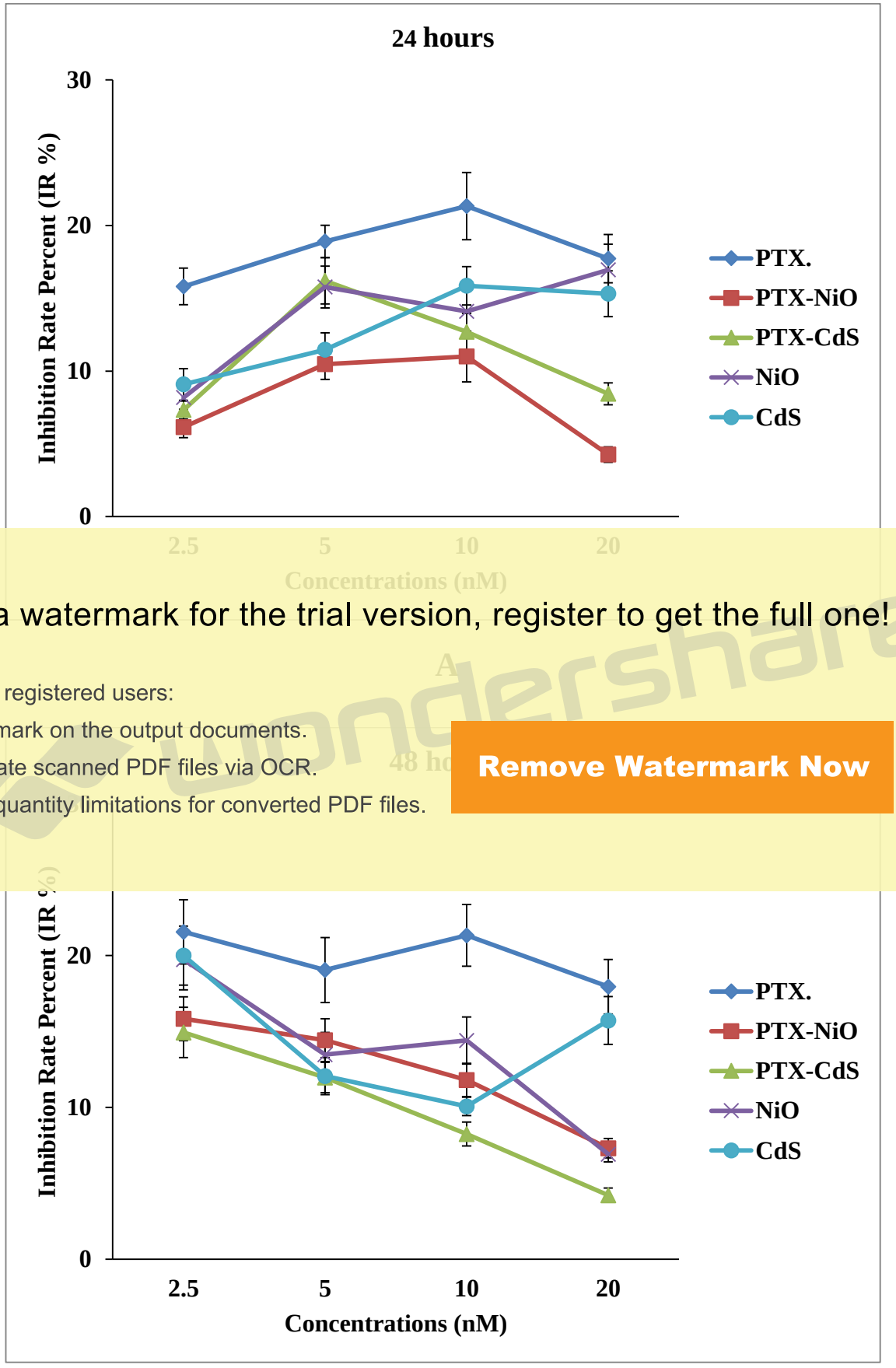

B

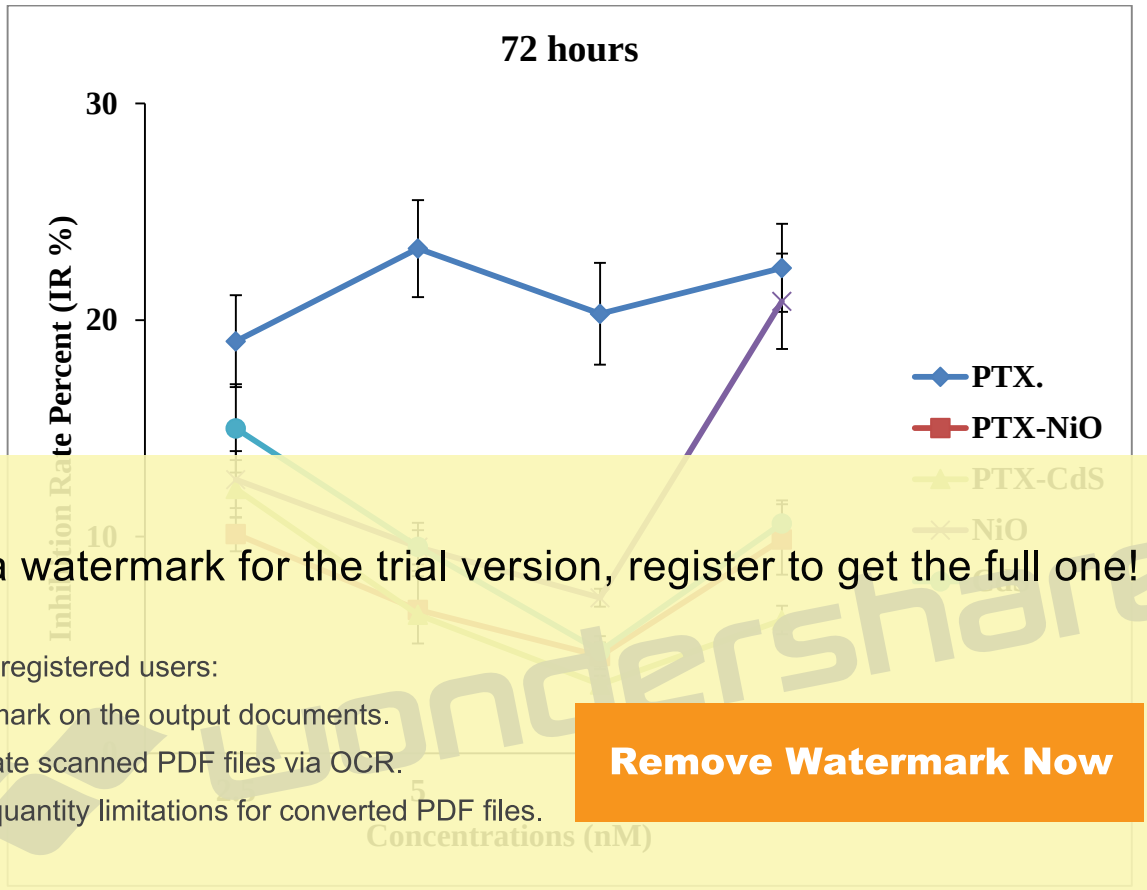

C

Figure (3-29): Comparative *in-vitro* cytotoxicity of pure paclitaxel, PTX loaded CdS nanoparticles, PTX loaded NiO nanoparticles, blank CdS nanoparticles and blank NiO nanoparticles showing the effect of concentration on their cytotoxic activity on MCF-10A cell line after (A) 24, (B) 48 and 72 h of exposure. Data points represent mean ± SD (n=3).

Chapter Four

4. Conclusions and Recommendations:

4.1 Conclusions:

1. Loading of clarithromycin and paclitaxel on the surface of the prepared CdS and NiO nanoparticles was performed by physical complex formation without any reaction of their functional groups which was approved by Ferrer Transform Infra-Red (FTIR), X-Ray Diffraction (XRD), zeta potential, Thermo-Gravimetric Analysis (TGA), Atomic Force Microscopy (AFM), Scanning Electron Microscopy (SEM) and Differential Scanning Calorimetric (DSC).

change in its solubility, but significant ($p<0.05$) increase in its antitumor activity on MCF-7 cell line accompanied with significant ($p<0.05$) reduction in its undesirable cytotoxic effect on normal mammary cell line (MCF-10A) indicating the selectivity and targeting action of the prepared PTX-CdS/NiO nanocarriers with reduced cytotoxic effect of the drug and the used metal nanocarriers.

4.2 Recommendations:

1. Formulation of clarithromycin and paclitaxel loaded on CdS and NiO nanoparticles in a suitable dosage form is recommended utilizing the enhanced solubility of clarithromycin and increased anticancer activity toward cancer cells (MCF-7) as well as decreased cytotoxicity toward normal cells (MCF-10A).

2. Comparative study in pharmacokinetic (absorption, distribution and bioavailability) and biological activity between the prepared drugs loaded on CdS and NiO nanoparticles after suitable dosage form achievement and conventional marketed dosage forms of these drugs is necessary.

3. Alternative methods for preparation of nanoparticles is recommended (such as low laser radiation method) in comparison with the chemical method.

References:

1. Ventola CL. The Nanomedicine Revolution. Part 1: Emerging Concepts Pharmacy and Therapeutics. 2012;37(9):512–25.
2. Sweeney AE. Nanomedicine concepts in the general medical curriculum: initiating a discussion. International journal of nanomedicine. 2015;10(1):7319–31.
3. Guo J-W, Lee Y-H, Huang H-W, Tzou M-C, Wang Y-J, Tsai J-C. Development of Taiwan’s strategies for regulating nanotechnology-based pharmaceuticals harmonized with international considerations. International journal of nanomedicine. 2014;9(2014):4773–83.
4. Arif T, Nisa N, Amin SS, Shoib S, Mushtaq R, Shawl MR. Therapeutic and Diagnostic Applications of Nanotechnology in Dermatology and Cosmetics. Journal of Nanomedicine & Biotherapeutic Discovery. 2015;2015(3):1-10.
5. [illegible] S, [illegible] T, Sahin A [illegible] delivery. OA Drug Design & Delivery [illegible]
6. Daughton CG, Ruhoy IS. Lower-dose prescribing: minimizing “side effects” of pharmaceuticals on society and the environment. Science of the Total Environment. 2013;443(2013):324-37.
7. Xu W, Ling P, Zhang T. Polymeric micelles, a promising drug delivery system to enhance bioavailability of poorly water-soluble drugs. Journal of drug delivery. 2013;2013(1):1-15.
8. Prabhakar U, Maeda H, Jain RK, Sevick-Muraca EM, Zamboni W, Farokhzad OC, et al. Challenges and key considerations of the enhanced permeability and retention effect for nanomedicine drug delivery in oncology. Cancer research. 2013;73(8):2412-7.
9. Krol S, Macrez R, Docagne F, Defer G, Laurent S, Rahman M, et al. Therapeutic benefits from nanoparticles: the potential significance of

nanoscience in diseases with compromise to the blood brain barrier. Chemical reviews. 2012;113(3):1877-903.

10. Chaturbedy P, Kumar M, Salikolimi K, Das S, Sinha SH, Chatterjee S, et al. Shape-directed compartmentalized delivery of a nanoparticle-conjugated small-molecule activator of an epigenetic enzyme in the brain. Journal of Controlled Release. 2015;217(1):151-9.

11. Desai PP, Date AA, Patravale VB. Overcoming poor oral bioavailability using nanoparticle formulations-opportunities and limitations. Drug Discovery Today: Technologies. 2012;9(2):87-95.

12. Pawar VK, Singh Y, Meher JG, Gupta S, Chourasia MK. Engineered nanocrystal technology: in-vivo fate, targeting and applications in drug delivery. Journal of Controlled Release. 2014;183(2):51-66.

13. Kamaly N, Xiao Z, Valencia PM, Radovic-Moreno AF, Farokhzad OC. Targeted polymeric therapeutic na[illegible]rticles: design, development and [illegible] Society R[illegible] 2012;41(7):2971-3010.

14. Yadav [illegible] M, Jain DK. [illegible] system. J Advanced Pharm Educ Res. 2011;1(4):201-13.

15. Oberdörster G. Safety assessment for nanotechnology and nanomedicine: concepts of nanotoxicology. Journal of internal medicine. 2010;267(1):89-105.

16. Manda R, Suthakaran R, Kaya V, Fouziya BS. A comparative review of recently developed particulate drug carrier systems. World Journal of Pharmacy amd Pharmaceutical Sciences. 2014;3(11):121-34.

17. Auffinger B, Morshed R, Tobias A, Cheng Y, Ahmed AU, Lesniak MS. Drug-loaded nanoparticle systems and adult stem cells: a potential marriage for the treatment of malignant glioma. Oncotarget. 2013;4(3):378-96.

18. Sutradhar KB, Amin ML. Nanotechnology in cancer drug delivery and selective targeting. ISRN Nanotechnology. 2014;2014(1):1-12.

19. Jena M, Mishra S, Jena S, Mishra SS. Nanotechnology-future prospect in recent medicine: a review. International Journal of Basic & Clinical Pharmacology. 2013;2(4):353-9.

20. Rangasamy M. Nano technology: A review. Journal of Applied Pharmaceutical Science 2011;1(2):8-16

21. Nikalje AP. Nanotechnology and its Applications in Medicine. Medicinal Chemistry. 2015;5(2):81-9.

22. Wahajuddin SA. Superparamagnetic iron oxide nanoparticles: magnetic nanoplatforms as drug carriers. International journal of nanomedicine. 2012;7(2012):3445–71.

23. Schumacher CM, Herrmann IK, Bubenhofer SB, Gschwind S, Hirt AM, Beck-Schimmer B, et al. Quantitative recovery of magnetic nanoparticles from flowing blood: trace analysis and the role of magnetic force. Advanced Functional

Kairdolf EA, Smith AM, Stoke

Semiconductor quantum dots for bioimaging and biodiagnostic applications. Annual review of analytical chemistry (Palo Alto, Calif). 2013;6(1):143-62.

25. Lalwani G, Henslee AM, Farshid B, Lin L, Kasper FK, Qin Y-X, et al. Two-dimensional nanostructure-reinforced biodegradable polymeric nanocomposites for bone tissue engineering. Biomacromolecules. 2013;14(3):900-9.

26. Qian W-Y, Sun D-M, Zhu R-R, Du X-L, Liu H, Wang S-L. pH-sensitive strontium carbonate nanoparticles as new anticancer vehicles for controlled etoposide release. International journal of nanomedicine. 2012;7(1):5781-92.

27. Kapadi SV, Gadhe L. Recent trend in nanopharmaceuticals: An overview. World Journal of Pharmaceutical Research. 2015;4(3):553-66.

28. Varma JR, Kumar TS, Prasanthi B, Ratna JV. Formulation and characterization of pyrazinamide polymeric nanoparticles for pulmonary tuberculosis: Efficiency for alveolar macrophage targeting. Indian journal of pharmaceutical sciences. 2015;77(3):258.

29. Wilczewska AZ, Niemirowicz K, Markiewicz KH, Car H. Nanoparticles as drug delivery systems. Pharmacological Reports. 2012;64(5):1020-37.

30. Athar M, Das AJ. Therapeutic nanoparticles: State-of-the-art of nanomedicine. Adv Mater Rev. 2014;1(1):25-37.

31. Gilkey M, Krishnan V, Scheetz L, Jia X, Rajasekaran A, Dhurjati P. Physiologically based pharmacokinetic modeling of fluorescently labeled block copolymer nanoparticles for controlled drug delivery in leukemia therapy. CPT: pharmacometrics & systems pharmacology. 2015;4(3):167-74.

32. Nagal A, Singla RK. Nanoparti[illegible] Delivery System: A Brief Review. Indo Global Jour[illegible] 2013;3(2):96-106.

33. Honary S, Zahir F. Effect of zeta potential on the properties of nano-drug delivery systems-a review (Part 1). Tropical Journal of Pharmaceutical Research. 2013;12(2):255-64.

34. Kaasalainen M, Mäkilä E, Riikonen J, Kovalainen M, Järvinen K, Herzig K-H, et al. Effect of isotonic solutions and peptide adsorption on zeta potential of porous silicon nanoparticle drug delivery formulations. International journal of pharmaceutics. 2012;431(1):230-6.

35. Mittal G, Sahana D, Bhardwaj V, Kumar MR. Estradiol loaded PLGA nanoparticles for oral administration: effect of polymer molecular weight and copolymer composition on release behavior in vitro and in vivo. Journal of Controlled Release. 2007;119(1):77-85.

36. Kalepu S, Manthina M, Padavala V. Oral lipid-based drug delivery systems–an overview. Acta Pharmaceutica Sinica B. 2013;3(6):361-72.

37. Chandra sekhar M, Narasimha Rao M, V.K.Prasad B. Vitality of Physics In Nanoscience and Nanotechnology. Journal of Applied Physics. 2015;7(1):1-5.

38. Zamani M, Prabhakaran MP, Ramakrishna S. Advances in drug delivery via electrospun and electrosprayed nanomaterials. International journal of nanomedicine. 2013;8(2013):2997-3017.

39. Omwoyo WN, Ogutu B, Oloo F, Swai H, Kalombo L, Melariri P, et al. Preparation, characterization, and optimization of primaquine-loaded solid lipid nanoparticles. International journal of nanomedicine. 2014;9(1):3865-74.

40. Ranjit K, AbdulBaquee A. Nanoparticle: An overview of preparation characterization and application. International Research Journal of Pharmacy. 2013;4(4):47-57.

41. Sharma B, Sharma A. Futu[illegible] development of anti-ageing formulations. Int J Pharm Pharm Sci. 2012;4(3):57-66.

42. Gauniya A, Mazumder R, Pathak K. Nanocrystals: A Challenge for Improved Drug Delivery Asian Journal of Biochemical and Pharmaceutical Research. 2014;4(3):282-92.

43. Sutradhar KB, Khatun S, Luna IP. Increasing possibilities of nanosuspension. Journal of Nanotechnology. 2013;2013(1):1-12.

44. Ochekpe NA, Olorunfemi PO, Ngwuluka NC. Nanotechnology and drug delivery part 2: nanostructures for drug delivery. Tropical Journal of Pharmaceutical Research. 2009;8(3): 275-87.

45. Arias JL, Ruiz MA, López-Viota M, Delgado ÁV. Poly (alkylcyanoacrylate) colloidal particles as vehicles for antitumour drug

delivery: a comparative study. Colloids and Surfaces B: Biointerfaces. 2008;62(1):64-70.

46. Gupta V, Nayak SK. Dendrimers: a Review on Synthetic Approaches. Journal of Applied Pharmaceutical Science. 2015;5(3):117-22.

47. Lohcharoenkal W, Wang L, Chen YC, Rojanasakul Y. Protein nanoparticles as drug delivery carriers for cancer therapy. BioMed research international. 2014;2014(1):1-12.

48. Taguchi K, Yamasaki K, Seo H, Otagiri M. Potential Use of Biological Proteins for Liver Failure Therapy. Pharmaceutics. 2015;7(3):255-74.

49. Li F-Q, Su H, Wang J, Liu J-Y, Zhu Q-G, Fei Y-B, et al. Preparation and characterization of sodium ferulate entrapped bovine serum albumin nanoparticles for liver targeting. International journal of pharmaceutics. 2008;349(1):274-82.

50. [illegible] AC, [illegible] for cell [illegible] Biointerfaces. 2015;136(1):514-26.

51. Akbarzadeh A, Rezaei-Sadabady R, Davaran S, Joo SW, Zarghami N, Hanifehpour Y, et al. Liposome: classification, preparation, and applications. Nanoscale Res Lett. 2013;8(1):1-9.

52. Moghassemi S, Hadjizadeh A. Nano-niosomes as nanoscale drug delivery systems: An illustrated review. Journal of Controlled Release. 2014;185(2014):22-36.

53. Basera K, Bhatt G, Kothiyal P, Gupta P. Nanoemugel: A novel formulation approach for topical delivery of hydrophobic drugs. World journal of pharmacy and pharmaceutical sciences. 2015;4(10):1871-86.

54. Joy J, Krishnakumar K, John A, Dineshkumar B. Current Research in Drug Targeting. Current Research in Drug Targeting. 2015;5(1):1-4.

55. López-García R, Ganem-Rondero A. Solid Lipid Nanoparticles (SLN) and Nanostructured Lipid Carriers (NLC): Occlusive Effect and Penetration Enhancement Ability. Journal of Cosmetics, Dermatological Sciences and Applications. 2015;5(2):62-72.

56. Patil J, Gurav P, Kulkarni R, Jadhav S, Mandave S, Shete M, et al. Applications of Solid Lipid Nanoparticle in Novel Drug Delivery System. British Biomedical Bulletin. 2013;1(2):103-18.

57. Kesarwani P, Rastogi S, Bhalla V, Arora V. Nanoparticulate drug delivery system to improve systemic absorption. International Journal of Research in Pharmaceutical and Nano Sciences. 2014;3(6):558- 69.

58. Mora-Huertas C, Fessi H, Elaissari A. Polymer-based nanocapsules for drug delivery. International journal of pharmaceutics. 2010;385(1):113-42.

59. Zhang X, Malhotra S, Molina M, Haag R. Micro-and nanogels with [illegible] synthesis [illegible] Chemical Society Reviews. 2015;44(7):1948-73.

60. Tejashri G, Amrita B, Darshana J. Cyclodextrin based nanosponges for pharmaceutical use: A review. Acta pharmaceutica. 2013;63(3):335-58.

61. Ahmed RZ, Patil G, Zaheer Z. Nanosponges–a completely new nano-horizon: pharmaceutical applications and recent advances. Drug development and industrial pharmacy. 2013;39(9):1263-72.

62. Maravajhala V, Papishetty S, Bandlapalli S. Nanotechnology in development of drug delivery system. International journal of pharmaceutical sciences & research. 2012;3(1):84-96.

63. Georgakilas V, Perman JA, Tucek J, Zboril R. Broad family of carbon nanoallotropes: classification, chemistry, and applications of fullerenes, carbon dots, nanotubes, graphene, nanodiamonds, and combined superstructures. Chemical Reviews. 2015;115(11):4744-822.

64. Prasad PV, Shrivastav TG. Nanotechnological Contribution to Drug Delivery System: A Reappraisal. Journal of Biomaterials and Nanobiotechnology. 2014;5(3): 194-9.

65. Liu M, Gan L, Chen L, Zhu D, Xu Z, Hao Z, et al. A novel liposome-encapsulated hemoglobin/silica nanoparticle as an oxygen carrier. International journal of pharmaceutics. 2012;427(2):354-7.

66. Kwon S, Singh RK, Perez RA, Neel EAA, Kim H-W, Chrzanowski W. Silica-based mesoporous nanoparticles for controlled drug delivery. Journal of tissue engineering. 2013;4(2013):1-18.

67. Volkov Y. Quantum dots in nanomedicine: recent trends, advances and unresolved issues. Biochemical and biophysical research communications. 2015;468(3):419-27.

68. HE D, WANG D, QUAN W, YU C. Application of Functionalize[illegible] Quantum Dots in Bioanalysis, Imaging and Targeting Delivery. Medical Science Journal of C[illegible] South Chin[illegible]

69. Khirwa[illegible], Kumar V, Dasho[illegible] delivery. Indo American Journal of Pharmaceutical Research. 2014;4(12):5599-610.

70. Singh D, McMillan JM, Kabanov AV, Sokolsky-Papkov M, Gendelman HE. Bench-to-bedside translation of magnetic nanoparticles. Nanomedicine. 2014;9(4):501-16.

71. Charitidis CA, Georgiou P, Koklioti MA, Trompeta A-F, Markakis V. Manufacturing nanomaterials: from research to industry. Manufacturing Review. 2014;1(11):1-19.

72. Hamouda IM. Current perspectives of nanoparticles in medical and dental biomaterials. Journal of biomedical research. 2012;26:143-51.

73. Conde J, Doria G, Baptista P. Noble metal nanoparticles applications in cancer. Journal of drug delivery. 2012;2012:1-12.

74. Adrjanowicz K, Zakowiecki D, Kaminski K, Hawelek L, Grzybowska K, Tarnacka M, et al. Molecular dynamics in supercooled liquid and glassy states of antibiotics: azithromycin, clarithromycin and roxithromycin studied by dielectric spectroscopy. . Molecular pharmaceutics. 2012;9(6):1748-63.

75. Vatsraj S, Chauhan K, Pathak H. Formulation of a Novel Nanoemulsion System for Enhanced Solubility of a Sparingly Water Soluble Antibiotic, Clarithromycin. Journal of Nanoscience. 2014;2014(1):1-7.

76. Morakul B, Suksiriworapong J, Leanpolchareanchai J, Junyaprasert VB. Precipitation-lyophilization-homogenization (PLH) for preparation of clarithromycin nanocrystals: Influencing factors on physicochemical properties and stability. International journal of pharmaceutics. 2013;457(1):187-96.

77. Patil MS, Vidyasagar G. Formulation, optimization and evaluation of floating tablets clarithromycin. International Journal of Pharmacy and Pharmaceutical Sciences. 2015;7(5):3[illegible]

78. Inoue Y, Yoshimura S, Tozuka [illegible] Y, et al. Application of ascorbic acid 2-glucoside as a solubilizing agent for clarithromycin: solubilization and nanoparticle formation. International journal of pharmaceutics. 2007;331(1):38-45.

79. Pereira JM, Mejia-Ariza R, Ilevbare GA, McGettigan HE, Sriranganathan N, Taylor LS, et al. Interplay of degradation, dissolution and stabilization of clarithromycin and its amorphous solid dispersions. Molecular pharmaceutics. 2013;10(12):4640-53.

80. Doucet-Populaire F, Capobianco J, Zakula D, Jarlier V, Goldman R. Molecular basis of clarithromycin activity against Mycobacterium avium and Mycobacterium smegmatis. Journal of Antimicrobial Chemotherapy. 1998;41(2):179-87.

81. Patingrao DL, Kadu P. Formulation and evaluation of clarithromycin gastroretentive dosage form. Journal of Chemical & Pharmaceutical Research. 2014;6(7):82-9

82. Adzitey F. Antibiotic Classes and Antibiotic Susceptibility of Bacterial Isolates from Selected Poultry; A Mini Review. World's Veterinary Journal. 2015;5(3):36-41.

83. Derakhshandeh K, Bahrami G, Mohammadi B, Alizadeh E. Oral Bioavailability and Pharmacokinetic Study of Clarithromycin in Different Dosage Forms in Iranian Healthy Volunteers. Journal of Bioequivalence & Bioavailability. 2014;6(6):206-11.

84. Akre HS, Mundhada DR, Bhaskaran S, Asghar S, Gandhi GS. Dry suspension formulation of taste masked antibiotic drug for pediatric use. Journal of Applied Pharmaceutical Science. 2012;2(7):

85. Amsden G. Anti-inflammatory effects of macrolides-an underappreciated benefit in the treatment of community-acquired respiratory tract infections and chronic inflammat Antimicrobial Chemotherapy. 2005;55(1):10-21.

86. Ni W, Shao X, Cai X, Wei C, Cui J, Wang R, et al. Prophylactic use of macrolide antibiotics for the prevention of chronic obstructive pulmonary disease exacerbation: a meta-analysis. PloS one. 2015;10(3):1-13.

87. Potter J, Capstick T, Ricketts W, Whitehead N, Kon O. A UK-based resource to support the monitoring and safe use of anti-TB drugs and second-line treatment of multidrug-resistant TB. Thorax. 2015;70(3):297-8.

88. Chu S, Deaton R, Cavanaugh J. Absolute bioavailability of clarithromycin after oral administration in humans. Antimicrobial agents and chemotherapy. 1992;36(5):1147-50.

89. Ramanathan G, Mahalakshmi N, Shiny ER, Suresh JI. Evaluation of Phytotoxic and Bioactive Potential of Paclitaxel from Fusarium solani. Int J Curr Microbiol App Sci. 2015;4(3):64-74.

90. Isah T. Natural Sources of Taxol. British Journal of Pharmaceutical Research. 2015;6(4):214-27.

91. Priyadarshini K, Aparajitha UK. Paclitaxel against cancer: a short review. Med chem. 2012;2(7):139-41.

92. Yang F-H, Zhang Q, Liang Q-Y, Wang S-Q, Zhao B-X, Wang Y-T, et al. Bioavailability enhancement of paclitaxel via a novel oral drug delivery system: paclitaxel-loaded glycyrrhizic acid micelles. Molecules. 2015;20:4337-56.

93. Surapaneni MS, Das SK, Das NG. Designing Paclitaxel drug delivery systems aimed at improved patient outcomes: current status and challenges. ISRN pharmacology. 2012;2012(1):1-15.

94. Shah M, Shah V, Ghosh A, Zhang Z, Minko T. Molecular Inclusion Complexes of β-Cyclodextrin Derivatives Enhance Aqueous Solubility and Cellular Internalization of Paclitaxel: Preformulation and in vitro Investigations. Pharmaceutical

Formulations Including Those Suitable for Use in Dogs. Journal of Veterinary Internal Medicine. 2015;29(4):1006-12.

96. Siddiqui S, Kumar S, Siddiqui A, Paliwal S, Kohli K, Mishra R. Analytical Approaches to Paclitaxel. Hamdard Medicus. 2012;55(3):17-25.

97. Kampan NC, Madondo MT, McNally OM, Quinn M, Plebanski M. Paclitaxel and its evolving role in the management of ovarian cancer. BioMed research international. 2015;2015(1):1-21.

98. Pillai G. Nanomedicines for cancer therapy: an update of FDA approved and those under various stages of development. SOJ Pharm Pharm Sci. 2014;1(2):1-13.

99. Sisodiya PS. Plant derived anticancer agents: A review. International Journal of Research and Development in Pharmacy and Life Sciences 2013;2(2):293-308.

100. Kaur Saharan H, Das S, Varshney P. Safety profile of Paclitaxel. International Journal of Pharmacy & Life Sciences. 2015;6(1):4177-94.

101. Chen N, Li Y, Ye Y, Palmisano M, Chopra R, Zhou S. Pharmacokinetics and pharmacodynamics of nab-paclitaxel in patients with solid tumors: Disposition kinetics and pharmacology distinct from solvent-based paclitaxel. The Journal of Clinical Pharmacology. 2014;54(10):1097-107.

102. Thagele R, Mishra A, Pathak A. Formulation and characterization of clarithromycin based nanoparticulate drug delivery system. Int J Pharm Life Sci. 2011;2(1):510-5.

103. Lotfipour F, Valizadeh H, Azhdarzadeh M, Zakeri-Milani P. Study of anti-microbial effects of Clarithromycin nanosuspensions against Staphylococcus aureus and Salmonella typhi. International Journal of Pharmaceutical Sciences 2012; 18(1):1-8

104. [illegible] Clarithromycin dissolution enhance[illegible] nanosuspensions using sonoprecipitation technique. Iranian journal of pharmaceutical research: IJPR. 2014;13(3):809-18.

105. Oktay B, Demir S, Kayaman-Apohan N. Magnetic nanoparticle containing thiol-ene crosslinked hydrogels for controlled and targeted release of hydrophobic drugs. Polymer Composites. 2016;10(1):241-4.

106. Fonseca C, Simoes S, Gaspar R. Paclitaxel-loaded PLGA nanoparticles: preparation, physicochemical characterization and in vitro anti-tumoral activity. Journal of Controlled Release. 2002;83(2):273-86.

107. Li F, Li J, Wen X, Zhou S, Tong X, Su P, et al. Anti-tumor activity of paclitaxel-loaded chitosan nanoparticles: An in vitro study. Materials Science and Engineering: C. 2009;29(8):2392-7.

108. Aygül G, Yerlikaya F, Caban S, Vural İ, Çapan Y. Formulation and in Vitro Evaluation of Paclitaxel Loaded Nanoparticles. Hacettepe Univ J Fac Pharm. 2013;33(1):25-40.

109. Lu J, Chuan X, Zhang H, Dai W, Wang X, Wang X, et al. Free paclitaxel loaded PEGylated-paclitaxel nanoparticles: Preparation and comparison with other paclitaxel systems in vitro and in vivo. International journal of pharmaceutics. 2014;471(1):525-35.

110. Bayindir ZS, Besiksi A, Yuksel N. Paclitaxel-loaded niosomes for intravenous administration: pharmacokineticsand tissue distribution in rats. Turkish journal of medical sciences. 2015;45(6):1403-12.

111. Ahamed M, Ali D, Alhadlaq HA, Akhtar MJ. Nickel oxide nanoparticles exert cytotoxicity via oxidative stress and induce apoptotic response in human liver cells (HepG2). Chemosphere. 2013;93(2):2141-7.

112. Raj KP, Sivakarthik P, Uthirakumar A, Thangaraj V. Cytotoxicity [illegible] nickel oxide [illegible] Journal of Chemical and Pharmaceutical Research. 2014;2014(1):269-71.

113. Vinardell Martínez-Hidalgo MP, Mitjans Arnal M. Antitumor activities of metal oxide nanoparticles. Nanomaterials 2015;5(2):1004-21.

114. Javed KR, Ahmad M, Ali S, Butt MZ, Nafees M, Butt AR, et al. Comparison of doxorubicin anticancer drug loading on different metal oxide nanoparticles. Medicine. 2015;94(11):1-6.

115. Adhikary J, Chakraborty P, Das B, Datta A, Dash SK, Roy S, et al. Preparation and characterization of ferromagnetic nickel oxide nanoparticles from three different precursors: application in drug delivery. RSC Advances. 2015;5(45):35917-28.

116. Essa HJ. Synthesis of porous nanoparticles and their use as a cytotoxic agent. J Fac Med Baghdad. 2014;56(3):325-8.

117. Malarkodi C, Rajeshkumar S, Paulkumar K, Vanaja M, Gnanajobitha G, Annadurai G. Biosynthesis and antimicrobial activity of semiconductor nanoparticles against oral pathogens. Bioinorganic chemistry and applications. 2014;2014(1):1-10.

118. Shivashankarappa A, Sanjay K. Study on Biological Synthesis of Cadmium Sulfide Nanoparticles by Bacillus licheniformis and Its Antimicrobial Properties against Food Borne Pathogens. Nanoscience and Nanotechnology Research. 2015;3(1):6-15.

119. Grinyte R, Garai-Ibabe G, Saa L, Pavlov V. Application of photocatalytic cadmium sulfide nanoparticles to detection of enzymatic activities of glucose oxidase and glutathione reductase using oxidation of 3, 3′, 5, 5′-tetramethylbenzidine. Analytica chimica acta. 2015;881(1):131-8.

120. Rockville M. General Methods of Analysis, des[illegible] method[illegible] and procedures for the quality contr[illegible] of p[illegible]armac[illegible]ical substances, [illegible]ination of Melting [illegible]nts Acco[illegible] USP35-NF30 [illegible] Pharmaco[illegible] Edition ed: Uni[illegible] (USP); 2014. p. 2033-4.

121. Muruganandam S, Anbalagan G, Murugadoss G. Optical, electrochemical and thermal properties of Co2+-doped CdS nanoparticles using polyvinylpyrrolidone. Applied Nanoscience. 2015;5(2):245-53.

122. Rao BS, Kumar BR, Reddy VR, Rao TS. Preparation and characterization of CdS nanoparticles by chemical co-precipitation technique. Chalcogenide Letters. 2011;8(3):177-85.

123. Adekunle AS, Oyekunle JA, Oluwafemi OS, Joshua AO, Makinde WO, Ogunfowokan AO, et al. Comparative Catalytic Properties of Ni (OH) 2 and NiO Nanoparticles Towards the Degradation of Nitrite (NO2-) and Nitric Oxide (NO). Int J Electrochem Sci. 2014;9(2014):3008-21.

124. Mohammadijooa M, Khorshidia ZN, Sadrnezhaadb S, Mazinanic V. Synthesis and characterization of nickel oxide nanoparticle with wide band

gap energy prepared via thermochemical processing. Nanoscience and Nanotechnology: An International Journal. 2014;4(1):6-9.

125. Liggins R, Burt H. Polyether–polyester diblock copolymers for the preparation of paclitaxel loaded polymeric micelle formulations. Advanced drug delivery reviews. 2002;54(2):191-202.

126. Doddayya H, Reddy R. Floating Tablets for Helicobacter Pylori Induced Peptic Ulcer Therapy: A Research Review on Formulation Studies, In Vitro and In Vivo Evaluation. Journal of Biomedical and Pharmaceutical Research. 2012;1(3):39-52.

127. Bonferoni M, Sandri G, Dellera E, Rossi S, Ferrari F, Mori M, et al. Ionic polymeric micelles based on chitosan and fatty acids and intended for wound healing. Comparison of linoleic and oleic acid. European Journal of Pharmaceutics and Biopharmaceutics. 2014;87(2014):1[illegible]

128. Nayeed S, Qamar F. Simple UV spectrophotometric assay of [illegible] Journal [illegible] 2014;6:382-5.

129. Kesarwani P, Tekade RK, Jain N. Spectrophotometric estimation of paclitaxel. International Journal of Advances in Pharmaceutical Sciences. 2011;2(2011):29-32.

130. Kumar SS, Manoj Kiran VN. Development and invitro characterization of paclitaxel sustained release microsphers. International Journal of Pharmacy Review & Research. 2015;5(4):338-44.

131. Jadhav KK, Reddy GA, Chowdary YA. Determination of absorption maxima (λmax) and Beer Lamberts range for paclitaxel by UV-Visible spectrophotometer. International Journal of Universal Pharmacy and Life Sciences 2012;2(2):37-41.

132. Namasivayam SKR, Singh V, Samydurai S. Metallic and non metallic nanoparticles incorporated meropenem and ceftazidime synthesis for the

improved antibacterial activity against human pathogenic bacteria. Der Pharma Chemica. 2014;6(6):121-7.

133. Pal SL, Jana U, Manna P, Mohanta G, Manavalan R. Nanoparticle: an overview of preparation and characterization. Journal of Applied Pharmaceutical Science. 2011;1(6):228-34.

134. Elias A, Crayton SH, Warden-Rothman R, Tsourkas A. Quantitative Comparison of Tumor Delivery for Multiple Targeted Nanoparticles Simultaneously by Multiplex ICP-MS. Scientific reports. 2014;4(2014):1-9.

135. Bykkam S, Ahmadipour M, Narisngam S, Kalagadda VR, Chidurala SC. Extensive studies on X-Ray diffraction of green synthesized silver nanoparticles. Advances in Nanoparticles. 2015;4(1):1-10.

136. Sierra-Ávila R, Pérez-Alvarez M, Cadenas-Pliego G, Padilla VC, Ávila-Orta C, Camacho OP, et al. Synthesis of Copper Nanoparticles Using Mixture of Allylamine and Polyallylamine. Journal of Nanomaterials. 2015;2015(1):1-8.

137. Pande N, Arshad SS, Hair Bejo [illegible] Synthesis and Characterization of Chitosan-Saponin Nanoparticle for Application in Plasmid DNA Delivery. Journal of Nanomaterials. 2015;2015(1):1-8.

138. Moosa AA, Ridha AM, Al-Kaser M. Process Parameters for Green Synthesis of Silver Nanoparticles using Leaves Extract of Aloe Vera Plant. International Journal of Multidisciplinary and Current research. 2015;3(2015):966-75.

139. Shahbaziniaz M, Foroutan SM, Bolourchian N. Dissolution Rate Enhancement of Clarithromycin Using Ternary Ground Mixtures: Nanocrystal Formation. Iranian journal of pharmaceutical research: IJPR. 2013;12(4):587-98.

140. Pandey S, Kumar S. Evaluation of the effect of hydrophilic polymer blend to extend the release of clarithromycin from prepared microcapsules. Journal of Pharmaceutical Scinces and Research. 2010;2(11):759-66.

141. Ahmad J, Mir SR, Kohli K, Chuttani K, Mishra AK, Panda A, et al. Solid-Nanoemulsion Preconcentrate for Oral Delivery of Paclitaxel: Formulation Design, Biodistribution, and γ Scintigraphy Imaging. BioMed research international. 2014;2014(1):1-12.

142. Sharma K, Deevenapalli M, Singh D, Chourasia MK, Bathula SR. Preparation and characterization of paclitaxel-loaded gliadin nanoparticles. Journal of Biomaterials and Tissue Engineering. 2014;4(5):399-404.

143. Filippousi M, Papadimitriou SA, Bikiaris DN, Pavlidou E, Angelakeris M, Zamboulis D, et al. Novel core–shell magnetic nanoparticles for Taxol encapsulation in biodegradable and biocompatible block copolymers: Preparation, characterization and release properties. International journal of pharmaceutics. [illegible]:221-30.

144. Gavini V, Murthy MS, Ku[illegible] Evaluation of Nanoparticulate Drug Delivery System Loaded With 5-Fluorouracil. Research Journal of Pharmaceutical Dosage Forms and Technology. 2014;6(4):243-8.

145. Apley M, Crist GB, Fellner V, Gonzalez MA, Hunter RP, Martinez MN, et al. Determination of Thermodynamic Solubility of Active Pharmaceutical Ingredients for Veterinary Species: A New USP General Chapter. 2015;41(3).

146. Elsayed I, Abdelbary AA, Elshafeey AH. Nanosizing of a poorly soluble drug: technique optimization, factorial analysis, and pharmacokinetic study in healthy human volunteers. International journal of nanomedicine. 2014;9(1):2943-53.

147. Valizadeh H, Mohammadi G, Ehyaei R, Milani M, Azhdarzadeh M, Zakeri-Milani P, et al. Antibacterial activity of clarithromycin loaded PLGA

nanoparticles. Die Pharmazie-An International Journal of Pharmaceutical Sciences. 2012;67(1):63-8.

148. Wang L, Li H, Wang S, Liu R, Wu Z, Wang C, et al. Enhancing the antitumor activity of berberine hydrochloride by solid lipid nanoparticle encapsulation. AAPS PharmSciTech. 2014;15(4):834-44.

149. Liebmann J, Cook J, Lipschultz C, Teague D, Fisher J, Mitchell J. Cytotoxic studies of paclitaxel (Taxol) in human tumour cell lines. British journal of cancer. 1993;68(6):1104-9.

150. Esfandyari-Manesh M, Mostafavi SH, Majidi RF, Koopaei MN, Ravari NS, Amini M, et al. Improved anticancer delivery of paclitaxel by albumin surface modification of PLGA nanoparticles. DARU Journal of Pharmaceutical Sciences. 2015;23(1):1-8.

151. Esfandyari-Manesh M, Mostafavi SH, Majidi RF, Koopaei MN, Ravari NS, Amini M, et al. Improved anticancer delivery of paclitaxel by albumin surface modification of PLGA nanoparticles. DARU Journal of Pharmaceutical Sciences. 2015;2015(1

152. Lin Y, Jiang D, Li Y, Han X, Yu D, Park JH, et al. Effect of sun ginseng potentiation on epirubicin and paclitaxel-induced apoptosis in human cervical cancer cells. Journal of ginseng research. 2015;39(1):22-8.

153. Huo ZJ, Wang SJ, Wang ZQ, Zuo WS, Liu P, Pang B, et al. Novel nanosystem to enhance the antitumor activity of lapatinib in breast cancer treatment: Therapeutic efficacy evaluation. Cancer science. 2015;106(10):1429-37.

154. Zhao M, Lei C, Yang Y, Bu X, Ma H, Gong H, et al. Abraxane, the Nanoparticle Formulation of Paclitaxel Can Induce Drug Resistance by Up-Regulation of P-gp. PloS one. 2015;10(7):1-19.

155. Prasath M, Arun RB, Revathy R. Synthesis and characterisation of Mn2+ doped CdS nanoparticles Journal of Chemical and Pharmaceutical Research. 2015;7(11):875-85.

156. Kishore N, Mukherjee S. Synthesis and Characterization of Mixed Ferrites. International Journal of Scientific and Research Publications. 2014;4(1):1-5.

157. Zhao Z, Li Y, Zhang Y. Preparation and Characterization of Paclitaxel Loaded SF/PLLA-PEG-PLLA Nanoparticles via Solution-Enhanced Dispersion by Supercritical CO 2. Journal of Nanomaterials. 2015;2015(1):1-7.

158. Hiremath JG, Khamar NS, Palavalli SG, Rudani CG, Aitha R, Mura P. Paclitaxel loaded carrier based biodegradable polymeric implants: preparation and in vitro characterization. Saudi Pharmaceutical Journal. 2013;21(1):85-91.

159. Jeyaprabha P, Sudhamani T. Design and characterization of clarithromycin beads using a biodegradable cationic polymer. Indian Journal of Research Journal of Pharmacy. 2013;4(3):1-8.

160. Zakeri-Milani P, Islambulchilar Z, Majidpour F, Jannatabadi E, Lotfipour F, Valizadeh H. A study on enhanced intestinal permeability of clarithromycin nanoparticles. Brazilian Journal of Pharmaceutical Sciences. 2014;50(1):121-9.

162. Adesina SK, Holly A, Kramer-Marek G, Capala J, Akala EO. Polylactide-Based Paclitaxel-Loaded Nanoparticles Fabricated by Dispersion Polymerization: Characterization, Evaluation in Cancer Cell Lines, and Preliminary Biodistribution Studies. Journal of pharmaceutical sciences. 2014;103(8):2546-55.

163. Hou Z, Zhao W, Zhang Q, Zheng W. Effect of Paclitaxel-loaded Nanoparticles on the Viability of Human Hepatocellular Carcinoma HepG2 Cells. Asian Pacific journal of cancer prevention: APJCP. 2014;16(5):1725-8.

164. Zhang Y, Yang M, Portney NG, Cui D, Budak G, Ozbay E, et al. Zeta potential: a surface electrical characteristic to probe the interaction of nanoparticles with normal and cancer human breast epithelial cells. Biomedical microdevices. 2008;10(2):321-8.

165. Honary S, Zahir F. Effect of zeta potential on the properties of nano-drug delivery systems-a review (Part 2). Tropical Journal of Pharmaceutical Research. 2013;12(2):265-73.

166. Kumar A, Singh N, Kaushik D. Taste Masking of Clarithromycin using Complexation with Ion exchange resin. International Journal of PharmTech Research. 2014;6(1):203-11.

167. Omar M, Makary P, Wlodarski M. A Review of Polymorphism and the Amorphous State in the Formulation Strategy of Medicines and Marketed Drugs. UK Journal of Pharmaceutical and Biosciences 20[illegible]5;3(6):[illegible]

168. Wang Y, Wang D, Fu Q, Liu D, Ma Y, Racette K, et al. Shape-[illegible] [illegible]particles wit[illegible] [illegible] worm-like, spherical, and fingerp[illegible] [illegible]2014;11(10):3766-71.

169. Ganesh M, Ubaidulla U, Hemalatha P, Peng MM, Jang HT. Development of Duloxetine Hydrochloride Loaded Mesoporous Silica Nanoparticles: Characterizations and In Vitro Evaluation. AAPS PharmSciTech. 2015;16(4):944-51.

170. Gulati K, Aw M, Losic D. Nanoengineered drug-releasing Ti wires as an alternative for local delivery of chemotherapeutics in the brain. International Journal of Nanomedicine 2012;7(1):2069-76.

171. Zendehdel M, Cruciani G, Kar FS, Barati A. Synthesis and study the controlled release of etronidazole from the new PEG/NaY and PEG/MCM-41 nanocomposites. Journal of Environmental Health Science and Engineering. 2014;12(1):1-9.

172. Terry AB, Salaam AD, Nyairo E, Thomas V, Dean DR. Plga nanoparticles for the sustained release of rifampicin. Journal of Nanogenomics and Nanomedicine. 2014;2(1):1-9.

173. Smitha K, Anitha A, Furuike T, Tamura H, Nair SV, Jayakumar R. In vitro evaluation of paclitaxel loaded amorphous chitin nanoparticles for colon cancer drug delivery. Colloids and Surfaces B: Biointerfaces. 2013;104(1):245-53.

174. Thagele R, Mishra A, Pathak A. Formulation and characterization of clarithromycin based nanoparticulate drug delivery system. International Journal of Pharmacy & Life Scinces. 2011;2(1):510-5.

175. Thadkala K, Nanam PK, Rambabu B, Sailu C, Aukunuru J. Preparation and characterization of amorphous ezetimibe nanosuspensions intended for enhancement of oral bioavailability. International journal of pharmaceutical investigation. 2014;4(3):131-7.

176. [illegible] K, Pal S[illegible] loaded PLGA [illegible]particles: preparati[illegible] and in vivo toxicity study. Nano Convergence. 2014;1(1):1-10.

177. Bhoskar M, Patil P. Developement and evaluation of paclitaxel loaded nanoparticles using 24 factorial design. International Journal of Current Pharmaceutical Research. 2015;7(2):64-72.

178. Onishi Y, Eshita Y, Ji R-C, Onishi M, Kobayashi T, Mizuno M, et al. Anticancer efficacy of a supramolecular complex of a 2-diethylaminoethyl–dextran–MMA graft copolymer and paclitaxel used as an artificial enzyme. Beilstein journal of nanotechnology. 2014;5(1):2293-307.

179. Martins KF, Messias AD, Leite FL, Duek EA. Preparation and characterization of paclitaxel-loaded PLDLA microspheres. Materials Research. 2014;17(3):650-6.

180. Zhang H, Liu G, Zeng X, Wu Y, Yang C, Mei L, et al. Fabrication of genistein-loaded biodegradable TPGS-b-PCL nanoparticles for improved

therapeutic effects in cervical cancer cells. International journal of nanomedicine. 2015;10(1):2461-73.

181. Rao A, Schoenenberger M, Gnecco E, Glatzel T, Meyer E, Brändlin D, et al., editors. Characterization of nanoparticles using atomic force microscopy. Journal of Physics: Conference Series; 2007: IOP Publishing.

182. Lu P-J, Huang S-C, Chen Y-P, Chiueh L-C, Shih DY-C. Analysis of titanium dioxide and zinc oxide nanoparticles in cosmetics. journal of food and drug analysis. 2015;23(3):587-94.

183. Drozdek S, Bazylińska U. Biocompatible oil core nanocapsules as potential co-carriers of paclitaxel and fluorescent markers: preparation, characterization, and bioimaging. Colloid and polymer science. 2016;294(1):225-37.

184. Rajan M, Raj V, Al-Arfaj AA, Murugan A. Hyaluronidase-triggered core-5-fluorouracil-loaded chitosan-PEG-gelatin polymer nanocomposites [illegible] drug delivery. [illegible] pharmaceutics. 2015;485(2):514-22.

185. Sun S-B, Liu P, Shao F-M, Miao Q-L. Formulation and evaluation of PLGA nanoparticles loaded capecitabine for prostate cancer. International Journal of Clinical and Experimental Medicine. 2015;8(10):19670-81.

186. Derman S, Mustafaeva ZA, Abamor ES, Bagirova M, Allahverdiyev A. Preparation, characterization and immunological evaluation: canine parvovirus synthetic peptide loaded PLGA nanoparticles. Journal of biomedical science. 2015;22(2015):1-12.

187. Tuncer Degim I, Kadioglu D. Cheap, suitable, predictable and manageable nanoparticles for drug delivery: quantum dots. Current drug delivery. 2013;10(1):32-8.

188. Dizaj SM, Vazifehasl Z, Salatin S, Adibkia K, Javadzadeh Y. Nanosizing of drugs: Effect on dissolution rate. Research in pharmaceutical sciences. 2015;10(2):95-108.

189. Junyaprasert VB, Morakul B. Nanocrystals for enhancement of oral bioavailability of poorly water-soluble drugs. Asian Journal of Pharmaceutical Sciences. 2015;10(1):13-23.

190. Yadollahi R, Vasilev K, Simovic S. Nanosuspension technologies for delivery of poorly soluble drugs. Journal of Nanomaterials. 2015;2015(1):1-13.

191. Mahalingam M, Krishnamoorthy K. Fabrication, Physicochemical Characterization and Evaluation of In vitro Anticancer Efficacy of a Novel pH Sensitive Polymeric Nanoparticles for Efficient Delivery of Hydrophobic Drug against Colon Cancer. Journal of Applied Pharmaceutical Science. 2015;5(11):135-45.

192. Taleb SAA, Ammar HO, Badawi AA, Mostafa DM. Novel Sustainable Nanocarrier Systems for Improving Drug [illegible]. Journal of Innovations in Pharmaceuticals and Biological Sciences. 2015;2(3):322-32.

[illegible] Lansoprazole. Journal of Applied Pharmaceutical Science Vol. 2015;5(4):20-5.

194. Sun J. Effect of particle size on solubility, dissolution rate, and oral bioavailability: evaluation using coenzyme Q. International journal of nanomedicine. 2012;7(2012):5733-44.

195. Kommavarapu P, Maruthapillai A, Palanisamy K. Preparation, Characterization and Evaluation of Elvitegravir-Loaded Solid Lipid Nanoparticles for Enhanced Solubility and Dissolution Rate. Tropical Journal of Pharmaceutical Research. 2015;14(9):1549-56.

196. Ma P, Mumper RJ. Paclitaxel nano-delivery systems: a comprehensive review. Journal of nanomedicine & nanotechnology. 2013;4(2):1-16.

197. Prabhu RH, Patravale VB, Joshi MD. Polymeric nanoparticles for targeted treatment in oncology: current insights. International journal of nanomedicine. 2015;10(1):1001—18.

198. Tang X, Cai S, Zhang R, Liu P, Chen H, Zheng Y, et al. Paclitaxel-loaded nanoparticles of star-shaped cholic acid-core PLA-TPGS copolymer for breast cancer treatment. Nanoscale research letters. 2013;8(1):1-12.

199. Wan C, Letchford K, Jackson JK, Burt HM. The combined use of paclitaxel-loaded nanoparticles with a low-molecular-weight copolymer inhibitor of P-glycoprotein to overcome drug resistance. International Journal of Nanomedicine 2013;8(1):379-91.

200. Zhu W, Lee S-J, Castro NJ, Yan D, Keidar M, Zhang LG. Synergistic Effect of Cold Atmospheric Plasma and Drug Loaded Core-shell Nanoparticles on Inhibiting Breast Cancer Cell Growth. Scientific reports. 2016;6(1):1-11.

[illegible] activity of paclitaxel-loaded [illegible] breast cancer cells. Biomacromolecules. 2013;14(6):2074-82.

الخلاصة

تقنية النانو هي تقنية الفهم والتحكم في المادة بأبعاد تتراوح تقريبا من 1- 100 نانومتربينما النواقل النانوية هي مواد بحجم النانو يتم استعمالها كوحدات نقل لمواد اخرى كالأدوية.

الكلارثرومايسين هو مضاد حيوي ماكروليدي و الذي يمتلك إمتصاص تحدده سرعة الذوبان وتوافر بيولوجي منخفض بعد إعطائه فمويا بسبب ذوبانيتة المنخفضة حيث أن الكلارثرومايسين ينتمي للصنف الثاني حسب نظام تصنيف الصيدلة الاحيائية والذي يمتلك ذوبانية قليلة ونفاذية عالية, بينما الباكليتاكسيل هو دواء مضاد للسرطان من الصنف الرابع والذي يمتلك ذوبانية قليلة و نفاذية قليلة, حيث أن طبيعتة المنجذبه للدهون وذوبانيتة المائية القليلة جدا إضافة لعدم إمتلاكة مجموعه فعالة قابلة للتأين تمثل التحديات الرئيسية للباكليتاكسيل أمام تحلله وتحرره من شكله الدوائي.

إن جزيئات كبريتيد الكادميوم (CdS) واوكسيد النيكل (NiO) النانوية قد تم تحضيرها وتحميل

الكلارثرومايسين و الباكليتاكسيل على سطح الجزيئات النانوية لكبريتيد الكادميوم واوكسيد النيكل تم

إنجازة بواسطة تكوين معقد فيزيائي بدون اي تفاعل كيمياوي لمجاميعها الفعالة.

إن دراسة الذوبانية/التحلل قد تم تطبيقها وأظهرت تحسنها بشكل ملحوظ ($p<0.05$) وبمعدل الضعف مع جزيئات كبريتيد الكادميوم النانوية وبمعدل ثلاث أضعاف مع جزيئات اوكسيد النيكل النانوية, بينما فحص الفعالية المضادة للبكتيريا أظهرعدم تأثرها بعد تحميل الكلارثرومايسين على النواقل النانوية. للباكليتاكسيل المحمل على جزيئات كبريتيد الكادميوم و اوكسيد النيكل النانوية قد أظهر تغير غير ملحوظ في الذوبانية ولكن أظهر زيادة بشكل ملحوظ ($p<0.05$) على فعاليتة المضادة للسرطان على خط خلايا سرطان الثدي (MCF-7) والمصحوبة بتقليل سمية الخلايا بشكل ملحوظ على خط خلايا الثدي الطبيعية (MCF-10A) بعد تحميلة على جزيئات كبريتيد الكادميوم و اوكسيد النيكل النانوية موضحا الاختيارية والاستهداف للخلايا السلطانية وإنخفاض السمية الخلوية للباكليتاكسيل والنواقل النانوية المعدنية على الخلايا الطبيعية.

جمهورية العراق

وزارة التعليم العالي والبحث العلمي

الجامعة المستنصرية

كلية الصيدلة

تحميل أدوية الكلارثرومايسين والباكليتاكسيل على

مصطفى رعد عبدالباقي
(بكلوريوس صيدلة 2009)

بإشراف

أ.م.د.نضال خزعل مرعي ***أ.د.عاشور حمود داوود***

1437 هجري **2016 ميلادي**